The role of ultraviolet (UV) A radiation and mitochondrial DNA mutations in progression and invasion of melanoma cells

Thesis submitted as requirement to fulfil the degree
„Doctor of Philosophy“ (Ph.D.)

at the
Faculty of Medicine
Eberhard Karls University
Tuebingen

by

Tarza Sherko Abdulkareem Baban

From
Kurdistan region
Iraq

2016

Dean: Professor Dr. I. B. Autenrieth

1. Reviewer: Professor Dr. med. Mark Berneburg

2. Reviewer: Professor Dr. rer. nat H. Peter Rodemann

Index

2. Index of figures

B. Introduction figures

D. Result figures

E. Discussion

3. Index of tables

B. Introduction table

C. Material and methods tables

F. Abbreviations

A. Abstract

Melanoma is a malignant tumor in which UVA (320-400nm) radiation is regarded to be an important risk factor. To date, the role of UVA in melanoma progression towards an invasive phenotype is still not adequately investigated. For most proliferating tumor cells the preference of aerobic glycolysis has been described as the Warburg effect. Here we examine the effect of UVA irradiation on changes in Warburg effect and tumor progression towards invasive potential. Upon UVA irradiation, melanoma cell lines from initial tumors show an induction of the Warburg effect with increased glucose consumption and lactate production, which is at least partially mediated by reactive oxygen species (ROS). Concomitantly with UVA treatment and the enhanced lactic acid production, tumor relevant proteases and *in situ* invasion is upregulated. Simultaneously, UVA increases intracellular concentrations of the progression markers transketolase and activated protein kinase Akt, both involved in metabolic changes that can be enhanced with proliferation. By using invasion assays we show that lactic acid, resulting from the UVA enhanced- and partially ROS mediated Warburg effect, increases the invasive potential of all melanoma cell lines investigated. Therefore, we recognize in melanoma cells, that production of lactic acid, induced by UVA irradiation, increases invasiveness of melanoma cells via expression of tumor relevant proteases. Additionally, we investigated the influence of UVA irradiation on initial melanoma and metastasizing melanoma in a 3D skin reconstruct model. Again, this UVA irradiation was able to increase the Warburg effect (glucose consumption and lactate production) and the transketolase activity and these effects were partially mediated by ROS. Furthermore, UVA treatment increased MMP9 and uPA expression and UVA treatment increased the invasion of melanoma cells in the skin reconstruct, which was verified by a histopathologist (section from Baban *et al*., in press).

Mitochondrial DNA (mtDNA) common deletion could be implicated in the progression of various cancer types but it has not been investigated in progression of melanoma. To investigate the role of mtDNA 4977bp deletion in the development of melanoma, we analyzed mtDNA 4977bp deletion in patients with nevi and different stages of melanoma. There we detected a highly significant change in the frequency of mtDNA 4977bp deletion. These findings could point to a selection mechanism against mtDNA 4977bp deletion, emphasizing the importance of functional mtDNA despite the observation of enhanced Warburg effect.

B. Introduction

1. Melanoma and ultraviolet radiation

1.1 Epidemiological data on melanoma

Melanoma is a malignant skin tumor deriving from melanocytic cells, characterized by high morbidity and mortality with a constantly rising incidence (Howe *et al.*, 2001; Jemal *et al.*, 2010), recent data indicate that the prevalence rate rose up 5 fold during the last 3 decades worldwide (Leiter *et al.*, 2014). It is estimated that 137,310 new cases of melanoma will be diagnosed and the lifetime risk rose to 1 in each 50 people by 2015 in the United States (US) (Rigel *et al.*, 2010; American cancer society cancer facts and figure, 2015) (figure 1).

A parisian physician Rene Laennec's had diagnosed and published the first case of melanoma in Europe approximately 210 years ago. There is substantial variation in melanoma rate within different ethnic population groups (Howe *et al.*, 2001), reported data show an increase in incidence rate by 3-7% per year in Caucasian population (Jhappan *et al.*, 2003). Melanoma is more common in fair skin types (Armstrong and Kricher, 2001) for example in the Scandinavian population, as their skin type expresses more pheomelanin (reddish yellow melanin) and less eumelanin (brownish black melanin). Eumelanin is a strong ultraviolet (UV) blocking pigment (Vincensi *et al*., 1998; Brenner and Hearing, 2008). The skin type represents one of the risk factors that influence melanoma development (John *et al*., 2013). Although melanoma may arise *de novo*, also there is a classical staging in melanoma development, where melanoma develop from initial tumor cells via radial growth phase (with tumor thickness less than 1mm patients mostly are cured after excision with surgery) and vertical growth phase (with tumor thickness more than 1mm, starts spreading to deeper layer of the dermis) to metastasizing melanoma (spreading to distant organs) (figure 2). One important aspect for prognosis and treatment is staging of melanoma, which depends on tumor thickness, mitotic rate, ulceration and metastasizing to lymph nodes and distant organs.

Epidemiological evidence indicates that UV radiation is involved in the generation of melanoma with approximately 65% of melanoma being caused by UV radiation (Bald *et al.*, 2014; Fears *et al.*, 2002; Tucker and Goldstein, 2003; Klug *et al.*, 2010*;* Armstrong and Kricker, 1993). Besides, some authors hypothesize a direct correlation between sunburn and the pathogenesis of melanoma (Dennis *et al.,* 2008).

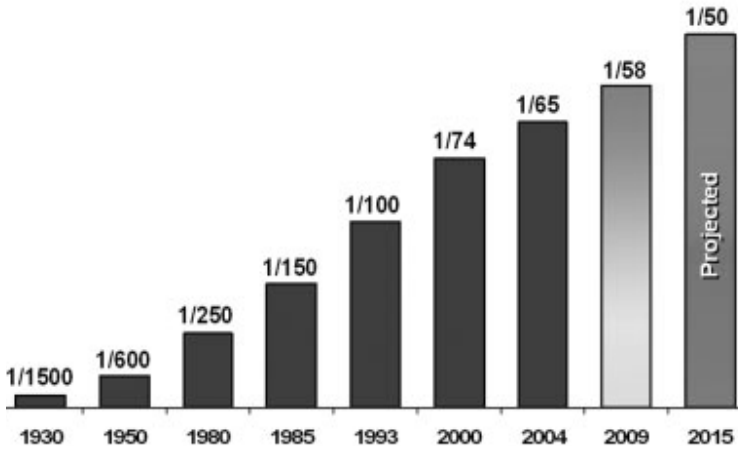

(Rigel *et al.,* figure 1, 2010)

Figure 1. Lifetime risk of invasive melanoma.

Increased lifetime risk of developing invasive melanoma in the US population from 1930 to 2015.

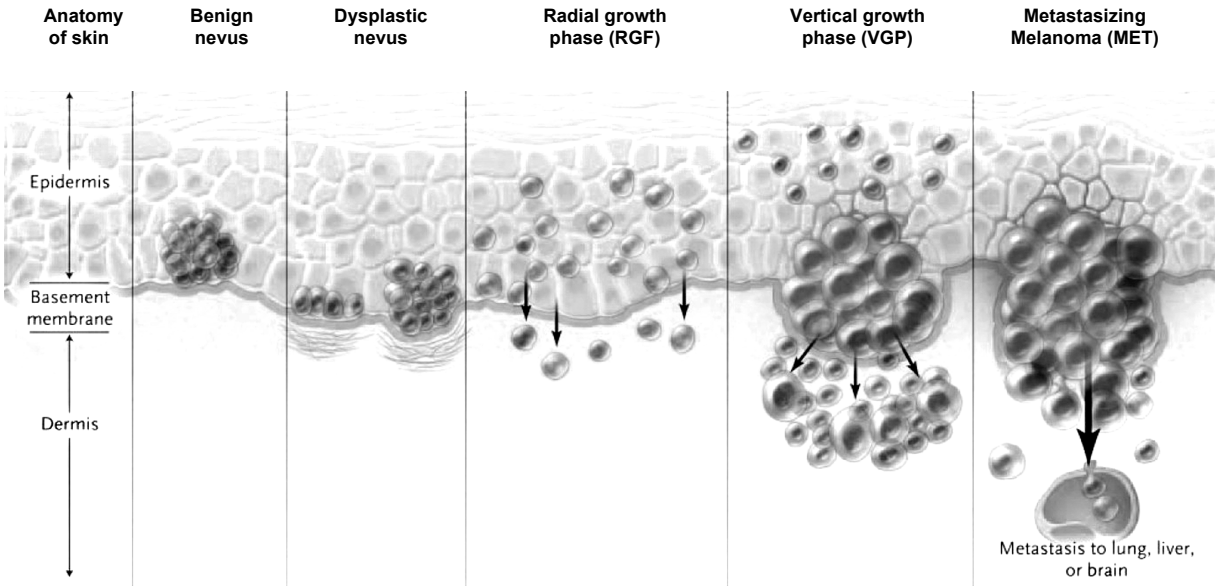

(Modified from Miller and Mihm, 2006)

Figure 2. Progression of melanoma.

In the staging model, melanomas develop from benign nevi cells via radial growth phase and vertical growth phase to metastasizing melanoma.

1.2 UV radiation and human skin

1.2.1 UV radiation

UV radiation is an electromagnetic radiation with the main natural source being the sun. The main artificial source for UV radiation is the tanning bed. The solar UV radiation is subdivided into three types according to wavelength and energy (Mogensen and Jemec, 2010):

- Ultraviolet A (UVA) has a wavelength between 320-400nm, which constitutes more than 95% of the solar UV radiation (Balk, 2011).
- Ultraviolet B (UVB) has a wavelength between 280-320nm, which constitutes less than 1% of the solar UV radiation (Rastogi *et al*., 2010; Balk, 2011).
- Ultraviolet C (UVC) has a wavelength between 100-280nm. It does not reach the surface of the earth because it is absorbed by the ozone layer in the atmosphere (Mogensen and Jemec, 2010).

The Intensity of solar UV radiation on earth surface depends on many factors, like time of daily exposure, the season, the altitude, the latitude and the UV reflection on the surfaces (Battie and Verschoore, 2012).

Another source of UV radiation is the tanning bed, which emits approximately (95%-99%) UVA and (1%-5%) UVB (Mogensen and Jemec, 2010) and intensity of tanning is mostly 10 times higher than solar radiation during midday (Balk, 2011). Studies showed that the risk for developing melanoma is increased up to 75% when tanning devices were used before the age of 35 years (Schulman and Fisher, 2009).

Since 2009, the World health organization (WHO) classified UV radiation as one of the carcinogenic factors (Mogensen and Jemec, 2010).

1.2.2 UV radiation effect on human skin

Exposures to UV radiation with acute high doses or chronic doses are considered as a risk factor for human body with profound change in the aging process and in tumorigenesis of the human skin (John *et al.,* 2013).

The long wavelength UVA radiation has the ability to penetrate the epidermis as well as the dermis and partially can reach the subcutaneous layer. UVA radiation mainly absorbs and induces damage in the dermis but UVB radiation penetrates the epidermis and upper layer of the dermis and it mostly absorbs and induces damage in the epidermis (Lee *et al.,* 2013) (figure 3).

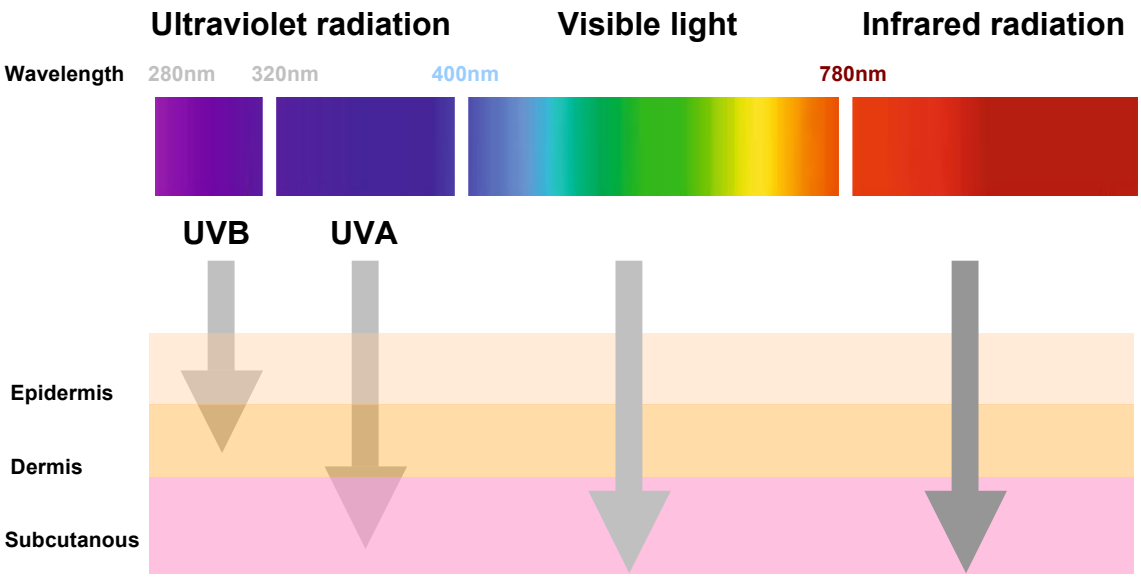

Figure 3. UV penetration in human skin.

UVA can penetrate the epidermis and dermis and UVB mainly penetrates the epidermis, both visible light and infrared radiation are capable to penetrate deeper than UV radiation.

1.2.3 Physiological relevance of UV radiation

Solar radiation has a wide range of biological effects. On the cellular level the energy of UVB radiation is absorbed by proteins and DNA molecules, causing direct DNA damage and mutations (Rastogi *et al*., 2010). The best described types of DNA damage, which are caused by UVB radiation, are cyclobutyl pyrimidine dimers (CPDs) and 6-4 photoproducts (6-4PPs) (Setlow *et al.,* 1993; Douki *et al.,* 2003; Besaratinia *et al.,* 2004; Pfeifer *et al.,* 2005), leading to genetic transitions.

UVA radiation is not significantly absorbed by DNA but it predominately induces the formation of reactive oxygen species (ROS) (Wittgen and Kempen, 2007; Beissert and Loser, 2008; Kappes *et al*., 2006). ROS are able to cause DNA damage, which can cause mutations, single strand breaks (SSBs) or double strand breaks (DSBs) in cellular DNA molecules (Wehner *et al.,* 1995; Folkard *et al.,* 2002). One of the most described UVA induced photoproduct in human skin is 8-oxo-7,8-dihydro-2'-deoxyguanosine (8oxoG) (Mouret *et al.,* 2006) (table 1).

Type of ultraviolet radiation	UVB (direct DNA damage)	UVA (indirect DNA damage)
DNA damage	Cyclobutyl pyrimide dimers (CPDs): -TT dimers -TC/CT dimers -CC dimers Pyrimidine-pyrimidone 6-4 photoproducts (6-4PPs)	Single strand breaks (SSBs) Double strand breaks (DSBs) 7,8-dihydro-8-oxo-2′-deoxyguanosine (8oxoG) 8-oxo-Adenin (8oxoA)
Some consequence of DNA damage	C-T or CC-TT transitions	T-G transversions

Table 1. DNA damage and consequence of DNA damage induced by UVB and UVA radiation.

1.3 Reactive oxygen species

Reactive oxygen species (ROS) are chemically reactive molecules, which are derived from oxygen (O_2) such as super oxide anions, hydroxyl radicals and peroxides (Poillet-Perez *et al.,* 2014). They can be formed endogenously by mitochondria via the electron transport chain and during mitochondrial dysfunction (Liemburg-Apers *et al.,* 2015) and additionally through nicotinamide adenine dinucleotide phosphate (NADPH) oxidase enzymes (NOX) and uncoupling of nitric oxide syntheses (NOS) (Liu-Smith *et al.,* 2014). Furthermore, ionizing radiation (IR), ultraviolet radiation (UV) and visible light are exogenous sources of ROS (Jalal *et al.,* 2014).

Detoxification of ROS is mediated by a number of defence mechanisms to achieve a balance between the production and the removal of ROS. An imbalance towards the pro-oxidative state is often referred to as “oxidative stress”.

Mechanisms of ROS detoxification are:

1. Enzymatic defence system against ROS, which is catalyzed by super oxide dismutase (SOD) and glutathione peroxidase.

2. Non Enzymatic defence systems against ROS are induced by antioxidant agents such as glutathione, vitamin C (ascorbic acid) and vitamin E (α-tocopherol) or Trolox (Khalid R, 2007).

ROS is able to cause nuclear and mitochondria DNA damage, additionally, ROS is involved in tumor progression, migration and invasion (Poillet-Perez *et al.,* 2014; Luanpitpong *et al.,* 2010). A study performed in melanoma cells showed that over stimulation of NOX enzyme, especially NOX1 enzyme, led to the enhancement in the expression of matrix metalloproteinase 9 (MMP9) and matrix metalloproteinase 2 (MMP2) and enhanced invasion *in vitro* (Liu *et al*., 2012).

1.4 DNA damage repair

Proper function and survival of all organisms depends on genome maintenance. A constant DNA damage from genotoxic agents is challenging several repair mechanisms for genome integrity. Besides, DNA damage can also occur during DNA replication, such as nucleotide misincorporation (Lindahl *et al.,* 1993; Jackson *et al.,* 2010).

Human cells counteract these threatening lesions by several efficient systems, which participate to detect DNA damage and mediate its repair such as base excision repair (BER), nucleotide excision repair (NER), mismatch repair, DNA strand repair mechanisms (non homologous end joining (NHEJ) and homologous recombination (HR)) (Zhang *et al.,* 2009).

Failure or incorrect repair of DNA lesions blocks genome replication and transcription, leading to mutations or different genomic aberrations that threaten cell functions and organisms viability. There are several diseases caused by DNA damage in humans, such as cancers and genetically inherited disorders (Hoeijmakers, 2001; Peltomaki *et al*., 2001), which are caused by defects in the DNA repair system, like in Xeroderma pigmentosum (XP) disease.

1.5 Oxidative stress and mtDNA mutagenesis caused by UV radiation

Mitochondrial DNA (mtDNA) consists of circular double stranded DNA, which has 16.5 kilobases (kb)s. The mitochondrial genome has 37 codes for the genes, which are important for normal mitochondrial function (Taanman, 1999), coding for 13 polypeptide genes provide protein instructions for complex I, III, IIII and IIIII, which

are involved in oxidative phosphorylation and the remaining genes code for transfer RNA (tRNA) and ribosomal RNA (rRNA), which are necessary for protein synthesis.
Histones in the nuclear DNA are necessary for nuclear packing and act against genetoxic events. Therefore, a lack of histone proteins in mitochondria can cause high rates of mtDNA mutagenesis, which is nearly 10 fold increased in mitochondrial DNA compared to nuclear DNA (nDNA) (Ballard and Whitlock, 2004; Tatarenkov and Avise, 2007).
As a major environmental factor, solar UV irradiation induces oxidative stress, which promotes mtDNA mutations through ROS, like mtDNA common deletion (Berneburg *et al*., 1997; Berneburg *et al*., 2004; Kaneko *et al.,* 2012). Therefore, mutation of mtDNA probably serves as a biomarker for cumulative UV radiation exposure and it has been shown, that mtDNA mutation is correlated with photoaging rather than chronological aging (Birch-Machin *et al*., 1998; Gendron *et al*., 2012) and UVA induced mtDNA mutation can persist even for more than 1.5 year (Berneburg *et al*., 2004).
The role of mutated mtDNA in the different tumors and in the different stages still is discussed controversially.

1.6 Common deletion of melanoma mtDNA

One of the best documented common mutation in mitochondrial DNA (mtDNA) molecules is a 4977bp deletion, which is also known as common deletion (Kamenish *et al*., 2006), normally correlated with the aging process or found in diseases, especially in premature skin aging (photoaging), which is associated with UV radiation (Berneburg *et al*., 2000) and cancer.
Various studies reported higher frequency of mtDNA common deletion in sunexposed sites, compared to sunprotected sites, in normal aged skin (Pang *et al*., 1994; Berneburg *et al*., 1997; Birch-Machin *et al*., 1998).
High metabolic activity and low proliferation rate in the tissues like heart, brain and muscle, accelerate the accumulation of mtDNA common deletion in contrast to fetal and young tissues (Cortopassi and Arnheim, 1990; Wallace *et al*., 1992; Bogliolo *et al*., 1999). As mtDNA mutations are important issues in carcinogenesis (Eshaghian *et al*., 2006), the frequency of mtDNA common deletion was investigated in various carcinomas. While some publications have found no changes in mtDNA mutation, others showed change in the frequency of mtDNA mutation in different tumors, in

breast cancer, gastric cancer, prostate cancer, colon carcinoma and head and neck cancer the frequency of mtDNA common deletion are compared with normal tissue, which are almost reduced or absent (Heerdt and Augenlicht, 1990; Fukushima *et al*., 1995; Habano *et al*., 1998, 1999; Kotake *et al.,* 1999; Shieh *et al*., 2004; Dani *et al*., 2004), furthermore, in some tumors for example in oral cancer and colorectal cancer it has been shown that the frequency of deleted mtDNA is declining proportionally during disease progression (Shieh *et al*., 2004; Chen *et al.,* 2011).

Up to now, there is a critical discussion about the level of mtDNA common deletion, which was found in different carcinomas.

It is known that UVA radiation induces skin tumors and it can also induce mtDNA common deletion (Berneburg *et al.,* 1999). In this context, it was important to investigate the mtDNA common deletion in skin cancer.

This was partially investigated in non melanoma skin cancer or in squamous cell carcinoma (SCC) and basal cell carcinoma (BCC). Previous work of our group showed a tendency of decreased in the level of mtDNA common deletion in (SCC) and (BCC) compared to surrounding tissues of these tumors (Kamenisch *et al*., 2007).

It has been reported in normal skin (non tumor) tissue of melanoma patients, that the level of mtDNA common deletion was associated with pigmentation of melanoma cells (Hubbard *et al.,* 2008).

1.7 Induction of melanoma by UV in different models

While it is clear, that UV radiation is one of the risk factor of squamous cell carcinoma (SCC) and basal cell carcinoma (BCC) (Ramos J *et al.,* 2006) so far, the role of UVA and UVB radiation is discussed controversially. Furthermore, the role of UVB and UVA radiation in melanoma carcinogenesis is not clear and since *in vivo* data are important to support the role of UV in the development and progression of malignant melanoma, currently there are some studies on the formation of melanoma with and without UV radiation exposure in different animal models.

1.7.1 Induction of melanoma without UV radiation

There are animal models that develop melanomas without exposure to UV radiation, or due to other reason rather than UV radiation. In mammalian animals, like in Sinclair swine, a main reason for melanoma is due to genetic hereditary factors, while

the histopathology of metastasizing process is well defined and similar to the human skin (Gomez-Raya *et al*., 2007).

In Camargue horses (gray skinned) melanoma can occur and the incidence rate of cutaneous melanomas tumors is high but it is significantly associated with age and 93.9% of tumors are located in non sun exposed regions (Fleury *et al*., 2000); therefore, development of melanoma is not related to solar irradiation.

Melanomas are described also in the Guinea pig and in the Syrian hamster models and these tumors are developed by the exposure to chemical carcinogen 7,12-dimethyl benz anthracene (DMBA) (Bardeesy *et al*., 2000) but not by exposure to UV irradiation alone, although UV can be able to enhance response to (DMBA).

1.7.2 Induction of melanoma with UV radiation

UV induces melanoma in Opossum (Monodelphis domestica) (Ley, 1991), when exposed to chronic sub-erythemal dose (Bardeesy *et al.,* 2000) but UVA alone was able to initiate melanocytic hyperplasia rather than malignant melanoma (Ley, 2001). However, opossum models are unsuitable to investigate, since the genetic pattern is poorly defined. Although difficulty to maintains this model limits the chance to use this model for genetic and immunologic study (Sabourin *et al*., 1992; Sherburn *et al*., 1998; Linan *et al.,* 2005), furthermore, melanomas are derived from the dermal layer and rarely are metastastic in contrast to the human malignant melanoma (Jhappen *et al*., 2003).

In non mammalian animals, like Xiphophorus fish, melanoma are developed either spontaneously or upon UV irradiation (Walter and Kazianis, 2001), furthermore, it was shown in a backcrossed hybrid Xiphophorus fish model, that both types of solar UV radiation, UVB (it mainly induces direct DNA damage) and UVA (it mainly induces indirect DNA damage) are capable to initiate melanoma (Mitchell *et al*., 2007). Using this model to investigate melanomagenesis is difficult, because there are wide differences, both phylogenetic and histologic in human skin compared to Xiphophorus fish.

Several years ago, different animal models were used to investigate the UV radiation as a causative factor for melanoma development. Recently, mice prominently are used to study melanomagenesis, because mouse genes are well described. But malignant melanomas are extremely rare in wild type mice and like other mammalian melanomas are derived from the dermis (not from the basal layer of the epidermis

like in human) because melanocytes are close to hair follicles and rarely metastasizes. Furthermore, there are only a few similarities in histopathology between mouse and human skin (Linanan *et al.,* 2005). Currently, different models of transgenic mice are available, which are providing pivotal insight in the role of a number of key pathways in melanomagenesis, which can facilitated transformation of melanocytes to neoplastic lesions. These models are: over expression of activated Rat sarcoma (RAS) genes, cyclin dependent kinase 4 genes (cCdk4) and receptor tyrosine kinase (RTK) genes or their ligands and inactivation of tumor protein (p53) gene or phosphatase and tensin homolog (PTEN), among others.

An early transgenic mouse model, which develop melanoma and shows UV radiation as reasonable cause is the transgenic mouse model for SV40 T-antigen described by (Kelsall and Mintz, 1998) and controlled by tyrosinase promoters (Bradl and Klein, 1991). Since these models suffered from different effects of the SV40 T-antigen, several problems may arise when analysing the relevant pathways.

One of the best-known transgenic mouse models, which is used for melanoma examination, is the hepatocyte growth factor/scatter factor (HGF/SF) mouse model, which will be described in detail in the next passage.

1.7.3 Hepatocyte growth factor/scatter factor (HGF/SF) mice

Recently, appropriate mouse models have been developed by Merlino and Colleagues (Marentt, 2000), in fact, all mouse models that have been mentioned before. In this model, the mouse is transgenic for a metallothionein (MET) gene promoter, which can be used to overexpress hepatocyte growth factor/scatter factor (HGF/SF). The c-Met is a multifunctional cytokine regulator, which is involved in different cellular behaviours that are related to tumorigenesis, like growth, motility and invasiveness (Comoglio and Boccaccio, 2001).

In human oncogenesis, irregularity of c-Met signaling or over expression of c-Met receptors has been implicated in cutaneous melanoma (Natali *et al.,* 1993; Jeffers *et al*., 1996).

The HGF/SF transgenic mouse is characterised by:

1- Akin to human melanocyte location, (HGF/SF) mouse melanocyte is localized in the epidermis or upper regions of the dermis and at the epidermal-dermal junction (Noonan *et al.,* 2001; Recio and Merlnio, 2002).

2- Histopathological appearance, stage progression and pathogenetic molecular aspect resemble human melanoma, which are induced by UV irradiation (Noonan *et al.,* 2001; Recio and Merlnio, 2002).

With this transgenic mouse model it has been shown that UVB has an effect in initiating cutaneous melanoma (De Fabo *et al.*, 2004), whereas UVA did not induce melanomas in a transgenic mouse model (HGF/SF) with an albino inbred background (De Fabo *et al.*, 2004; Noonan *et al.*, 2001).

Interestingly, later on it has been demonstrated in the mice transgenic for (HGF/SF) with pigment-inbred background, that irradiation with a single neonatal high dose of UVA (Noonan *et al.,* 2012) is capable to induce melanotic tumors (figure 4).

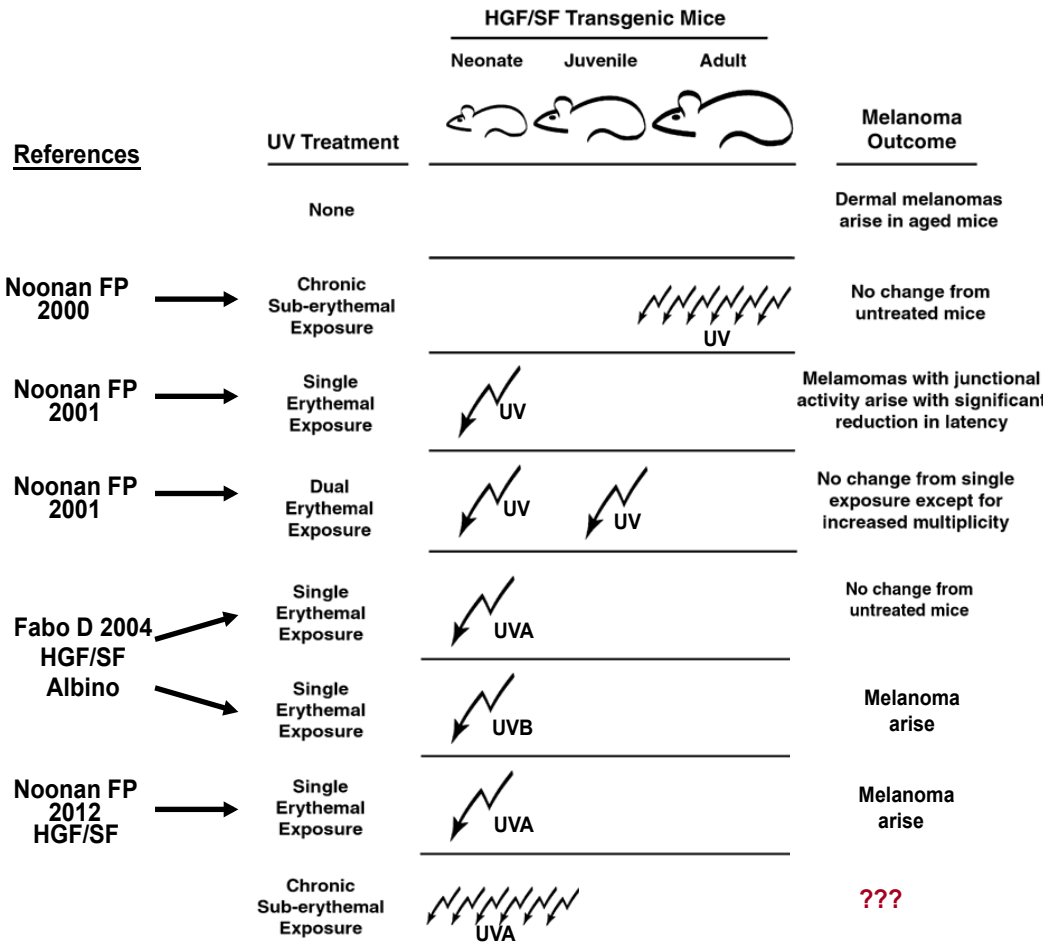

(Modified from Jhappen *et al.*, 2003)

Figure 4. UV influence on induction of melanoma in HGF/SF transgenic mice.

Melanoma in HGF/SF transgenic mice can be induced by UVB and UVA irradiation, but depends on type and dose of UV irradiation and on inbred background.

The latter study strongly supports the role of a single neonatal high dose of UVA radiation in the pathogenesis of melanoma. Furthermore, single neonatal UVA irradiation is mimicking sunburn reactions in childhood, but they do not mimic normal physiological UVA exposure, where humans are typically exposed to several low doses of solar UVA radiation.
These models show clearly that UVA as well as UVB are cancer-promoting agents and are capable to induce melanoma. Still the question on the role of UVA in progression of melanoma remains unanswered.

Two important points during progression of initial melanomas are invasion, which requires specific proteases and proliferation that requires specific metabolic demands, like the Warburg effect and increased transketolase activity.

2. Glycolysis and tumor metabolism

Glycolysis is an important metabolic pathway for energy production. It means conversion of glucose $C_6H_{12}O_6$ to pyruvate CH_3COCOO^- in the cytoplasm. The first step is the phosphorylation of glucose by hexokinase enzyme, which is a key enzyme of the glycolysis pathway. Through this pathway, cellular energy in the form of adenosine triphosphate (ATP) and reduced nicotinamide adenine dinucleotide (NADH) are produced. Furthermore, pyruvate can be metabolized by two different pathways that are described in the next passage (Alfarouk *et al.,* 2014) (figure 5 and 6).

2.1.1 Decarboxylation of pyruvate

Preferably under aerobic condition, in this pathway pyruvate is degraded to acetyl-CoA, and then enters the citric acid cycle, which occurs in the mitochondria matrix. Multiple enzymes are involved in completely oxidizing acetyl-CoA into carbon dioxide and a reducing agent NADH.
NADH participates in oxidative phosphorylation, there it is oxidized to NAD^+ and the electrons of NADH are transferred to an electron acceptor (oxygen O_2 molecule) in the electron transport chain. The energy achieved in this process is stored in the proton gradient and used to produce ATP via the ATP synthase.

Moreover, the TCA cycle provides intermediate components, which are used as precursors for the biosynthesis of other molecules such as fatty acids and different amino acids (Lunt and Vander Heiden, 2011), the total cellular energy produced from 1 mole of glucose is about 36 moles of ATP (figure 5).

2.1.2 Anaerobic glycolysis

Under hypoxic conditions, resting cells for energy production turn to anaerobic glycolysis instead of oxidative phosphorylation, because insufficient amount of O_2 limits ATP synthesis by the electron transport chain inside the mitochondria.

In the cytoplasm, pyruvate is converted to lactate by lactate dehydrogenase enzyme (LDH) and in this process NADH is convert to NAD+, which is needed in glycolysis and also is involved in the continuous glucose flux through glycolysis by glyceraldehyde 3 phosphate to 1,3 bisphosphoglycerate transformation (Hamanaka and Chandel, 2012). Anaerobic glycolysis typically is seen in excess in skeletal muscles, when sufficient amount of oxygen is not available and in erythrocytes because they lack mitochondria. From 1 moles of glucose only 2 moles of ATP are generated (figure 5).

2.1.3 Aerobic glycolysis or Warburg effect

Many tumor cells prefer aerobic glycolysis for energy production, even if adequate amounts of O_2 are present, this phenomenon is known as Warburg effect. It was discovered more than 80 years ago by Otto Heinrich Warburg (1883–1970), a German scientist, who laureate the Nobel prize in physiology (1931) for the discovery of the nature and mode of action of the respiratory enzyme.

In oncology, Warburg focused on the metabolism and the respiration of cancer cells. He describes the metabolic preference of proliferating cells, as well as tumor cells, using high rate of glycolysis, followed by lactic acid fermentation in the cytosol for energy production, which is known as aerobic glycolysis (figure 5). Compared to the lower rate of glycolysis and subsequent oxidation of pyruvate in the mitochondria, as it occurs in resting cells. He assumed, that cancer is caused by dysfunctionality of the mitochondrial metabolism (Warburg, 1956). Meanwhile, different studies have shown the functionality of mitochondria (Frezza and Gottlieb, 2009) and the phenomenon of aerobic glycolysis would be only the metabolic demand of proliferative cells, such as tumor cells, which is necessary for their growth and proliferation, since they require

more metabolites in demand for nucleotide, lipid and amino acid formation (Zu and Guppy, 2004).

Nowadays, the Warburg effect phenomenon is used in clinical diagnosis; a glucose analogue, such as fludeoxyglucose (^{18}F) is used and detected by positron emission tomography, because fludeoxyglucose (^{18}F) is taken up by high glucose consuming cells, like tumor cells (Gambhir, 2002).

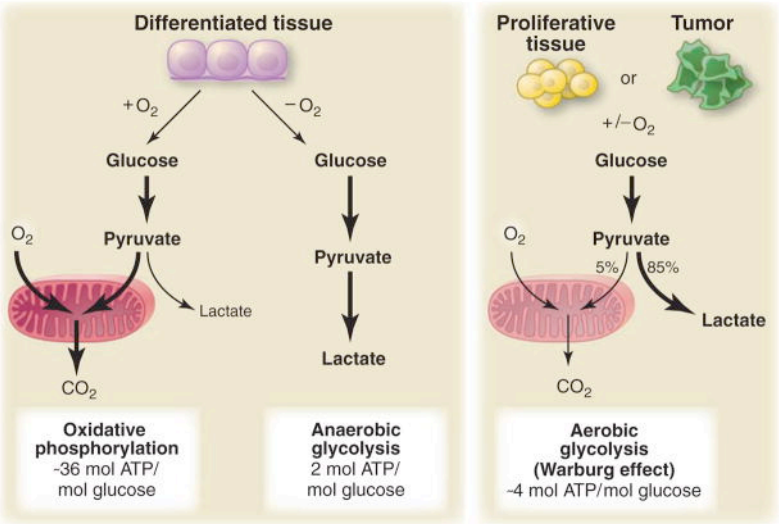

(Vander Heiden *et al.,* 2009)

Figure 5. Glucose metabolism in normal and tumor cells.

2.2 Tumor metabolism and pentose phosphate pathway

Pentose phosphate pathway is the metabolic pathway occurring in the cytoplasm and generating NADPH and ribose sugars. NADPH acts as a reducing equivalent in the biosynthesis of lipids, nucleotides and amino acids. Pentose (5 carbon atoms) sugars are important for nucleotides and nucleic acid synthesis.

The pentose phosphate pathway generally consists of 2 phases (Patra and Hay 2014):

2.2.1 Oxidative phase: Glucose 6-phosphate is converted to ribulose 5-phosphate and $NADP^+$ is reduced to NADPH (figure 6).

Reaction: glucose 6-phosphate + 2 $NADP^+$ + H_2O

↓

ribulose 5-phosphate + 2 NADPH + 2 H^+ + CO_2

2.2.2 Non-oxidative phase: from ribulose 5-phosphate, ribose-5-phosphate and intermediate glycolysis compounds are generated to fuel the glycolysis pathway (figure 6).

Reaction: 3 ribulose-5-phosphate

↓

1 ribose-5-phosphate + 2 xylulose-5-phosphate

↓

2 fructose-6-phosphate + glyceraldehyde-3-phosphate

2.2.3 Transketolase like 1 enzyme

Transketolase like 1 (TKTL1), an isoenzyme of the transketolase (Schenk *et al.,* 1998), is a key enzyme of the pentose phosphate pathway (Berthon *et al.*, 1992), as mentioned before it provide cells with components that are crucial for proliferation, survival and nucleotide synthesis in the non oxidative phase of the pentose phosphate pathway, like ribose sugar (Koolman and Röhm *et al.,* 1998) (figure 6).

An increase in TKTL1 is another metabolic change, found in many tumor cells including melanoma, which is therefore used as a tumor biomarker for highly proliferative cancers (Diaz-Moralli *et al.*, 2011; Langbein *et al.*, 2006) and as indicator for poor patient outcome (Lange *et al.,* 2012). It has been shown in melanoma, lymphoma and SCC (non melanoma skin cancer) that the expression of TKTL1 is increased compared to controls (Lange *et al.,* 2012) and in the SCC (non melanoma skin cancer), TKTL1 over expression significantly correlates with tumor thickness and the mitotic rate (Lange *et al.,* 2012). Furthermore, inhibition of TKTL1 decreases proliferation in the tumor cell (Du *et al.,* 2004; Yuen *et al.,* 2010). Expression of TKTL1 protein and glucose transporter 1 (GLUT1) both together was shown to be

indicative for a poor patient outcome in oral SCC (non melanoma skin cancer) (Grimm *et al.*, 2014).

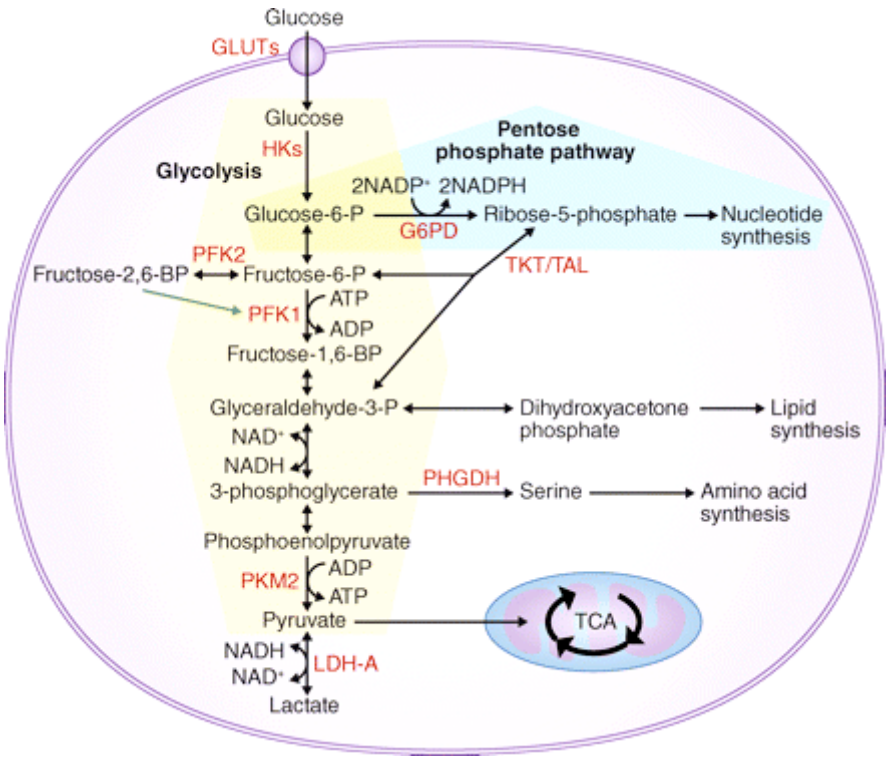

(Hamanaka and Chandel, 2012)

Figure 6. Glycolysis and pentose phosphate pathway.

3. Invasion of melanoma cells

Another important step in melanomagenesis is invasion, which requires specific proteases to invade adjacent tissue (figure 2).

3.1 Matrix metalloproteinases

Matrix metalloproteinases (MMPs) are zinc dependent endopeptidases and a most prominent family of extracellular proteinases (Gross and Lapiere, 1962).

Humans are expressing different types of MMPs in an enzymatically inactive state, which are called proenzymes. When these substrates convert into an active proteolytic enzyme, they are capable to degrade all kinds of extracellular matrix

proteins (Sternlicht and Werb, 2001). MMPs can be inhibited endogenously by tissue inhibitor of metalloproteinases (TIMPs).

MMPs are playing a role in several physiological process, like cell proliferation, differentiation, angiogenesis, migration and apoptosis (Egeblad and Werb, 2002; Page-McCaw *et al*., 2007; Kessenbroc *et al.,* 2011).

In tumorigenesis, MMPs are an outstanding family of proteinases and changes in protolysis homeostasis are important for tissue invasion and metastasis (Liotta *et al.,* 1980).

In vivo MMP activity can be detected by using a radiolabel inhibitor of MMP like 18F-MMP and 123I-MMP inhibitors by PET and SPECT, that accumulates in the tumor (Furumoto *et al.,* 2003; Schafers *et al.,* 2004).

Several investigations have shown in humans, that MMPs are expressed in the tumor and the tumor-associated stromal tissue in different carcinomas (Löffek *et al.,* 2005) and increased level of activated MMP2 is associated with malignant progression in brain tumours (Yamamoto *et al.,* 1996), lung tumor (Tokuraku *et al*., 1995), gastric carcinomas (Nomura et al, 1995) and in melanoma (Hoffman *et al.,* 1999; Redondo *et al.,* 2005). Furthermore, previous studies strongly implicate an important role of activated MMP2 in melanoma progression.

Studies on MMP1 expression also showed that it could be expressed by tumor periphery in advanced melanomas (Airola *et al.,* 1999).

UV irradiation induces over expression of MMP1 and MMP10 in a SCC (non melanoma skin cancer) (Ramos *et al.,* 2005). UV irradiation promotes melanoma progression through MMP9 activation (Shellman *et al.,* 2006) and by MMP9-siRNA treatment, migration and invasion are significantly inhibited both in *in vitro* and *in vivo* (Tang *et al*., 2013).

3.2 Urokinase plasminogen activator

Urokinase plasminogen activator (uPA) is another protease, which is involved in thrombolysis and the degradation of extracellular matrix proteins. It has been shown that the over expression of urokinase, correlates with tumor malignancy, as it facilitates invasion and the process of metastasis (Keleg S *et al.,* 2003).

Particularly, it was shown that uPA and MMP9 are activated in IFNgamma/TNFalpha-stimulated cells during invasion of melanoma cells (Bianchini *et al*., 2006).

4. Cell signaling and metabolism in melanoma

Signal transduction pathways are necessary in normal cellular processes to transfer signals between extracellular and intracellular cell stimuli, which are most often achieved by protein kinases and its transcription factors. In cancer cells signal transduction pathways are often deregulated (Giancotti FG, 2014). Deregulation in signaling pathways is important for understanding melanoma development and progression.

One of the major environment factors, which can trigger development of melanoma, is UV radiation, by inducing genetic and epigenetic alterations (Katiyar SK *et al.,* 2012).

Major signaling pathways, which are involved in human melanoma pathogenesis, are MAPK/ERK (mitogen activated protein kinases/extracellular signal regulated kinases) and PI3K/AKT/mTOR (phosphoinositide 3 kinase/AKT/mammalian target of rapamycin) pathways, which promote proliferation, survival, angiogenesis and invasion of melanoma (Yajima *et al.,* 2012), these pathways will be explained in detail in (figure 7).

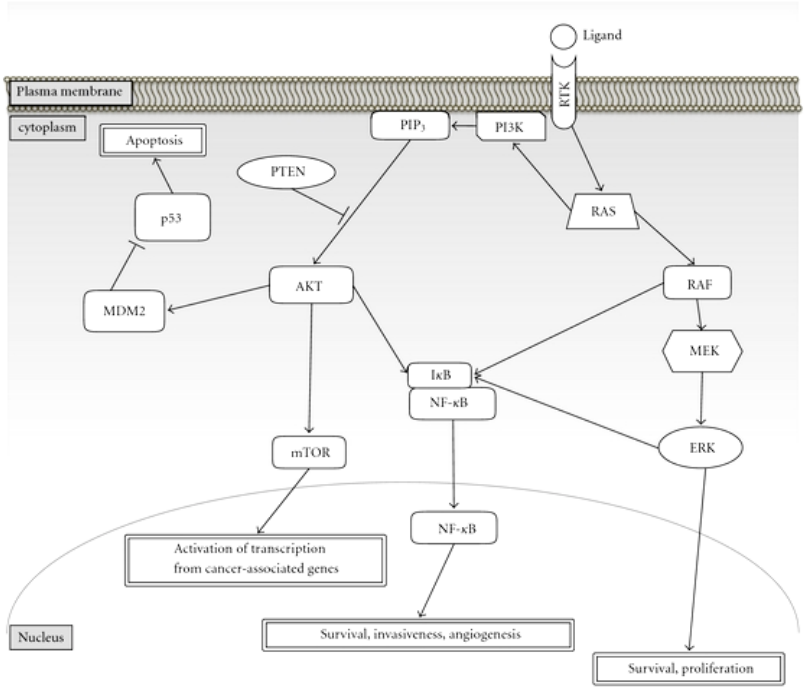

(Yajima *et al.,* 2012)

Figure 7. Melanoma signaling pathway affects development and progression.

4.1 MAPK pathway in melanoma

A common pathway which is activated during melanoma progression is the MAPK pathway (Goodall J, 2004), this pathway is usually activated through receptor tyrosine kinases (RTK) and then the signal is transferred to RAS proteins, like HRAS, KRAS, and NRAS, which then activate RAF proteins, like ARAF, BRAF and CRAF, subsequently activating MEK and ERK proteins and finally resulting in activation of transcription in the nucleus (figure 7).

Deregulation or permanent activation of the MAPK pathway plays an important role in tumorigenesis of multiple human cancers such as prostate, breast, bladder, lung cancer, as well as melanoma (Inamdar *et al.,* 2010). High mutation rates of MAPK pathway genes have been reported for the NRAS, BRAF and ERK genes and mutation rates for these genes are about 15-30%, 50-70% and 90% in human cancer (Davies *et al.,* 2002; Cohen *et al.,* 2002).

4.2 PI3K pathway in melanoma

Another signaling cascade of malignant melanoma, which is implicated in initiation, proliferation, progression and invasion via induction of cell survival cascades and inhibition of apoptosis cascades, is PI3K/AKT/mTOR signaling (Bunney and Katan, 2010; Majewski e*t al.,* 2004). When PI3K protein is activated, it phosphorylates Akt protein kinase, which leads to the activation of Akt and mTOR. Interestingly, Akt phosphorylation at serine 473 is present in the majority of immunohistologically-investigated melanomas (Dhawan *et al.*, 2002) (Baban *et al*., in press) and activation of Akt is dramatically increased with melanoma progression (Dai *et al.,* 2005) (figure 7). It was shown, that over activation of AKT may be able to transform radial growth melanoma (RGP) to vertical growth melanoma (VGP) and thus, an overexpression of Akt increases the production of ROS and induces more glycolytic metabolism (Govindarajan *et al.,* 2007).

Additionally, it has been shown that increased glycolysis and overexpression of TKTL1 is associated with the activation of Akt (Volker *et al.,* 2008) (Baban *et al*., in press).

4.3 UVA irradiation induces cell signaling

UV radiation is able to induce many cell signaling pathways and most of these pathways are involved in induction of skin carcinogenesis, originating at cytoplasmic membrane receptors (Zhang *et al.,* 2001), such as epidermal growth factor receptor (EGFR). UVA for example, is able to induce tyrosine phosphorylation of EGFR without ligand binding (dependant or independent) but it depends on the type of UV and the subsequent dose (Kneble *et al.*, 1996).

It has been shown, that an EGFR overexpression correlates with tumor progression (Correia *et al.,* 2014) in many tumors, especially in head and neck, ovarian, cervical, bladder and oesophageal cancers (Nicholson *et al.,* 2001). Furthermore, several chemotherapeutic treatments, that are targeting EGFR tyrosine kinase, are used clinically to decrease cancer proliferation, invasion and metastasis by tyrosine kinase inhibitors (Noonberg and Benz, 2001).

After EGFR activation upon UVA irradiation, the signal is transferred to downstream ribosomal protein S6 kinases, p70 (S6K) and p90 (RSK) via PI3K and ERKs and EGFR(-/-) cells have the same effect like the one achieved with tyrosine kinase inhibitors (AG1478 and PD153035) (Zhang *et al.*, 2001).

4.4 Hypoxia-inducible factor 1 upregulation in melanoma

The Hypoxia-inducible factor 1 alpha (HIF1α) is a transcription factor that mediates transcriptional responses upon hypoxia by activating the transcription of different target genes, which are associated with glycolysis and have a role in various cellular processes in a hypoxic microenvironment (figure 8) (Demaria *et al.,* 2010).

The overexpression of hypoxia-inducible factor 1 (HIF1) in many tumors, such as head and neck cancer, cervical cancer and renal cell carcinoma induced by hypoxia, is associated with tumor progression (Kuphal *et al.,* 2010). In contrast to other tumors, it has been shown that in malignant melanoma even in normoxic condition, HIF1 activity is increased, due to constitutive HIF1α activation that is regulated by ROS (Kuphal *et al.,* 2010).

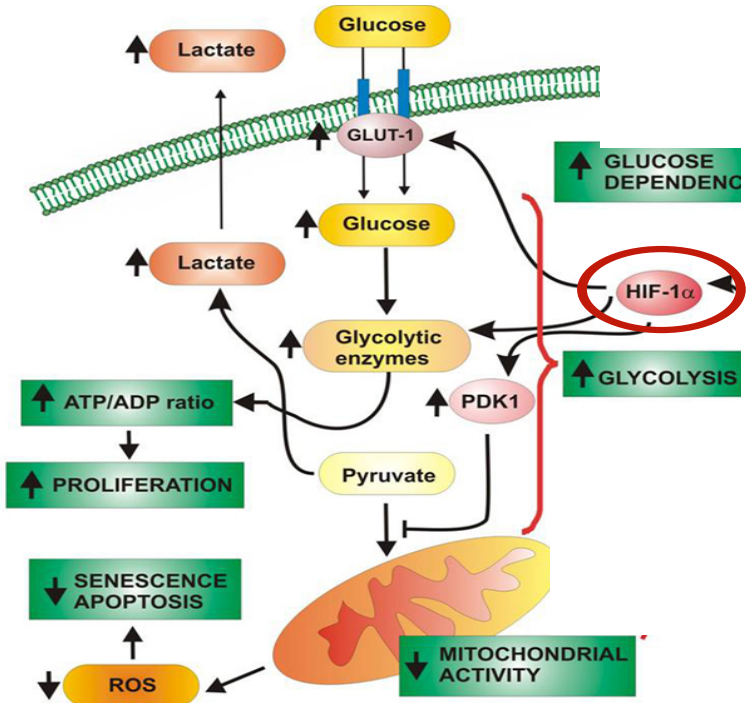

(modified from Demaria *et al.,* figure 8, 2010)

Figure 8. HIF1α influence on the transcription of different genes.

ROS, which can occur from damage or deregulation of mitochondria in hypoxic condition (Comito *et al.,* 2011) and upon UV radiation in normoxic condition is able to upregulate HIF1α protein (Gidanian *et al.,* 2008).

Activation of HIF1 is important for cancer development and progression, meanwhile data have shown, that treating melanoma cells with an antioxidant (ROS quencher) was able to decrease HIF1α protein expression and HIF1 activity (Kuphal *et al.,* 2010). Inactivation of HIF1α leads to the reduction of pyruvate dehydrogenase kinase 3 (PDK3) expression, which induces transport of pyruvate to the mitochondria.

Subsequently, melanoma metabolism drives toward oxidative phosphorylation, instead of aerobic glycolysis and thus, glycolysis rate decreases (Kluza *et al.,* 2012) (figure 8).

4.5 Poly ADP ribose polymerase 1

Poly ADP ribose polymerase 1 (PARP1) or NAD+ ADP- ribosyl transferase 1 is an enzyme which has a role in DNA damage signaling, in mediating basal excision repair and DNA strand break repair (Godon C *et al.,* 2008). Furthermore, it is important for differentiation, proliferation and tumor transformation (Rojo *et al.,* 2012; Wang *et al.,* 2015). For PARP synthesis, NAD+ is required as substrate and during PARP overactivation cells require more NAD+, subsequently inducing a progressive ATP depletion. PARP activation can be induced in ssDNA damage, like upon exposure to radiation (figure 9).

Overexpression of PARP1 is associated with cutaneous malignant melanoma progression, since it is highly expressed in advanced stage of melanoma and correlates with melanoma thickness (Csete *et al.,* 2008; Staibano *et al.,* 2005).

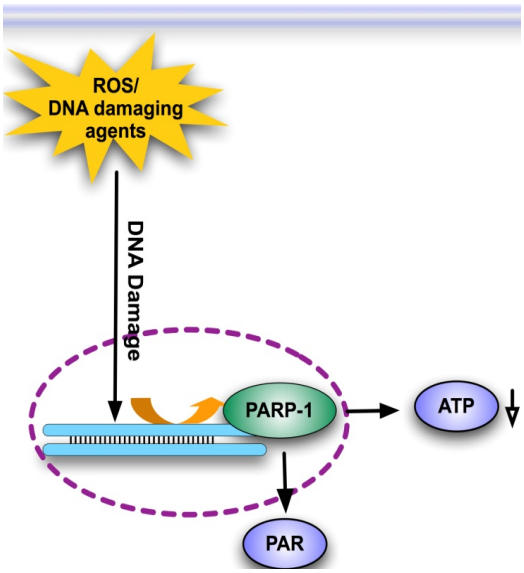

(Modified from Huang and Shen figure 2., 2009)

Figure 9. PARP1 overactivation under the condition of oxidative stress increases ATP consumption.

5. Purpose of this work

Previous literature showed that UVA radiation has physiologic relevance and is capable to induce melanoma in animals. The role of UVA radiation in melanoma progression in humans is not clear, thus the aim of our project was to investigate:

5.1 Role of UVA irradiation in melanoma metabolism and progression

It remains unclear if UVA radiation of initial melanoma is able to induce progression of melanoma cells. To investigate this, we irradiated cell lines of initial melanomas (IM) and metastasizing melanomas (MM) with chronic sublethal doses of UVA. The effect of UVA irradiation on glucose consumption, lactate production, different metabolites, transketolase activity, Akt expression, MMP and uPA transcriptional activity and invasive potential were determined.

We investigated UVA dependent influence in glucose uptake and in lactate production, which was partially mediated by UVA induced ROS. This UVA induced and ROS mediated enhanced lactate production leads to the change of MMPs and uPA transcription and finally it influenced invasiveness of the UVA treated melanoma cells, which was shown in *in vitro* invasion assay and in skin reconstructs. Additionally, we analyzed the influence of UVA on different metabolic pathways, like pentose phosphate pathway, TCA cycle, and lipid metabolism because most of the proliferating tumor like melanoma have a metabolic demand for progression. This work was done *in vitro,* in melanoma cells, together with a cooperation partner, specialized on investigation of metabolites with NMR spectroscopy (Prof Gronwald, University of Regensburg).

To interfere with UVA induced metabolic changes and to investigate the mediators of the persistence of these effects, it is important to identify cellular signaling cascades, which facilitate UVA induced Warburg effect as a potential target for anticancer therapies. As it is known, that UV irradiation has an effect on EGFR and IGFR signaling we started to investigate EGFR and IGFR signaling. First results showed change in the internalization rate of EGFR and IGFR upon UVA irradiation, compared to unirradiated samples, pointing to an UVA effect on these two receptors.

5.2 Role of mtDNA mutations in progression and invasion of melanoma cells

Mitochondria play a pivotal role in metabolism and their role in carcinogenesis in the context of the Warburg effect is of actual interest. Although the need for mitochondrial ATP generation could be decreased in tumor cells, mitochondrial metabolism is still needed for anabolic processes like amino acid synthesis (Wallace *et al.,* 2005). We found, that UVA radiation induces Warburg effect but on the other hand has mutagenic effects on mtDNA in human keratinocytes and fibroblasts (Berneburg *et al.,* 1999). If these deletions accumulate, they can disturb the mitochondrial metabolism. UVA radiation is known to induce large scale deletions in mtDNA, the so called common deletion, which are considered as marker deletions for UVA exposure.

To investigate the role of mtDNA 4977bp deletions and UVA exposure in human melanoma, the level of common deletion of melanoma tissue and control epidermal tissue from the same patient was analyzed from microdissected histological samples in cooperation with Prof. Röcken (Department of Dermatology, University of Tuebingen) and Prof. Seeger (Department of Gynecology, University of Tuebingen). We found that, the normalized level of mtDNA 4977bp deletion is different in normal nevi, dysplastic nevi and during progression of melanoma. These findings support the importance of functional mtDNA during carcinogenesis. Interestingly, the alteration of mtDNA 4977bp deletion level during carcinogenesis points to possible selection mechanisms during these process.

C. Material and methods

1. Material

1.1 Devices

Devices	Model	Company
Centrifuge	Biofuge pico; Biofuge fresco/ Heraeus, Multifuge 3S-R	Thermo Waltham/ Dreieich, Hanau
Clean bench	Hera Safe KS 18	Heraeus, Frotscher
Electrophoresis chamber	Power Pac Basic, Power Pac 300	BioRad, Munich
ELISA reader	Multiscan Ex	Thermo, Waltham
FACS	BD FACS Calibur	BD bioscience, Heidelberg
FACS sorter	BD FACS Aria-cell sorter	BD bioscience, Heidelberg
Fluorescence reader	Tristar LB 941	Berthold technology, Bad Wildbad
Gel-documentation, UV transilluminator	RH-5.1 darkroom hood, easy 442K camera	Herolab, Wiesloch
Gel-electrophoresis apparatus	Protean II, modell 45-2020i	BioRad, Munich
Heating block mixer	Thermomixer comfort LS2	LS2 Eppendorf, Hamburg
Incubator	Heracell 240	Thermal/Kendro Dreieich/Hanau
Laser capture microdissection apparatus	Pix Cell IIe	Arcturus engineering Inc.; Mountain view, California
Microscope	Axiovert25 Invers, Axiovert200 fluorescence, HBO100	Zeiss, Jena
PCR-Machine	Primus 96 plus	MWG Biotech, Ebersberg
pH-meter	CG842	Schott, Wertheim
Photometer	Bio photometer 6131	Eppendorf, Hamburg
Pipet aid	Pipette boy	Hirschman, Eberstadt
Pipettes	Research, Reference	Eppendorf, Hamburg
Real time PCR machine	Light Cycler®480/iCycler	Roche, Mannheim/ BioRad, Munich
Rotary table	KDE 015	MTE, Weinstadt-Endersbach/ UKT, Tuebingen
Sonifier	Sonoplus HD2070	Bandelin, Berlin
Wb transfer system	Trans blot turbo	BioRad, Munich

UVA lamp	Sellasol 1200	Sellas, Gevelsberg
Vortexer	Reax top	Heidolph, Kelheim
Water bath	WB22 funke	Medingen, Freital
X-ray film processor	Optima mammo X-ray film processor	Rontgen Bender

Table 2. Device manufacturer.

1.2 Kits

Kits	Company
BCA protein assay	Pierce, Rockford
GO glucose assay	Sigma, Deisenhofer
iScript cDNA synthesis	BioRad, Munich
Lactate reagent	Trinity biotech, Wicklow
Novex zymogram gelatine gel	Life technologies, Darmstadt
Nucleospin RNA II	Macherey-nagel, Duren
QIAamp DNA-mini	Qiagen, Hilden
QCM™ Matrix 24 well invasion assay	Millipore, Billerica
Sso Fast EvaGreen Supermix	BioRad, Munich
uPA ELISA kit antibody	Abcam, Cambridge

Table 3. Used kits with it source.

1.3 Antibodies

Antibodies	Catalog number	Manufacture
Anti glucose transporter GLUT1	ab652	Abcam, Cambridge
Anti MMP9 antibody	ab38898	Abcam, Cambridge
Anti urokinase antibody	ab24121	Abcam, Cambridge
APC anti human EGFR	352905	Biolegend, San Diego
β actin (8H10D10) mouse mAb	3700S	Cell signalling technology
GAPDH (14C10)	2118	Cell signalling technology
pADPr (10)	sc-56198	Santa cruz biotechnology
Phospho Akt (Ser473)	9271	Cell signalling technology
Phospho EGF receptor	3777	Cell signalling technology

Purified mouse anti-human HIF1α	610958	BD bioscience, Heidelberg
Anti S100 antibody	Z0311	Dako, Germany

Table 4. Primary antibodies used for western blot and FACS.

1.4 Primer

1.4.1 DNA repair gene primer

Primer	Annealing temperature °C	Sequence	Company
ATM	46	AAGTGAAAACTTATTGGGAAAACAG TTGCTGGCTCATGTAACGTC	Biomers
ATR	51	CGCTGAACTGTACGTGGAAA CAATTAGTGCCTGGTGAACATC	Biomers
BAX	60	CATGGAGCTGCAGAGGATGAT TTGCCGTCAGAAAACATGTCA	Eurofins MWG Operon
BCL2	60	GGCTGGGATGCCTTTGTG GCCAGGAGAAATCAAACAGAGG	Eurofins MWG Operon
BRCA1	52	ATCATTCACCCTTGGCACA CATGGAAGCCATTGTCCTCT	Biomers
BRCA2	52	ACATGCCCACAGGGTGTC CACATCTGCCCAATTGCAT	Biomers
ERCC1	50	GAAATTTGTGATCCCCTCGAC GATCGGAATAAGGGCTTGG	Biomers
CHK2	52	AAGCCAGAGAATGTTTTACTGTCA CTTGGAGTGCCCAAAATCAG	Biomers
HR23A	50	GTCACCATCACGCTCAAAAC CTTCTCCTTTAGCACCTTCACC	Biomers
HR23B	50	GCAGCAACTACGACAGCAAC CTGAGGCTGATTCCGTAAAAA	Biomers
MDM2	52	CCATGATCTACAGGAACTTGGTAGTA TCACTCACAGATGTACCTGAGTCC	Biomers
P21	52	TCACTGTCTTGTACCCTTGTGC GGCGTTTGGAGTGGTAGAAA	Biomers
P53	60	CCCAGCCAAAGAAGAAACCA GTTCCAAGGCCTCATTCAGCT	Eurofins MWGOperon
PARP1	54	CTTGCTGCTTGTTGAAGAT AGGCTGCTTTGTCAAGAA	Biomers

XPA	46	GACACAGGAGGAGGCTTCATT TCGCATATTACATAATCAAATTCCATA	Biomers
XPB	50	ACTGGATGGAGCTGCAGAAT GGAGACATAGGGCACCAGAC	Biomers
XPC	60	GCCGAGACCTTGAGACCATA TCCATGTGTTTTGCCTGAAA	Biomers
XPD	50	TTGAGACCCGGGAGGATATT ATGCCATCAGGGACCACA	Biomers
XPE	50	CCCCTCAATTCAGATGGCTA GGTGAGGGTGCTATTGTTGG	Biomers
XPF	50	GAGGCAGAAAATGAGAGTGAA CATGTTCGGTCATCACTTGC	Biomers
XPG	50	CCAAGCGCAGAAGAACATTA TTAAGCAAGCCTTTGAGTTGG	Biomers

Table 5. Primer used for DNA repair gene analysis.

1.4.2 Protease gene primer

Primer	Annealing temperature °C	Sequence	Company
MMP1	54	CACCAAGGACAAGCACAG ACACAGTAGGCCAGGTCTCG	Biomers
MMP2	54	CCCCAAAACGGACAAAGAG CTTCAGCACAAACAGGTTGC	Biomers
MMP3	54	CAAAACATATTTCTTTGTAGAGAGGACAA TTCAGCTATTTGCTTGGGGAAA	Eurofins MWGOperon
MMP9	54	GAACCAATCTCACCGACAGG GCCACCCGAGTGTAACCATA	Biomers
MMP13	54	CCAGTCTCCGAGGAGAAACA AAAAACAGCTCCGCCGCATCAAC	Biomers
MMP15	54	ACGGTCGTTTTGTCTTTTCA GTCAGCGGCTGTGGGTAG	Biomers
TIMP1	54	TGGATAAACAGGGAAACACTG GATGGACTCTTGCACATCAT	Biomers
uPA	54	TTGCTCACCACAACGACATT GGCAGGCAGATGGTCTGTAT	Biomers

Table 6. Primer used for protease gene analysis. (Baban *et al.*, in press)

1.4.3 mtDNA common deletion and HIF1α primer

Primer (gene expression)	Annealing temperature °C	Sequence	Company
CD	54	ACC CCC ATA CTC CTT ACA CTA TTC AAG GTA TTC CTG CTA ATG CTA GGC	Biomers
HIF1α	54	GTTTACTAAAGGACAAGTCACC CTCCCTTCAACAAACAGAA	Biomers

Table 7. Common deletion and HIF1α primer.

1.4.4 House keeping gene primer

Primer	Annealing temperature °C	Sequence	Company
β actin	46-60	GCACCCAGCACAATGAAGA CGATCCACACGGAGTACTTG	Biomers
GAPDH	46-60	CACCAAGGACCAAGCAGACAG ACACAGTAGGCCAGGTCTCG	Biomers
IS	54	GAT TTG GGT ACC ACC CAA GTA T AAT ATT CAT GGT GGC TGG CAG TA	Biomers

Table 8. Primer used as house keeping genes.

1.5 List of Human melanoma cell lines

Cell line	Growth phase of melanoma	Abb.	Source
WM 35	Initial growth phase, radial growth phase	**IM**	Prof. Schittek, Department of Dermatology, Tuebingen
WM 1552c	Initial growth phase, radial growth phase	**IM**	Zentrum für Medizinische Forschung (ZMF),Tuebingen
WM 3211	Initial growth phase, radial growth phase	**IM**	Zentrum für Medizinische Forschung (ZMF),Tuebingen
Sbcl2	Initial growth phase,	**IM**	Prof. Schittek, Department

	radial growth phase		of Dermatology, Tuebingen
WM 115	Initial growth phase, vertical growth phase	**IM**	Prof. David Melton, Cancer research center, Edinburgh
WM 793	Initial growth phase, vertical growth phase	**IM**	Prof. Schittek, Department of Dermatology, Tuebingen
BLM	Advanced growth phase, metastasizing melanoma	**MM**	Prof. Schittek, Department of Dermatology, Tuebingen
WM 1205	Advanced growth phase, metastasizing melanoma	**MM**	Prof. Schittek, Department of Dermatology, Tuebingen
WM 451 LU	Advanced growth phase, metastasizing melanoma	**MM**	Prof. Schittek, Department of Dermatology, Tuebingen
WM 266-4	Advanced growth phase, metastasizing melanoma	**MM**	Prof. Bauer, Department of Dermatology, Tuebingen

(Baban *et al.,* in press)

Table 9. Human melanoma cell lines.

1.6 Chemicals

Chemical	Source
Acrylamide / Bisacrylamide (30% / 0.8%)	Roth, Karlsruhe
Agarose	Roth, Karlsruhe
Amiroride	Santa cruz biotechnology
Antibiotic-antimycotic solution	PAA, Pasching
Anthelios XL, LSF 50+, spray	La Roche-posay, Asnieres-Cedex
Bovine serum albumin	Sigma, Deisenhofen
Calcium chloride	Sigma, Deisenhofen
3-Cholamidopropyl-dimethylammonio-1-propansulfonate (CHAPS)	Sigma, Deisenhofen
2-Deoxy-D glucose	Sigma, Deisenhofen
D (-) Mannitol	Roth, Karlsruhe
Dntp Set, PCR grade	Qiagen, Hilden
Diglycine (Gly – Gly)	Fluka, Buchs
Dimethylsulfoxide (DMSO)	Sigma, Deisenhofen
Disodium hydrogen phosphate (Na2HPO4)	Fluka, Buchs
Dithionite	Fluka, Buchs
DPBS	Life technologies, Darmstadt

Dulbecco's phosphate buffered saline 1x (PBS)	PAA, Pasching Sigma, Steinheim
Dulbecco's modified eagle medium (DMEM), 1 g/l and 4.5 g/l glucose with glutamine	PAA, Pasching Sigma, Steinheim
Eosin y solution	Merck, Darmstadt
Ethanol 100%	Merck, Darmstadt
Ethylene diamine tetraacetic acid (EDTA)	Roth, Karlsruhe
Fetal bovine serum (FBS)	Thermo science, Waltham
Formaldehyde	Roth, Karlsruhe
Formalin	Roth, Karlsruhe
GelRed	Biotium, Hayward
Glycine	Roth, Karlsruhe
GM 6001	Santa cruz biotechnology
Marker 100bp plus DNA-leiter	Fermentas, St. Leon Rot
HBSS	Life technologies, Darmstadt
Haematoxylin	Dako, United State
Horseradish peroxidase (HRP)	Life technologies, Darmstadt
H_2O nuclease free	Qiagen, Hilden
Hydrochloric acid (HCl)	Sigma, Deisenhofen
Hydrogen peroxide (H_2O_2)	Roth, Karlsruhe
Potassium chloride (KCl)	Roth, Karlsruhe
Potassium dihydrogen phosphate (KH_2PO_4)	Roth, Karlsruhe
Potassium hydroxide (KOH)	Sigma, Deisenhofen
Protease inhibiter tablet	Roth, Karlsruhe
L (+) Lactic acid	Roth, Karlsruhe
Lithium-hydroxypyruvat	Roth, Karlsruhe
Magnesium chloride ($MgCl_2$)	Fluka, Buchs
Methanol	VWR, Darmstadt
Milk powder	DM, Karlsruhe
Novex sharp pre-stained protein standard	Life technologies, Darmstadt
Sodium carbonate (Na_2CO_3)	Roth, Karlsruhe
Sodium chloride (NaCl)	Merck, Darmstadt
Sodium dichloroacetate	Sigma, Deisenhofen
Sodium fluoride	Roth, Karlsruhe
Sodium hydrogen phosphate (Na_2HPO_3)	Sigma, Deisenhofen
Sodium hydroxide	Merck, Darmstadt
Sodium phosphate	Sigma, Deisenhofen
Sodium dodecyl sulphate (SDS)	Fluka, Buchs

Paraformaldehyde	Sigma, Deisenhofen
PCR buffer 10x	Qiagen, Hilden
Phenylmethanesulfonyl fluoride (PMSF)	Sigma, Deisenhofen
Propanol	Merck, Darmstadt
Propionaldehyde	Fluka, Buchs
Tetraalkylammonium carbonate	Sigma, Deisenhofen
Streptomycin / Amphotericin B	PAA, Pasching
Thiaminepyrophosphate	Sigma, Deisenhofen
Thiazolyl blue tetrazolium bromide (MTT)	Sigma, Deisenhofen
Triphenyltetrazoliumchloride	Sigma, Deisenhofen
Tris	Sigma, Deisenhofen
Tris glycine SDS	Invitrogen, Darmstadt
Triton 100X	Roth, Karlsruhe
Trolox (6Hydroxy-2,5,7,8 tetramethylchromane-2-carboxylic acid)	Sigma, Deisenhofen
Trypanblue	Biochrom, Berlin
Trypsin EDTA 0,5%	Gibco, United state
Tween^{R} 20	Roth, Karlsruhe
Ultra low range DNA ladder I	PeqLab, Erlangen
Vitamin B1 (Thiamine)	Sigma, Deisenhofen
Zink chloride	Sigma, Deisenhofen

Table 10. List of chemicals used during experiments.

1.7 Materials

Material	Company
Adhesive clear qPCR seals sheets	Biozym, Hessisch Oldendorf
Capsure marcoLCM caps	Life technologies, Darmstadt
Cell culture flasks	Greiner, Frickenhausen
Capillary tips	Biozym, Hessisch Oldendorf
Cryo tubes	Greiner, Frickenhausen
Cuvettes	Ratiolab GmbH, Dreieich-Buchschlag
Glassware	Schott AG, Mainz
Falcons	Greiner, Frickenhausen
Filter tips	Greiner, Frickenhausen
Freezing container “Mr Frosty“	Thermo science, Waltham

Neubauer cell counting chamber	Hecht, Sondheim/ Rhon
PCR reaction eppendorfs	Biozym, Hessisch Oldendorf
Petri dishes	Greiner, Frickenhausen
Plastic container for centrifuges	BD bioscience, Heidelberg
Plastic pipettes	Costar, Fernwald
PVDF transfer membranes hybond	GE-Healthcare, Freiburg
Reaction eppendorfs (1ml)	Eppendorf, Hamburg
Slides superfrost /plus	R.Langenbrink, Emmendingen
Sterile filter (0,22 µm)	Millipore, Billerica
Syringes	Greiner, Frickenhausen
96 well-PCR plates	Peqlab, Erlangen
Well plates	Greiner, Frickenhausen
Whatman paper	GE-Healthcare, Freiburg

Table 11. List of material and plastic goods used during experiments.

1.8 Buffer

1.8.1 Cell Culture medium

- **Cell Culture medium for melanoma cells**:

  89 % DMEM
  10 % FCS
  1 % Streptomycin / Amphotericin B

- **Cell Culture medium for fibroblast cells:**

  89 % MEM
  10 % FCS
  1 % Streptomycin / Amphotericin B

- **Cell Culture freezing medium for melanoma cells:**

  30 % DMEM
  60 % FCS
  10 % DMSO

❖ Sterile filtered FCS solution was aliquoted and stored at -20 °C for several months.

1.8.2 Gel electrophoresis (agarose) buffers

- **TAE buffer:**

2	mM	EDTA
1	mM	NaAc
40	mM	Tris HCl
		pH 8.0

- **Loading buffer:**

0.2	%	Bromphenol blau
50	%	Glycerine
50	%	TAE-buffer

- **2% agarose gel:**

2% agarose (w/v) prepared with the appropriate amount of 1x TAE buffer.

- **5% agarose gel:**

5% agarose (w/v) prepared with the appropriate amount of 1x TAE buffer.

1.8.3 Transketolase buffer and reaction solution

- **Lysis buffer:**

0.5	mM	Benzamidine
40	mM	Citrate
40	mM	Sodium phosphate
0.25	mM	Phenylmethanesulfonyl fluoride (PMSF)
		pH 6

- **Reaction solution:**

360	µl	Gly-Gly (50 mM)
120	µl	Lithium hydroxypyruvat (250 mM)
60	µl	MgCl2 (90 mM)
60	µl	Thiamine pyruphosphat (24 mM)
10	µl	177 ng/ml Thiamine

1.8.4 Western blot buffers

- **Lysis buffer:**

150	mM	Sodium chloride
1	%	Nonidet P-40
0.5	%	Sodium deoxycholate
0.1	%	Sodium dodecyl sulphate (SDS)
		Protease inhibitors
		pH 7.4

- **10x SDS-PAGE buffer:**

2	M	Glycine
1	%	SDS
250	mM	Tris
		bidest H_2O
		pH 8.3 - 8.5

- **WB semidry buffer:**

0.2	M	Glycine
20	%	Methanol
25	mM	Tris
		bidest H_2O
		pH 8.5

- **10x TBS (Tris buffered saline):**

8	%	NaCl
200	mM	Tris
		bidest H_2O
		pH 7.6

- **TBS Tween 20 (TBST):**

0.1% Tween 20 in 1x TBS.

- **Blocking buffer:**

5% non-fat dry milk or bovine serum albumin (BSA) in TBST.

2. Methods

2.1 Cell culture

2.1.1 Cell culture maintenance

Human melanoma cells of the different progression levels from vertical growth phase (VGP), radial growth phase (RGP) and metastasizing melanoma (MM) (table 9) for cultivation and progression were cultured in cell culture flasks with DMEM medium, complemented with 10% FCS and 1% antibiotic-antimycotic solution (streptomycin/amphotericin B) at 37°C in a humidified atmosphere enriched with 5% CO_2 in an incubator (Baban *et al.,* in press). Melanoma cells are adherently growing cells and every 2-3 days the medium was renewed.

For splitting, when the flask is a proximally 80% confluent, cells were washed with PBS X1 then treated with 3ml of the pre-warmed trypsin solution for 5 min to detach cells, for stopping trypsin reaction, 3-5ml of DMEM medium, complemented with 10% FCS was added, to inactivate proteolysis effect of trypsin. After transferring the required volume of cell suspension into new flasks, each flask was filled with DMEM and the flasks were placed in the incubator to allow cells to settle down and attach again.

2.1.2 Cryopreservation

When the cells in the flasks reached confluence, cells were detached, using trypsin as described before and reaction was inhibited with complete DMEM. The cell suspension was centrifuged at 1500 rpm for 5 min. After discarding the supernatant, the precipitated pellet was resuspended in 1ml of freezing medium and cell suspension was transferred to freezing vials and stored in -80 °C for 24 hr. For long term storage cells were transferred to liquid nitrogen.

For culturing cells, after thawing, they were immediately transferred to a tissue culture flask containing pre-warmed DMEM. Melanoma cells were cultivated in an incubator, all steps of thawing should be performed quickly.

The day after thawing the cells, the medium of cell culture flasks was exchanged with fresh DMEM (1 g/l low glucose media).

2.1.3 Cell counting with Neubauer chamber

The Neubauer chamber or hemocytometer is a device used to determine the number of cells per unit volume. The grid area in the counting chamber is divided into 9 large squares, each square has a surface area of 1 mm^2 and depth of 0.1 mm after putting the glass cover over it.

After cells were harvested, they were diluted and counted in a volume ratio of 1:1 with trypanblue and pipetted and drawn by capillary force to grid area in a Neubauer chamber. A light microscope was used to count live cells in the counting fields.

To calculate total cell number in absolute volume, all cells in 4 large squares were counted (by light microscope) then the average count was founded, which was multiplied by chamber factor 10 000 (cell/ml) and the dilution factor. To get the total cell number in a specific volume, the number was multiplied by total volume in ml:

Cells per ml = average count x dilution factor x 10 000

Cells per total volume = average count x dilution factor x 10 000 x volume

2.2 Determination of cell viability and proliferation by MTT assay

Equivalent number of each melanoma cell line was irradiated with UVA radiation within different doses from 4 to 10 J/cm^2 three times daily for 4 consecutive days. After UVA irradiation, melanoma cell lines were treated with tetrazolium dye MTT (3-(4,5-dimethylthiazol-2-yl)-2,5-diphenyltetrazolium bromide), using a concentration of 5 mg/ml and incubated at 37°C for 3.5 hr.

Cells were treated 15 min with MTT solvent (4mmole HCl, 0.1 % nodent in isopropanol), cell viability and proliferation was measured, using ELISA reader at optical density of 590 nm.

2.3.1 UVA irradiation

Irradiation was carried out according to and as described (Berneburg *et al.*, 2005; Kamenisch *et al.*, 2010; Koch *et al.*, 2001). Briefly, cells were irradiated with a UVA irradiation lamp with different doses from 4 to 10 J/cm^2 of UVA three times daily for 4 consecutive days (Baban *et al.,* in press).

For UVA irradiation experiment, equivalent number of each melanoma cell lines was seeded and cultivated in 10cm or 15cm diameter of adherent cell culture Petri dishes in DMEM with 4.5 g/l glucose (high glucose media). During irradiation DMEM was

replaced by PBS X1 and collected in a sterile Falcon to avoid chemical changes in the medium by UVA irradiation. Petri dishes were placed on a turntable to uniformly irradiate whole petri dishes, treatment was three times per day, with 4 hr intervals between irradiation coarse, to give cells enough time for entire recovery.

Periodically, UVA emitted energy by UVA lamp was re-measured, which was necessary for calculating the exact exposure time for each dose.

For each experiment and according to each cell line a control (without irradiation) was included.

2.3.2 Chemical treatment during UVA irradiation

Cells were treated with Trolox (6-hydroxy-2,5,7,8-tetramethylchroman-2-carboxylic acid) during the irradiation, with a dose of 20µM, which is similar to doses observed in plasma (20-100µl/l) after oral Trolox treatment. Cells were treated with 2-DG (2 deoxy-D-glucose) during the irradiation, with doses of 10µM and 5.5mM, which are similar to 2-DG concentrations (1.76 mM) observed in the blood of patients with 2-DG treatment (Yamaguchi *et al.*, 2011). Cells were treated 12 hr with lactic acid to induce MMPs and uPA transcription with a dose of 20mM, which is close to concentrations that are observed in the micromillieu of tumors (Serganova *et al.*, 2011). For inhibition of uPA, amiloride (3,5-diamino-6-chloro-N-(diaminomethylene)pyrazine-2-carboxamide) was used at doses of 7µM during irradiation and recovery and 0.1mM during invasion assay. For MMPs inhibition, GM6001 (N-[(2R)-2-(Hydroxamidocarbonylmethyl)-4-methylpentanoyl]-L-tryptophan methyl amide) was used at doses of 10nM during irradiation and recovery and 1µM during invasion assay (section from Baban *et al.,* in press).

2.4 Glucose measurement

Glucose measurement was performed according to instruction of glucose go assay (sigma) in the cell culture supernatant. Glucose is oxidized by glucose oxidase reagent to gluconic acid and H_2O_2, o-dianisidine and peroxidase in the reagent reacts with H_2O_2 to produce a brown colored product (oxidized o-dianisidine), later on a stable pink colored product is formed by addition of 12N sulfuric acid H_2SO_4.

The maximum absorption intensity of pink colored products was directly proportional to the total amount of glucose in the samples at 540 nm.

Procedure for glucose measurement

1. After irradiation courses supernatant was collected immediately
2. Dilution of cell culture media was done with bidest.H_2O
   Low glucose medium (1g/l) was diluted 1:10
   High glucose medium (4.5g/l) was diluted 1:100
3. Blank: 100µl diluted pure media
4. Standard preparation: standard (1mg/ml) was diluted 1:20 with ddH_2O
5. Reaction steps were followed as described in manual of glucose go protocol assay.

Calculation

Whole amount of glucose, which was consumed by cells in the supernatant, was calculated by the difference of glucose in beginning compared to the end of experiments.

The glucose consumption [mg] = entire glucose [mg] – residual glucose [mg]

The amount of glucose consumption in the supernatant [mg] was normalized to the number of cells [million cells] after irradiation courses. Throughout the experiment the same volume of media was used for all samples.

For glucose measurement in skin reconstructs lysate, the skin reconstructs were weighted and immediately incubated in 50µl of PBS X1 at 95°C for 5 min. Glucose concentration was measured by using glucose go assay protocol, as described above.

2.5 Lactate measurement by color enzymatic method

Principle of enzymatic approach

Lactate measurement was performed according to the protocol of the lactate kit (Trinity biotech), instruction for cell culture supernatant; lactate reagent contains oxidase, peroxidase enzymes and chromogen precursors to form a colored product.

The maximum absorption intensity of colored products was directly proportional to the total amount of lactate in the samples at 540 nm.

Procedure for lactate measurement

1. After irradiation courses supernatant was collected immediately
2. Supernatant was mixed with lactate reagent in volume ratio of 1:100
3. Blank: 100µl diluted pure media
4. Standard preparation:
   40 mg/dl standard was used in volume ratio of 1:100
5. Rest of procedure was performed according to the lactate kits protocol.

Calculation

The amount of lactate produced by cells in the supernatant, as determined in [mg] was normalized to the number of cells [million cells] after irradiation courses. Throughout the experiment the same volume of media was used for all samples.
For lactate production measurement in skin reconstructs, the skin reconstruct was weighted and immediately incubated in 50µl of PBS at 95°C for 5 min. Then, lactate concentration was measured by using lactate reagent assay Kit protocol (Baban *et al.,* in press).

2.6 Transketolase activity measurement

Transketolase activity was measured colorimetrically. Briefly, after UVA irradiation, cells were harvested, pelleted and lysed by addition of transketolase lysis buffer. 45µl of mixture1 (120µl Li-HPA (250 mM), 60µl MgCl2 (90 mM), 60µl TPP (24 mM), 360µl Gly-Gly (50 mM), 10µl 177 ng/ml thiamine) was incubated with 45µl of cell lysate and 20µl propionaldehyde. This reaction mix was incubated for 72 hr at RT. Afterward it was incubated with Gly-Gly (50 mM) and 10 mg tetraalkylammonium carbonate (polymer-bound carbonate resin beads) for 24 hr at RT, followed by treatment tetrazolium red (0.2% in methanol). This assay as described by (Smith *et al.*, 2006), has been adapted and modified to the needs of the irradiation experiment. For transketolase activity measurement, the skin reconstructs were weighted and subsequently transketolase activity was measured calorimetrically as described above. Measurement was carried out at 492 nm optical density, using an ELISA reader (Baban *et al.,* in press).

2.7 Nuclear magnetic resonance spectroscopy

NMR spectroscopy is a research technique mostly used in biochemistry to determine the chemical properties of atoms and molecules by taking the advantage of magnetic properties of particular atomic nuclei.

Equivalent numbers of different melanoma cell lines were irradiated with 6 J/cm^2, three times daily for 4 consecutive days. After UVA irradiation course, melanoma cells were harvested and detached with ethanol by mechanical force, then supernatant and cells were stored at -80°C until sending to University of Regensburg for NMR analysis.

UVA induced metabolic change was investigated, the uptake or secretion of different metabolomics such as amino acids in the supernatant and cell pellets of control and UVA irradiated melanoma cells, in cooperation with the University of Regensburg (Prof Gronwald) by NMR.

Changes in metabolomics concentration in [µM] within the supernatant and melanoma pellets with and without UVA irradiation, were normalized to protein concentration. Data are presented as mean value with standard deviation of 3 independent experiments.

2.8 Fluorescence activated cell sorting

Fluorescence activated cell sorting (FACS) is a biotechnical method used for sorting a heterogeneous population of living cells into two or more subpopulations, based on distinct fluorescent labeling of each cell type.

The initial targets of UVA signaling in melanoma cells are Epidermal growth factor receptor (EGFR) and Insulin-like growth factor receptor (IGFR). To investigate the influences of UVA irradiation on both receptors, FACS analysis was performed. For that purpose, equivalent number of different melanoma cell lines were irradiated with 6 J/cm^2, three times daily for 4 consecutive days. After UVA irradiation course, melanoma cells were harvested and stained with EGFR antibody and IGFR antibody by incubating for 1 hr at 37°C. After the incubation period with antibodies, cells were centrifuged for 5 min at 1500 rpm and the pellet was washed twice with 10 ml PBS and resuspended in medium (MEM + 10% FCS).

Indirectly, by detection of IGFR and EGFR on cellular surface with fluorescent-labeled antibodies, the mean value of internalized EGFR and IGFR population was estimated.

2.9 DNA isolation

Instructional information and detailed manual of the QIAamp DNA micro kit from Qiagen protocols for molecular biology experiment was used to carry out DNA extraction in the laser micro dissection tissues.

DNA genome purification was performed for human tissue sections, which were isolated by laser capture micro dissection microscope from paraffin embedded slices. Genomic DNA was used for of analysis mitochondrial common deletion gene expression by PCR (table 17 and 18). All steps were rapidly carried out after DNA isolation, as DNA is not stable. All steps were performed at room temperature.

2.10 RNA isolation

According to instructional information and detailed manual of the RNA NucleoSpin®II kit from Macherey-nagel, RNA genome purification from cell culture cells was performed.

Cells were harvested, pelleted and then resuspended in 300 µl of lysis buffer contained in the kit. Subsequently RNA was eluted in 60µl RNAase free H_2O. All procedure steps were carried out at RT. Measurement of RNA and DNA concentration and purification success was done with the spectrophotometer.

2µl of RNA sample was diluted in 60µl double bidest.H_2O and bidest.H_2O was used as a blank for photometer calibration. A measurement of optical density or UV absorbance at 260 nm wavelengths for nucleic acid was used to determine nucleic acid concentration. The RNA and DNA concentration was calculated, using photometer software. Then, 2% agarose gel electrophoresis was done for verifying purification of RNA.

2.11 cDNA Synthesis

Complementary DNA (cDNA) is a double strand DNA, which was synthesized from messenger RNA (mRNA) template by reverse transcriptase enzyme during reverse transcription polymerase chain reaction (RT-PCR). The cDNA synthesis was synthesized according to iscript synthesis kit for cDNA synthesis (table 12 and 13).

Components	Volume
1. 5X iscript reaction mix	4 µl
2. Iscript reverse transcriptase	1 µl
3. Nuclease free H_2O	X µl
4. RNA (1µg)	X µl
Total volume / reaction	20µl

Table 12. cDNA synthesis setup.

Phase	Duration	Temperature
1	5 min	25 °C
2	30 min	42 °C
3	5 min	85 °C
Hold	5 min	4 °C

Table 13. cDNA synthesis protocol.

2.12 Real time PCR

Real time PCR is a method, used to amplify and quantify target DNA genetic molecules (Mats Nilsson, 2002; Thore Hillig, 2012; Kameisch *et al.,* 2010).

After cDNA synthesis by RT-PCR protocol (described in table 12 and 13), DNA quantification was determined with real time PCR protocol, by using EvaGreen Supermix and specific primer pairs (shown in table 6,7 and 8). Roche light cycler instrument was used in this study for analysis of expression level of different proteases and protein kinases that are involved in melanoma invasion and cell signaling pathways respectively. GAPDH and β actin were used as housekeeping genes that were chosen as they showed a stable expression. Additionally, internal standard (IS) primer (table 8) was used in real time PCR of mtDNA common deletion gene expression as housekeeper for relative relation to the total amount of mtDNA (described in table 14, 15, 16 and 17) (Koch *et al.,* 2001). The amplification products of the target genes were normalized to the amplification products of the housekeeping genes. Delta Ct (ΔCt) was measured between target gene Ct and housekeeping gene Ct. Fold change or the value of difference of target gene

between (ΔCt) treated and (ΔCt) untreated were calculated as $2^{-\Delta(\Delta Ct)}$, which means the difference in the target gene between treated and control samples (Livak and Schmittgen, 2001).

After real time PCR, 5% agarose gel electrophosis was performed for the amplification products to detect bands with the size of the gene product.

Components	Volume
EvaGreen Supermix	12.5 µl
Primer forward	0.025 µl
Primer reverse	0.025 µl
cDNA	1 µl
Nuclease free H_2O	11.5 µl
Total volume / reaction	25 µl

Table 14. Real time PCR setup.

Phase	Temperature	Duration
Pre incubation	95 °C	5 min
Amplification	95 °C	10 sec
	54 °C	10 sec
	72 °C	10 sec
Melting	95 °C	10 sec
	65 °C	1 min
	95 °C	
Cooling	40 °C	10 sec

Table 15. Real time PCR protocol for MMPs and uPA.

Components	Amount
EvaGreen Supermix	12,5 µl
Primer forward	0.125 µl
Primer reverse	0.125 µl
DNA 250 ng	X µl

Nuclease free H_2O	X µl
Total volume / reaction	25 µl

Table 16. Real time PCR setup for mtDNA common deletion.

Phase	Temperature	Duration
Pre incubation	95 °C	5 min
Amplification	95 °C	10 sec
	58 °C	10 sec
	72 °C	10 sec
Melting	95 °C	10 sec
	65 °C	1 min
	95 °C	
Cooling	40 °C	10 sec

Table 17. Real time PCR protocol for mtDNA common deletion by light Cycler.

Real time PCR protocol, which was used in experimental setup for MMPs and uPA gene expression, was used for other primers with annealing temperature adapted, according to each primer.

Phase	Temperature	Duration
Denaturation	95 °C	2 min
Amplification	95 °C	5 sec
	58 °C	10 sec
	72 °C	5 sec
Melting	65 °C	10 sec
Cooling	15 °C	Hold

Table 18. Real time PCR protocol for mtDNA common deletion by iCycler

2.13 Agarose gel electrophoresis

Agarose gel electrophoresis is the most effective way for separation DNA fragments by size (length in base pairs) for visualization and purification purpose by an electrical field, because DNA is negatively charged as it has phosphate group.

Amplification products through agarose gel matrix migrate toward a positive electrode but the rate of migration depends on gel density and length of DNA fragments. To accurately determine the size of DNA fragment in the gel matrix, DNA ladder (array of DNA fragments of known size) from (PEQ gold ultra low range DNA ladder I) was used that runs alongside DNA samples and has defined band sizes.

The 2% agarose gel electrophoresis was performed for isolated RNA and 5% agarose gel electrophoresis was performed for DNA after PCR. Samples were prepared, by mixing with a loading buffer, which contains bromophenol blue (acts as staining dye that is able to absorb UV radiation) and GelRed (an intercalating nucleic acid fluorescent dye illuminates around 312 nm of UV wave length). Loading buffer was prepared in concentration of 1:2000 ratio volumes GelRed to bromphenol blue, bands were photographed, using UV transilluminator. The running buffer was TEA buffer and gels were run within 100 Voltage for 20-40 min at RT.

2.14 Protein measurement

BCA protein assay reagent A and B (Pierce, USA) was used for protein measurement, as indicated in the manufactures protocol.

2.15 Western blot

Western blot is a protein immunoblot method, used to separate different proteins according to their length of the polypeptide by sodium dodecyl sulfate-polyacrylamide gel electrophoresis (SDS-PAGE) and subsequent detection of target protein by a specific antibody on the membrane after blotting.

Sample preparation

After protein quantification, using BCA protein assay kit, the same amount of proteins in µg/µl of samples were mixed with tris glycine X2 SDS, then heated at 95°C for 5 min for denaturation.

Polyacrylamide gel preparation

Upper gel solution	Amount / Gel	Lower gel Solution	Amount / Gel
Stacking buffer	3.8 ml	Separating buffer	7.3 ml
Acrylamide	0.85 ml	Acrylamide	2.65 ml
TEMED	3.75 µl	TEMED	17.5 µl
APS	37.5 µl	APS	60 µl

Table 19. 8% Polyacrylamide gel preparation (upper and lower) gels.

Marker**:** 6µl of Novex ® Sharp protein standard marker from invitrogen LC5800 was used to determine protein molecular weight. Gel run was started with 90 Voltage then changed to 120 Voltage until the protein bands are at the bottom of the gel.

Blotting OF PVDF membrane

Semidry method was used for blotting proteins on a hydrophobic polyvinylidene difluoride (PVDF) membrane. The membrane was activated with 100% methanol and equilibrated in semidry buffer for 30 sec and whartman paper were seaked in semidry buffer. Blotting was performed with Trans blot turbo transfer system at 25 Voltage for 10 min.

Only for EGFR proteins, the tank method was used for blotting on hydrophobic polyvinylidene difluoride (PVDF) membranes and it was performed at 100 Voltage for 2 hr at RT.

Blocking

This step was performed to block unspecific binding proteins on a hydrophobic polyvinylidene difluoride (PVDF) membrane

- Blocking buffer for non-phosphorylated proteins:

5% (w/v) non fat dry milk in TBST was used for 1 hr at RT with rotation.

- Blocking buffer for phosphorylated proteins:

5% (w/v) BSA in TBST was used for 1 hr at RT with rotation.

Primary antibody

Membranes were incubated over night with primary antibodies, diluted in TBST at 4°C.

Secondary antibody:

The IgG Horseradish peroxidase (HRP) anti mouse or rabbit was used, according to each species for 1 hr at RT with rotation.

Developing

According to LumiGlo kit protocol, development was done by an auto processor X-ray film detector (Optimax mammo-X-ray film processor) in a darkroom. X-ray film (Amersham hyper chemiluminescence films) was used for detection of chemiluminescent signals from the membrane, after putting it in a light proof cassette and exposing it for an appropriate time period, then the film was developed.

Scanned x-ray film was analyzed by Adobe photoshop and Microsoft excel for densitometric comparison of detected bands relative to housekeeping protein β actin.

2.16 Zymography

For zymography, the proteins of the supernatant, which was treated with UVA, Trolox and lactic acid, were concentrated by using protein concentrators 9K MWCO, 7m (thermo scientific, Germany). Concentrated supernatants were diluted 1:1 in 2X tris-glycine SDS buffer without heating and subsequently electrophoresis was performed with a 10% tris-glycine gel, containing 0.1% gelatine (invitrogen, Germany). Gel run was performed at 125 Voltage for 90 min, followed by incubation in renaturating buffer (invitrogen, Germany) at RT. After incubating overnight in the developing buffer (invitrogen, Germany) they were stained with Simply blue safestain for 1 hr (invitrogen, Germany). The activity and concentration of MMP2 and MMP9 proteases has analyzed by measuring the size of digested bands in the gelatin gels normalized to the number of cells. The size of digested bands was quantified by measuring the cumulative intensity of pixels within the digested band with ImageJ (section from Baban *et al.,* in press).

2.17 uPA assay

Quantitative detection of human uPA was performed according to uPA (URK) human ELISA kit (abcam, Germany) protocol. Briefly, supernatant of IM and MM cells treated with UVA, Trolox or lactic acid were concentrated by using protein concentrators, 9K MWCO, 7m (as described before in paragraph 2.16). The concentrated supernatant was applied to the precoated wells with uPA antibody. After washing, HRP was

added to wells to link it with uPA antibody. After washing, the human uPA concentration in the supernatant was measured in a microplate reader at 450 nm optical density (section from Baban *et al.,* in press).

2.18 *In vitro* cell invasion assay

Cell invasion assay was performed, according millipore cell invasion assay protocol (millipore, Germany). Briefly, 250000 melanoma cells were incubated per insert, for 24 hr with and without treatment and the fraction of invaded cells was determined fluorometrically, using fluorescence plate reader with a 480/520 nm filter set (section from Baban *et al.,* in press).

2.19 Skin reconstructs model

Skin reconstruct model is a three dimensional (3D) skin culture that consists of dermal layers, which is a mixture of normal human fibroblast within a biocollagen matrix and epidermis layer. Epidermis layer contains normal human keratinocytes and melanoma or melanocytes that were seeded on dermas layer. Using the skin reconstruct mode, we are able to fill the gap between *in vitro* experiments in human cells and *in vivo* experiments in mice. Skin reconstructs were prepared in collaboration with (Dr. Tobias Sinnberg, working group of Prof. Birigit Schittek, University of Tuebingen). To investigate the influence of UVA irradiation on skin reconstructs, glucose uptake, lactate production and transketolase activity were measured in different conditions in skin reconstructs lysate and the supernatant of skin reconstructs as described before.

For immunohistochemistry, after fixation with histofixation solution (4% formalin) overnight, skin reconstructs were paraffin embedded, serially sectioned using microtome. 2µm thick sections were seated on Superfrost (poly-L-lysin) glass slides, and then analyzed by H&E staining and S100 antibody, which is a specific antibody for human melanoma cells (staining with H&E and treating with S100 antibody were done by Histopathology Department of Dermatology hospital, Tuebingen).

2.20 Statistical analysis

Data are shown as the mean with standard deviation of at least three independent experiments and statistical significance was tested with Student's t-test and a two sided p value < 0.05 was considered significant**.**

C. Results

1. Role of ultraviolet (UV) radiation in progression and invasion of melanoma cells

1.1 UVA radiation decreased survival and viability of melanoma cells

We investigated the effect of different UVA radiation doses on survival and viability of human melanoma cells (initial melanoma derived from vertical horizontal growth phase (IM) and metastasizing melanoma (MM)) by determination of viable cell number with trypanblue and 3-(4,5-dimethylthiazol-2-yl)-2,5-diphenyltetrazolium bromide (MTT), before and after the experiment (figure10) (section from Baban *et al.,* in press).

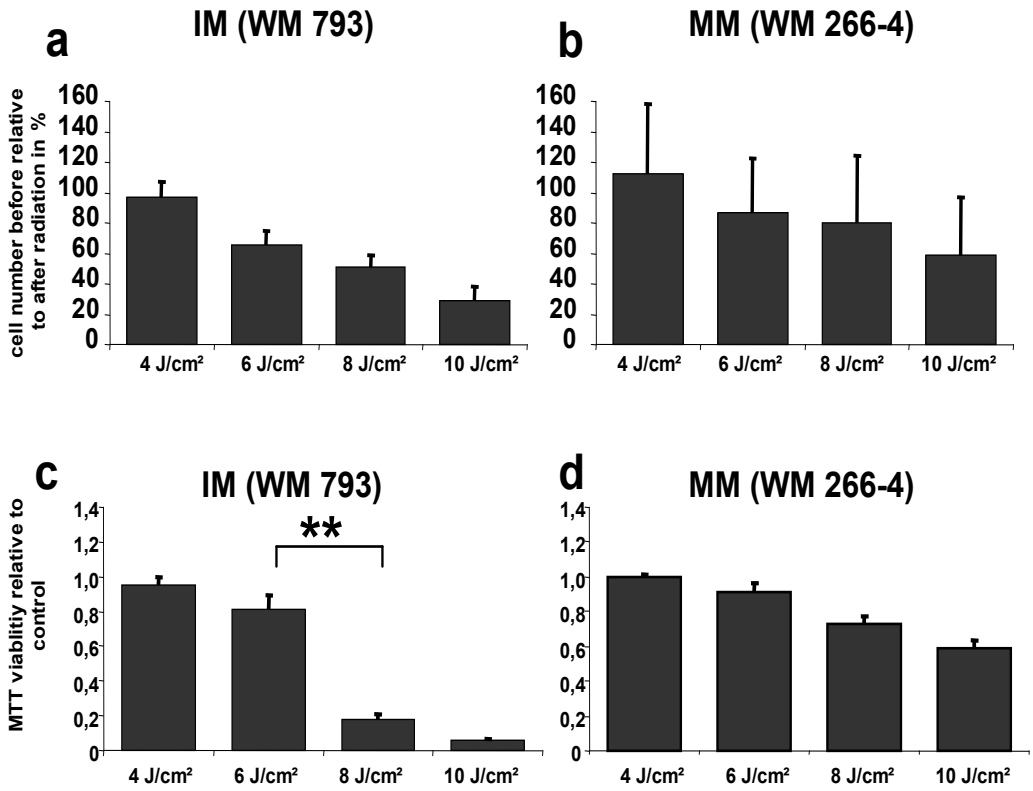

(section from Baban *et al.,* in press)

Figure 10. Influences of UVA irradiation on cell survival and viability.

Melanoma cell lines from initial melanoma (IM) and metastasizing melanoma (MM) were irradiated with different doses from 4 to 10 J/cm^2 of UVA three times daily for 4 consecutive days.

a-b. Trypanblue was used for viable cell number determination.

The number of cells after experiment relative to number of cells at beginning of the experiment is displayed. The number of cells decreased in a dose dependent manner upon UVA irradiation. Data are shown as mean value of at least three independent experiments with standard deviation (section from Baban *et al.,* in press).

c-d. MTT was used to determine the number of viable cells. Displayed is the MTT viability relative to unirradiated control. The MTT viability decreased in a dose dependent manner upon UVA irradiation. Data are presented as mean values of at least three independent experiments with standard deviation (section from Baban *et al.,* in press).

The decrease in cell viability was moderate at doses of 4 J/cm² and 6 J/cm², but a significant decrease in MTT viability assay (students t-test; $p<0.01$) was observed from 6 J/cm^2 to 8 J/cm^2 in IM cells (figure 10 c).

1.2 UVA induced glucose consumption and lactate production

Most proliferating tumor cells are characterized by enhanced glucose consumption and increased lactate production. To investigate the influence of UVA radiation on glucose uptake and lactate production, melanoma cells were irradiated three times daily for 4 consecutive days (figure 11) (section from Baban *et al.,* in press).

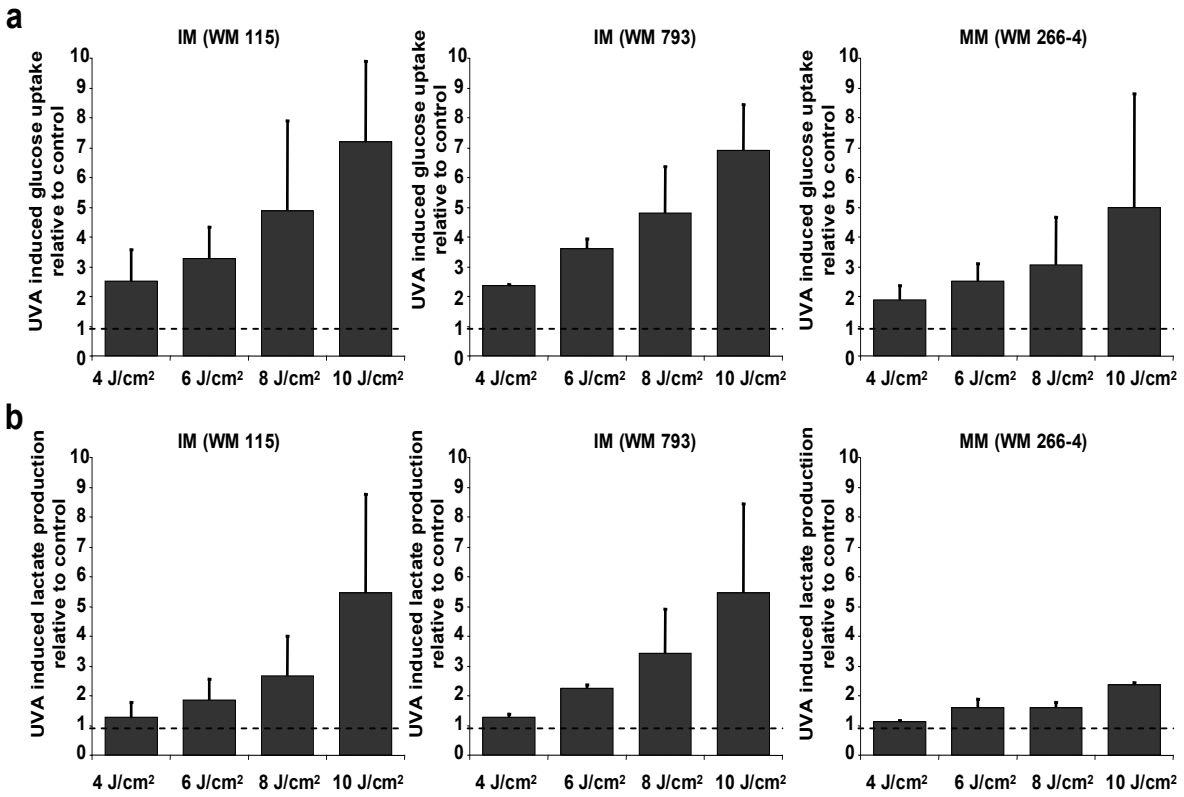

(section from Baban *et al.,* in press)

Figure 11. UVA induced a dose dependent upregulation of the Warburg effect.
Melanoma cell lines from initial melanoma (IM) and metastasizing melanoma (MM) were irradiated with different doses from 4 to 10 J/cm^2 of UVA three times daily for 4 consecutive days and glucose consumption and lactate production relative to cell number was measured.

a. Repetitive UVA irradiation with different UVA doses increases glucose consumption relative to control in a dose dependent manner. Data are presented as mean values of at least three independent experiments with standard deviation (section from Baban *et al.,* in press).
b. Repetitive UVA irradiation with different UVA doses increased lactate production and glucose consumption relative to control in a dose dependent manner. Data are presented as mean values of at least three independent experiments with standard deviation (section from Baban *et al.,* in press).

Glucose consumption and lactate production are increased upon UVA radiation. This effect was observed for different doses of UVA irradiation, partially showing a dose dependent upregulation of the Warburg effect (figure 11).

Since irradiation with 6 J/cm^2 represents a physiological relevant dose during normal sun exposure (Baczynska *et al.,* 2013; Gerber *et al.,* 2002; Mecherikunnel and Duncan, 1982; Miyamura *et al.,* 2011; Parisi and Wong, 2000; Turnbull and Parisi, 2003) and higher doses in our experiments had a strong effect on MTT viability and cell survival, further experiments were performed with an irradiation dose of 6 J/cm^2 (figure 12) (section from Baban *et al.,* in press).

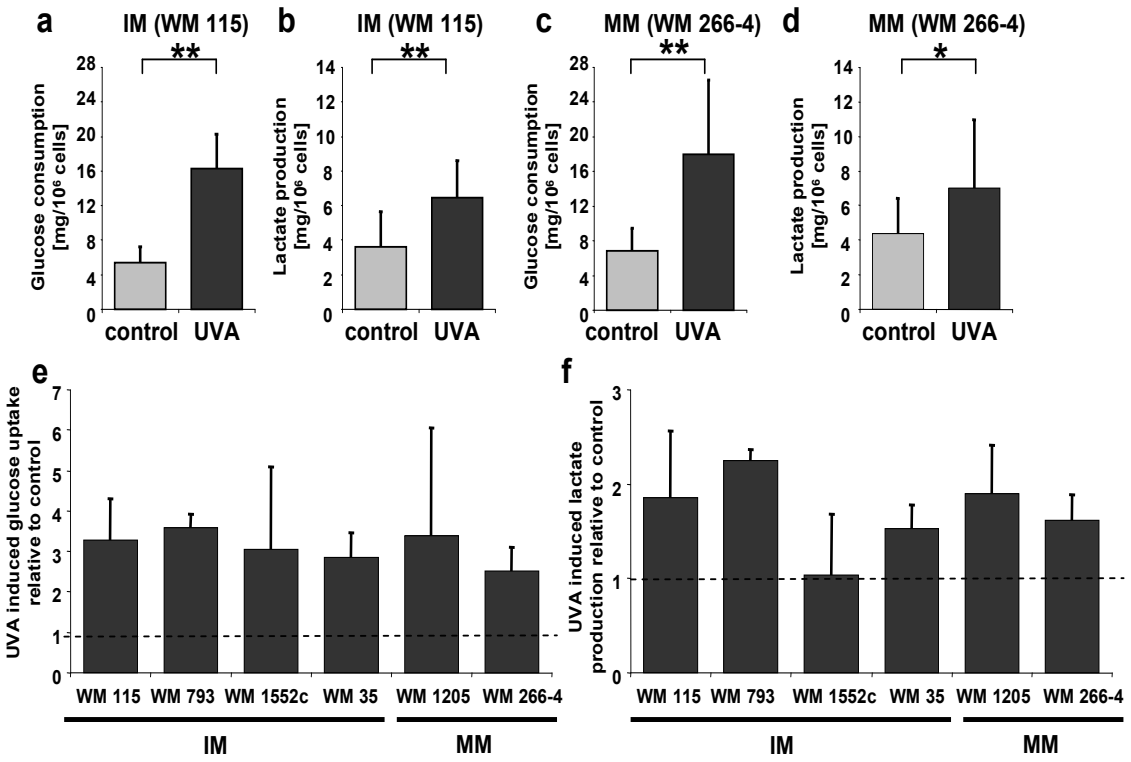

(section from Baban *et al.,* in press)

Figure 12. UVA significantly induced Warburg effect.
Melanoma cell lines from initial melanoma (IM) and metastasizing melanoma (MM) were treated repetitively with 6 J/cm^2 UVA three times daily for 4 consecutive days.

a-b. Repetitive UVA irradiation with 6 J/cm^2 increased glucose consumption (students t-test; $p<0.01$) and lactate production (students t-test; $p<0.05$) in IM cells. Glucose consumption and lactate production are displayed relative to cell number. Data are presented as mean value with standard deviation of at least four independent experiments (section from Baban *et al.,* in press).
c-d. UVA irradiation with 6 J/cm^2 increased glucose consumption (students t-test; $p<0.01$) and lactate production (students t-test; $p<0.05$) in MM cells. Glucose consumption and lactate production are displayed relative to cell number. Data are presented as mean value with standard deviation of at least five independent experiments (section from Baban *et al.,* in press).
e-f. UVA irradiation with 6 J/cm^2 increased glucose consumption and lactate production compared to unirradiated control, with different genetic background in IM and MM cells. Data are presented as mean value with standard deviation of at least three independent experiments (section from Baban *et al.,* in press).

Upon UVA irradiation with 6 J/cm^2, melanoma cell lines showed significant (students t-test; $p<0.01$) upregulation of UVA induced Warburg effect by increased glucose consumption (figure 12 a and c) and lactate production (figure 12 b and d).
Despite different genetic background every IM and MM investigated, tended to induce glucose consumption (figure 12 e) and lactate production (figure 12 f) with 6 J/cm^2 UVA.
Therefore, further experiments were performed with an irradiation dose of 6 J/cm^2.

1.3 UVA decreased pH value of the medium

Different melanoma cell lines showed increased glucose consumption and lactate production upon UVA radiation. To investigate it melanoma cells also secrete not only lactate but also lactic acid, the pH in the medium was measured after UVA radiation (figure 13) (section from Baban *et al.,* in press).

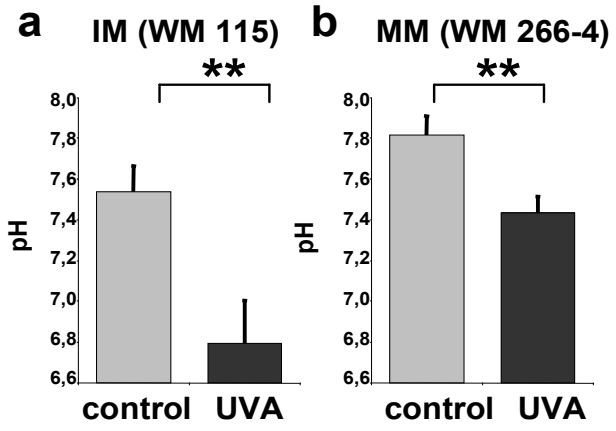

(section from Baban *et al.,* in press)

Figure 13. UVA decreased pH value of the medium.

Melanoma cell lines from initial melanoma (IM) and metastasizing melanoma (MM) were treated repetitively with 6 J/cm^2 UVA three times daily for 4 consecutive days, then pH measurement was performed.

a-b. The pH values are displayed after UVA radiation, repetitive UVA irradiation with 6 J/cm^2 significantly (students t-test; $p<0.01$) decreased the pH value of the IM and MM cell lines. Data are presented as pH value of the medium as mean value of at least three independent experiments with standard deviation (section from Baban *et al.,* in press).

As a consequence of increased release of lactic acid in to the medium, the pH in the medium decreased significantly (students t-test; $p<0.01$) compared to unirradiated control (Figure 13). Increased acidity or decreased pH value of media after UVA treatment indicates that UVA induces the Warburg effect.

1.4 Effect of antioxidant on Warburg effect

Since exposure to UVA irradiation generates reactive oxygen species (ROS) (Meewes *et al.*, 2001) we tested whether UVA-induced Warburg effect in melanoma cells is ROS mediated by coincubation with ROS quencher Trolox. Cells were treated with Trolox (6-hydroxy-2,5,7,8-tetramethylchroman-2-carboxylic acid) (Sigma Aldrich, Germany) during the irradiation regimen with a dose of 20µM, which is similar to doses observed in plasma (20-100µl/l) after oral Trolox treatment (figure 14) (section from Baban *et al.,* in press).

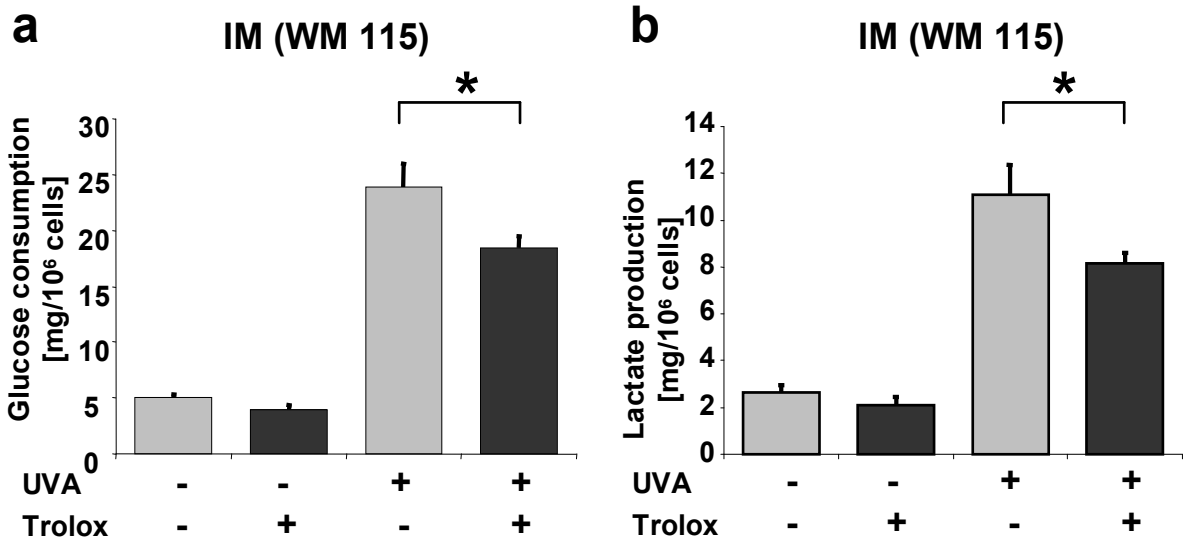

(section from Baban *et al.,* in press)

Figure 14. UVA increased Warburg effect is partially mediated via reactive oxygen species (ROS).

Melanoma cell lines from initial melanoma (IM) were treated repetitively with 6 J/cm^2 UVA three times daily for 4 consecutive days then glucose consumption and lactate production with addition of ROS quencher relative to cell number were measured.

a-b. Treatment of melanoma cells with and without ROS quencher Trolox and repetitive UVA irradiation with 6/cm^2. ROS quencher Trolox significantly (students t-test; $p<0.05$) attenuates UVA induced glucose consumption and lactate production. Data are presented as mean value with of at least three independent experiments with standard deviation (section from Baban *et al.,* in press).

The UVA induced increase in glucose consumption and lactate production compared to unirradiated control was mediated by ROS, since treating cells with ROS quencher Trolox partially attenuated the Warburg effect (figure 14).

1.5 Effect of glycolysis inhibitor

Additionally the effect of UVA induced increase in glucose consumption and lactate production in the presence of the inhibitor of glycolysis was investigated, to verify it UVA enhanced glucose consumption and lactate production is related to enhanced glycolysis. Melanoma cell lines from IM were treated with or without the inhibitor of glycolysis, 2-deoxy-D-glucose (2-DG), which reversely blocks activity of glucose kinase, a key enzyme of the glycolytic pathway, within a concentration 5.5mM of glycolytic inhibitor 2-DG during UVA irradiation (figure 15) (section from Baban *et al.,* in press).

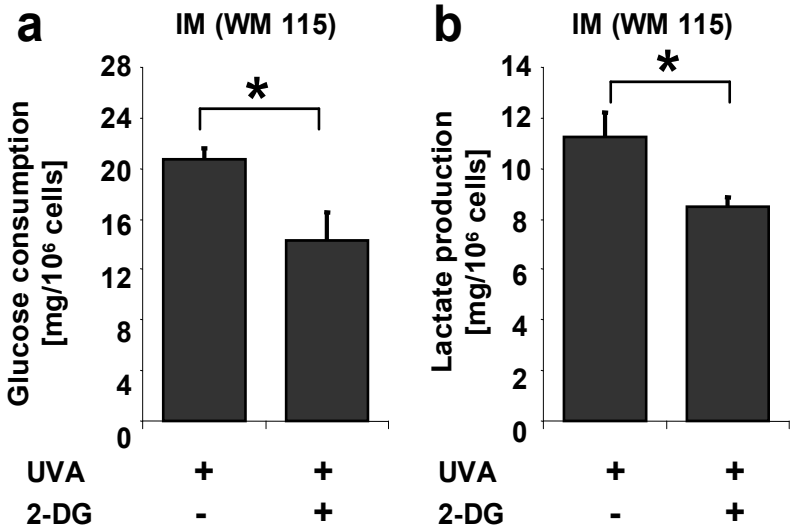

(section from Baban *et al.,* in press)

Figure 15. UVA induced Warburg effect is inhibited by glycolytic inhibitor.

Initial melanoma (IM) cell lines were treated repetitively with 6 J/cm^2 UVA three times daily for 4 consecutive days then glucose consumption and lactate production relative to cell number with or without addition of glycolytic inhibitor was measured.

a-b. UVA induced glucose consumption and lactate production could be decreased significantly (students t-test; $p<0.05$) in the presence of 2-deoxy-D-glucose (2-DG). Glucose consumption and lactate production are presented as mean value with standard deviation of triplicates as representative of at least four independent experiments (section from Baban *et al.,* in press).

In consequence, we found that 5.5 mM of 2-deoxy-D-glucose (2-DG) significantly (students t-test; $p<0.05$) diminished UVA induced glucose consumption and increased lactate production (figure 15).

1.6 UVA radiation enhanced transketolase activity

Transketolase is a key enzyme of the pentose phosphate pathway, which is highly expressed in many tumors and is used as an important prognostic tumor marker (Langbein S *et al.,* 2006). To determine the effect of UVA radiation on the activity of transketolase enzyme, melanoma cell lines from IM and MM were irradiated with different doses from 4 to 10 J/cm^2 of UVA three times daily for 4 consecutive days. Afterwards, transketolase activity relative to cell number was measured with a colorimetric assay (figure 16) (section from Baban *et al.,* in press).

a

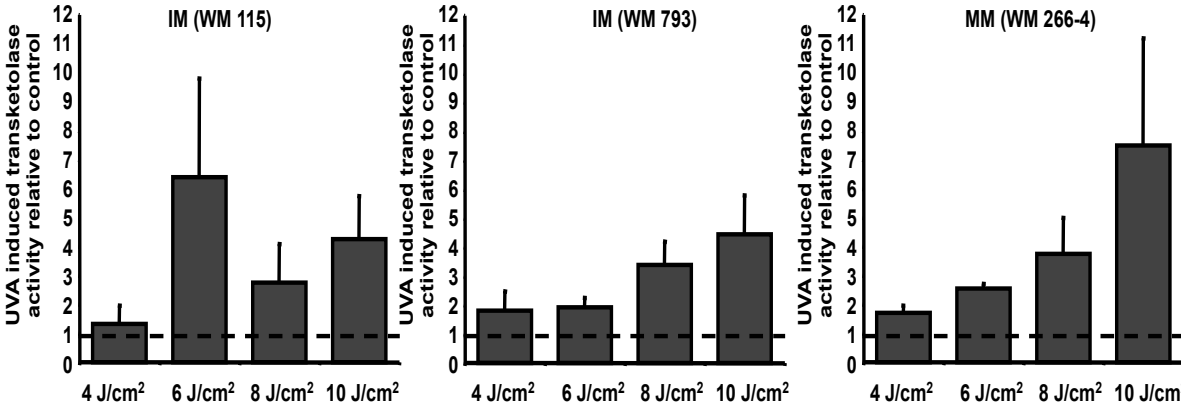

b

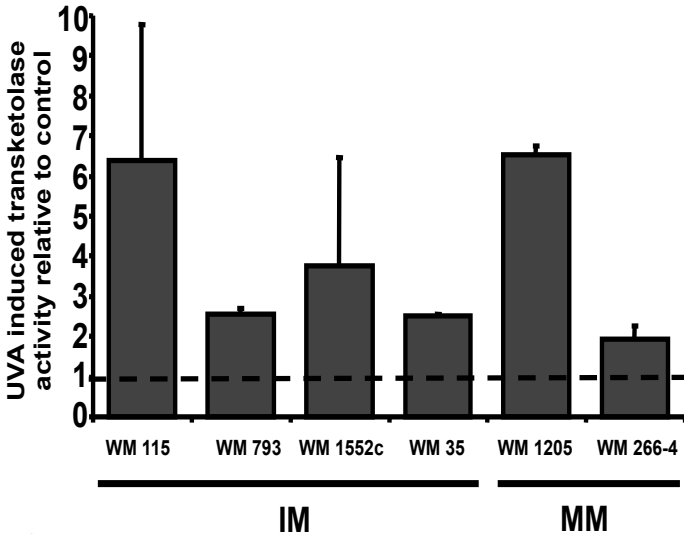

(section from Baban *et al.,* in press)

Figure 16. UVA radiation enhanced transketolase activity.

Repetitive UVA irradiation with different doses three times daily for 4 consecutive days in melanoma cell lines from initial melanoma (IM) and metastasizing melanoma (MM).

a. UVA irradiation with 4 to 10 J/cm^2 increased transketolase activity relative to control partially in a dose dependent manner. Data are shown as mean value of at least three independent experiments with standard deviation (section from Baban *et al.,* in press).

b. UVA irradiation with 6 J/cm^2 increased tranketolase activity compared to unirradiated control, with different genetic background in IM and MM cells. Data are presented as mean value with standard deviation of three independent experiments (section from Baban *et al.,* in press).

Different doses of UVA irradiation, partially showing a dose dependent upregulation of transketolase activity (figure 16 a) and despite different genetic background every IM and MM cell line, investigated was tended to induce transketolase activity (figure 16 b) upon UVA treatment with 6 J/cm^2 UVA.

1.7 Effect of antioxidant on transketolase activity

To investigate the effect of UVA irradiation on transketolase activity and whether UVA irradiation induces transketolase activity via ROS, different melanoma cell lines from IM and MM were irradiated with 6 J/cm^2 and treated with and without ROS quencher Trolox at a dose of 20µM during the irradiation course, transketolase activity was measured using a colorimetric assay (figure 17).

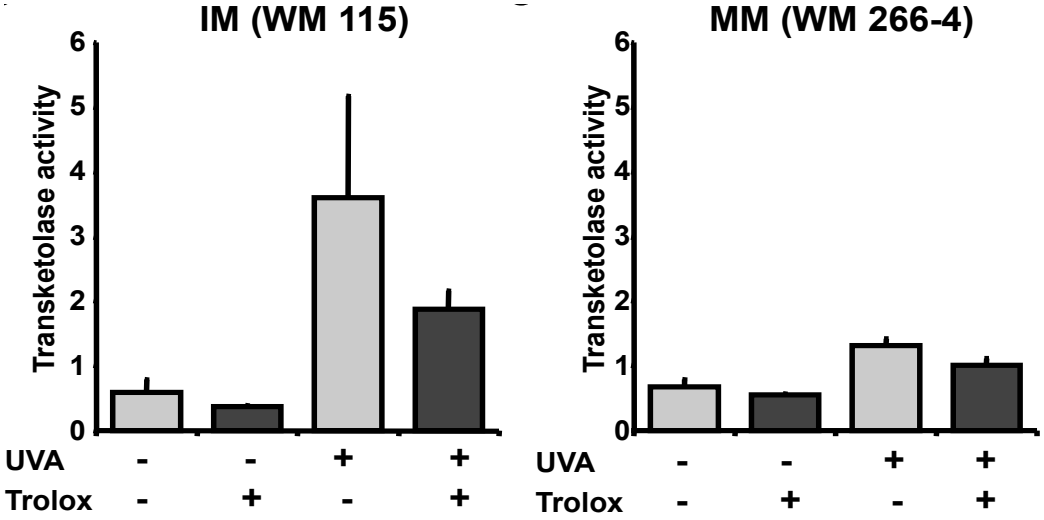

(section from Baban *et al.,* in press)

Figure 17. UVA radiation enhanced transketolase activity was partially mediated via ROS. Repetitive UVA irradiation with 6 J/cm^2 of UVA enhanced transketolase activity in initial melanoma (IM) and metastasizing melanoma (MM) cells and additional treatment with the ROS quencher Trolox attenuated this effect. Displayed is the transketolase activity relative to cell number, and as representatives of three independent experiments with standard deviation (section from Baban *et al.,* in press).

Simultaneously, increased transketolase activity upon treatment with 6 J/cm^2 of UVA was visible in investigated melanoma cells. This UVA enhanced transketolase activity in IM cells was strongly dependent on UVA induced ROS, as addition of the ROS quencher Trolox attenuated UVA induced transketolase activity (figure 17).

1.8 Persistence of UVA induced Warburg effect after UVA radiation

To test whether the UVA induced Warburg effect persists beyond cessation of UVA treatment, melanoma cells from IM were UVA irradiated with 6 J/cm^2 for 4 days and afterwards seeded for growth on a new plate for another 5 days without irradiation (figure 18 a). Subsequently, glucose consumption, lactate production and transketolase activity with and without ROS quencher Trolox were measured (figure 18 b-d) (section from Baban *et al.,* in press).

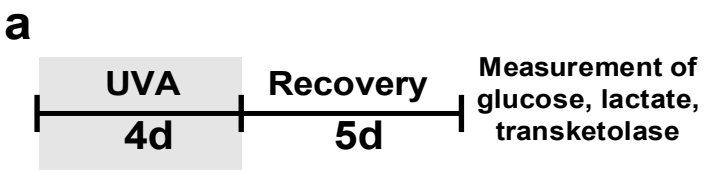

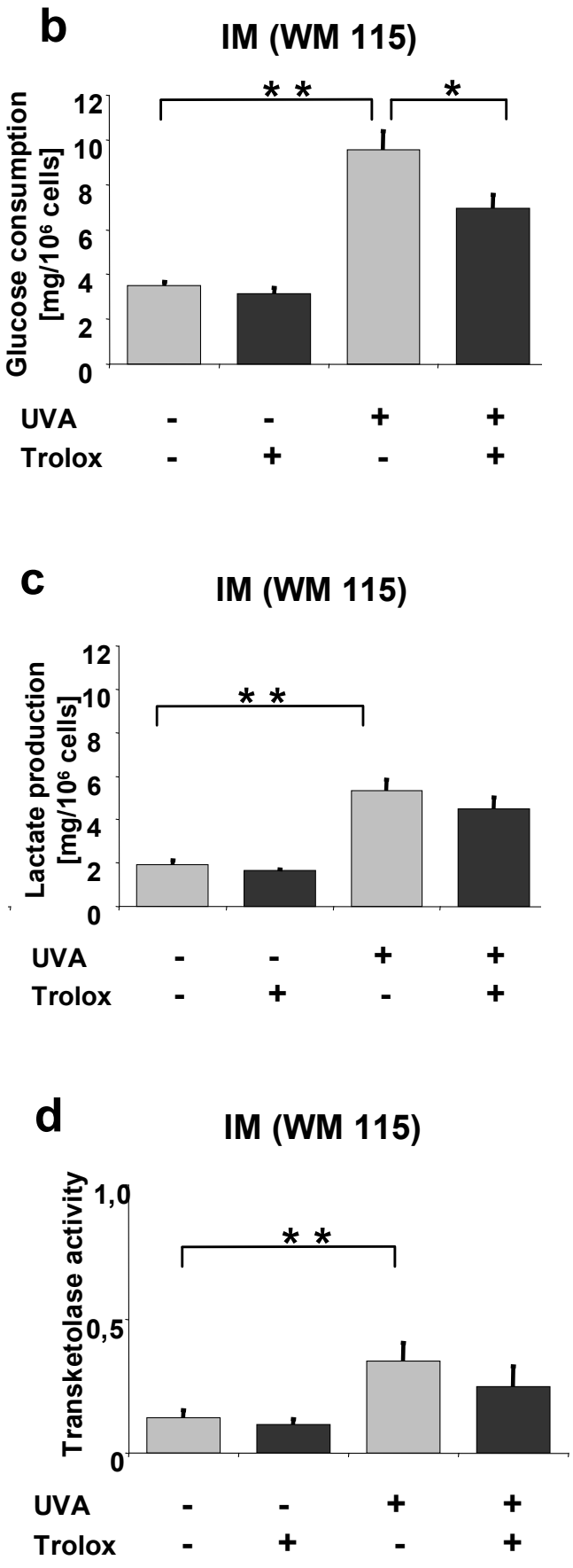

(section from Baban *et al.*, in press)

Figure 18. UVA enhanced Warburg effect and transketolase activity is partially ROS mediated and persists 5 days after UVA treatment.

a. Melanoma cell lines were irradiated 4 days with subsequent recovery for 5 days.

b-d. Glucose consumption, lactate production and transketolase activity relative to cell number were measured before and after the experiment, UVA enhanced glucose consumption, lactate production and trasketolase activity was still significantly (students t-test; $p<0.01$) increased 5 days after the last UVA irradiation (figure 9 b-d). This long term effect of UVA induced glucose consumption and lactate production was comparable in magnitude to the immediate UVA induced Warburg effect and was also ROS mediated as addition of ROS quencher Trolox decreased this long term persistence (section from Baban *et al.,* in press).

When compared to unirradiated controls, UVA mediated induction of glucose consumption and lactate production continued 5 days after cessation of the last UVA irradiation (figure 18 b-c). Again, this UVA induced long term persistence of elevated glucose consumption and lactate production was partially ROS mediated, similar to the immediate UVA induced Warburg effect, as addition of ROS quencher Trolox again reduced this long term persistence (figure 18 b-c). Similar to the UVA induced Warburg effect, UVA induced transketolase activity also persisted (figure 18 d) even 5 days after irradiation and was still significantly higher than in unirradiated controls. This UVA induced persistent increase in transketolase activity could be partially attenuated by the ROS quencher Trolox (figure 18 d) (section from Baban *et al.,* in press).

1.9 Measurement of influenced UVA irradiation on different metabolomics by NMR spectroscopy

To further analyze UVA induced metabolic changes, we investigated the production and consumption of different metabolites in the supernatants and melanoma cell pellets with NMR analysis in collaboration with the University of Regensburg (Prof Gronwald).

1.9.1 Detection of UVA induced Warburg effect by NMR spectroscopy

We investigated in greater detail UVA induced Warburg effect by NMR spectroscopy in the supernatants of control and UVA irradiated melanoma cells. Melanoma cell lines from IM and MM were irradiated with 6 J/cm^2 of UVA three times daily for 4 consecutive days, without recovery (figure 19). According to the NMR protocol, sample preparation was performed, which described in the material and method section.

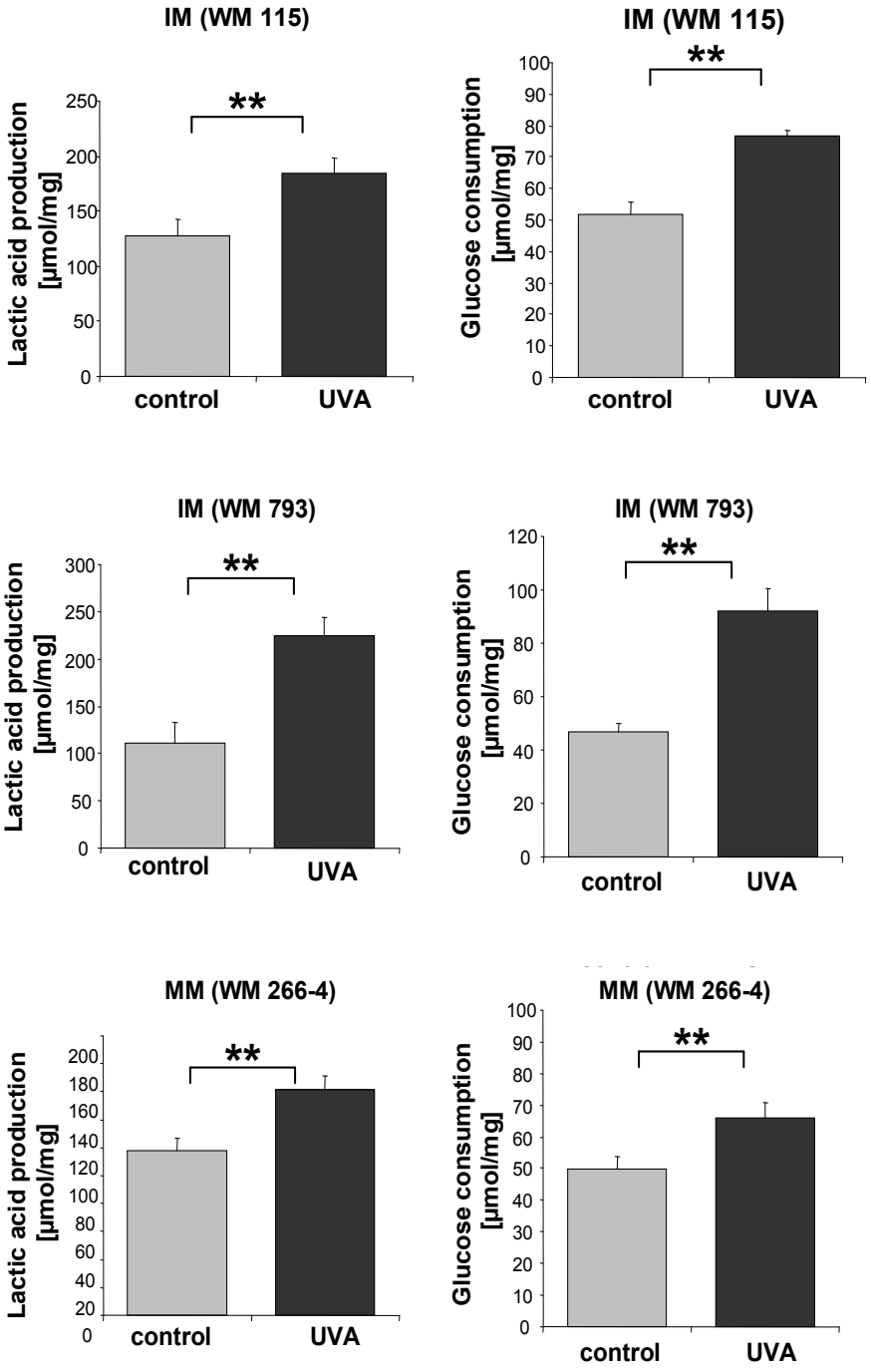

Figure 19. UVA induced Warburg effect analyzed by NMR spectroscopy.

UVA induced Warburg effect in the supernatant of initial melanoma (IM) and metastasizing melanoma (MM) cells was investigated by NMR spectroscopy. Glucose consumption and lactate production significantly (students t-test; $p<0.05$) increased by UVA irradiation and were normalized to mg of total cell protein content. Data are presented as mean value with standard deviation of three independent experiments.

The NMR spectroscopy result of UVA induced Warburg effect showed increased glucose consumption and lactate production, which is confirming our result of UVA induced Warburg effect by color enzymatic method (figure 12). The results are

displayed in µmol/mg as they were normalized to mg of total cell protein content in melanoma cell lines (figure 19).

1.9.2 Investigation of UVA induced differences in metabolomics of melanoma cells in the supernatant by NMR spectroscopy

To investigate further UVA induced metabolic changes, we analyzed the secretion (figure 20 a) or uptake (figure 20 b) of different metabolites in the supernatant of control and UVA irradiated melanoma cell lines from IM and MM by NMR spectroscopy (figure 20 a and b). Comparision of the metabolism of different cancer cells and primary cells revealed differences in some metabolites already discussed in literature, as some of these metabolites have been investigated in these studies (Scott DA.*et al*., 2011; Dettmer *et al.,* 2013).

a

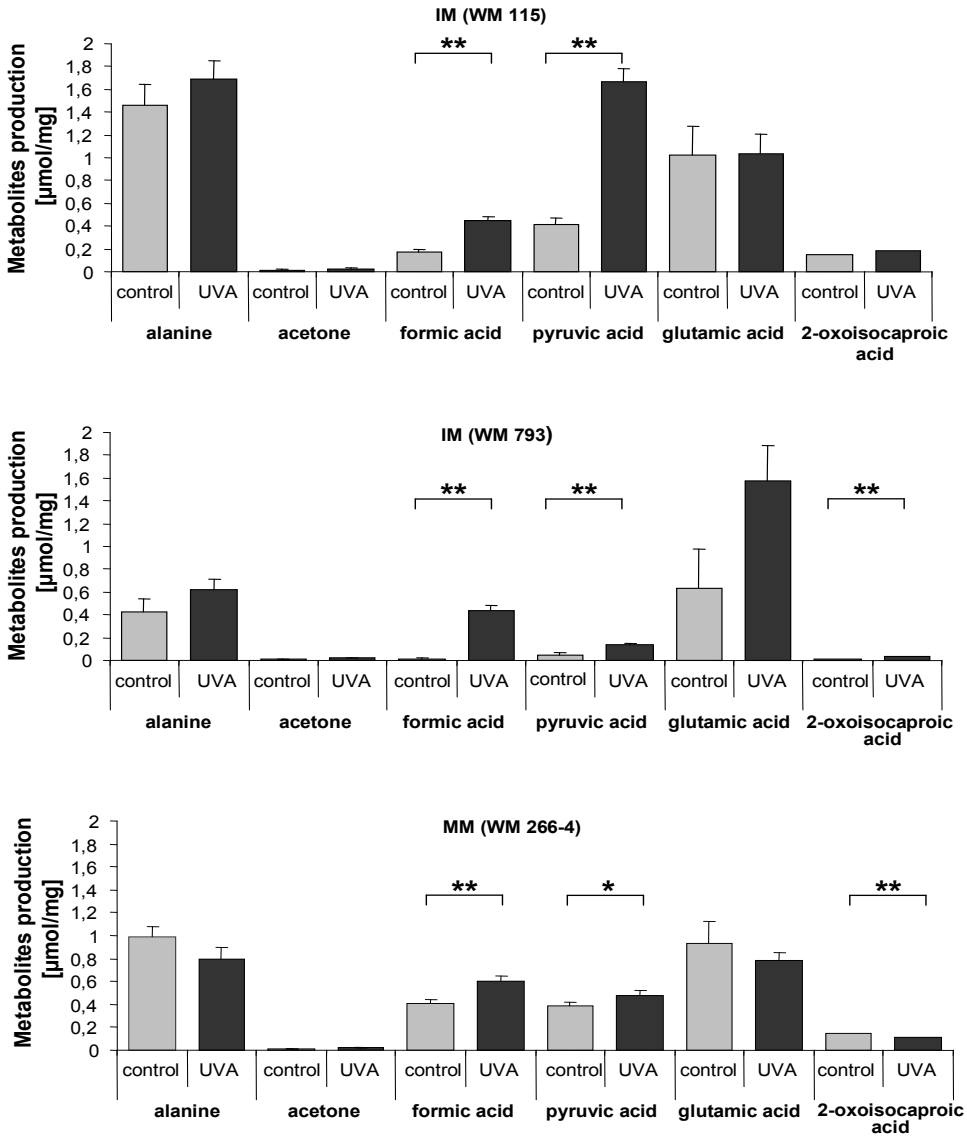

b

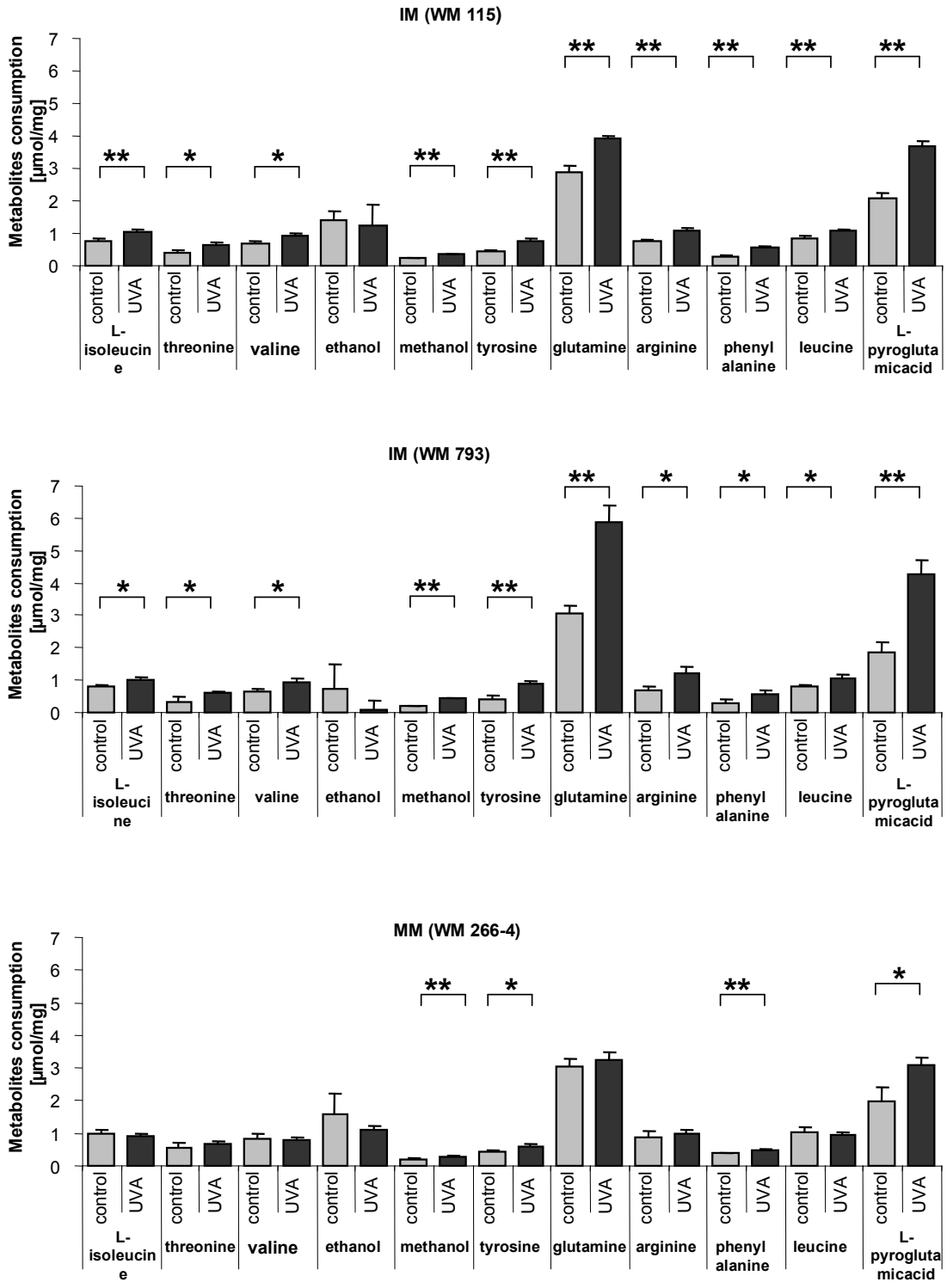

Figure 20. Change of metabolites upon UVA irradiation in the supernatant of melanoma cells.
Change of metabolites in the supernatant of melanoma cell lines from initial melanoma (IM) and metastasizing melanoma (MM) with and without 6 J/cm^2 UVA irradiation. Displayed are levels relative to mg of total cell protein content and data are presented as mean value with standard deviation of three independent experiments.

a. Secretion of metabolites changed upon UVA irradiation. Treatment with UVA irradiation significantly (students t-test; $p<0.05$) increased secretion of formic acid and pyruvic acid in the supernatant of IM and MM cells.
b. Treatment of melanoma cells with UVA irradiation changed consumption of metabolites in the supernatant and the consumption of L-isoleucine, threonine, valine, tyrosine, glutamine, arginine, phenylalanine, leucine and L-pyroglutamicacid was significantly (students t-test; $p<0.05$) increased upon UVA irradiation in IM cells.

The secretion of different metabolites in the supernatant of melanoma cells from IM and MM significantly (students t-test; $p<0.05$) increased secretion of formic acid and pyruvic acid upon UVA irradiation (figure 20 a).
Furthermore, the consumption of metabolites in the supernatant of melanoma cell lines from IM was significantly (students t-test; $p<0.05$) increased for L-isoleucine, threonine, valine, tyrosine, glutamine, arginine, phenylalanine, leucine and L-pyroglutamicacid consumption and for MM only tyrosine, phenylalanine and L-pyroglutamicacid consumption was significantly (students t-test; $p<0.05$) increased, upon UVA irradiation (figure 20 b).

1.9.3 Investigation of UVA induced differences in metabolomics of melanoma cells in the pellets by NMR spectroscopy

Furthermore, UVA induced metabolic changes were investigated in the melanoma cell pellets. The concentration of metabolites inside melanoma cells from IM and MM of control and UVA irradiated cells was detected by NMR spectroscopy (figure 21).

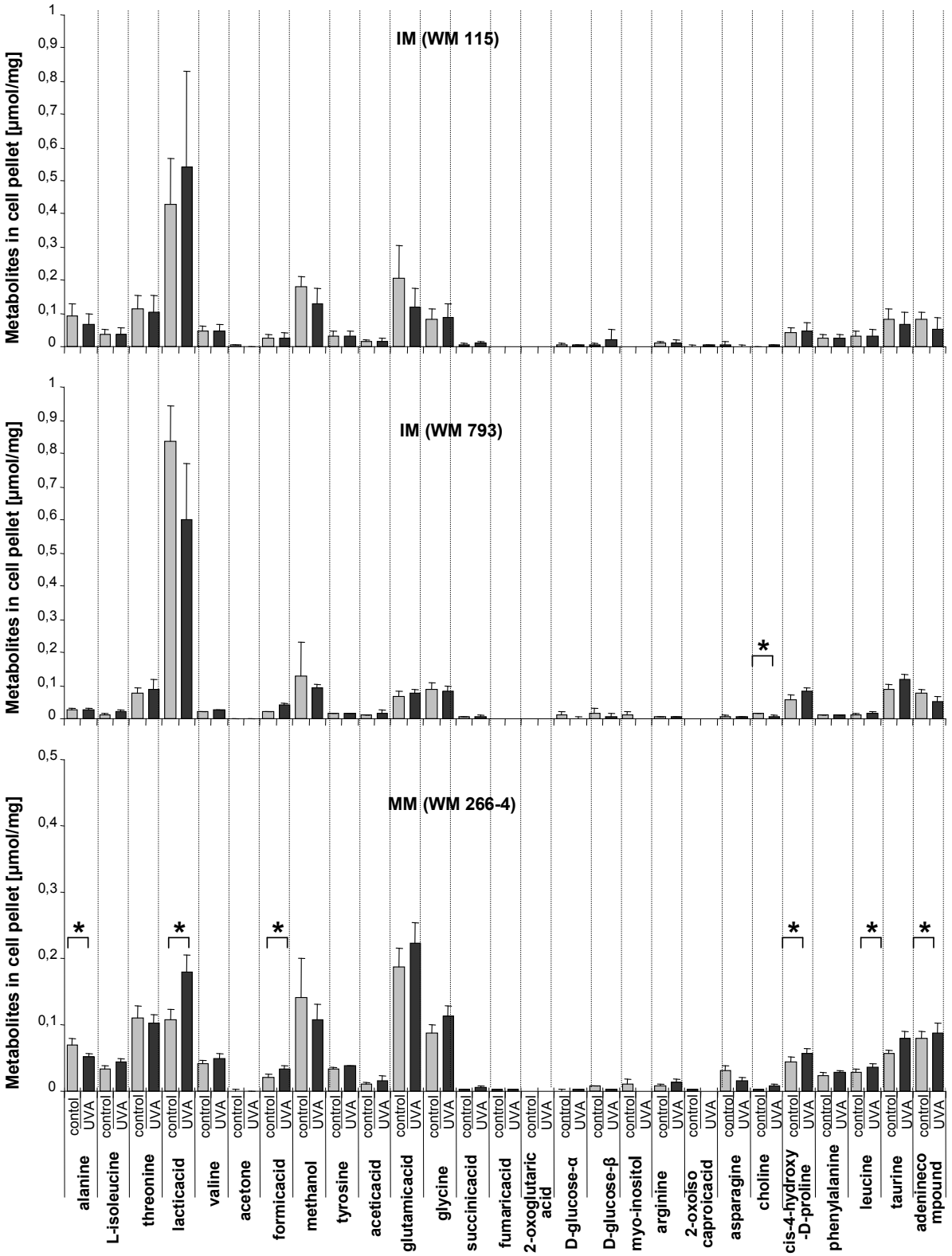

Figure 21. Change of metabolites upon UVA irradiation in the melanoma cell pellets.

Change of metabolites in the melanoma cell pellets of melanoma cells from initial melanoma (IM) and metastasizing melanoma (MM) with and without 6 J/cm^2 UVA irradiation are displayed relative to mg of total cell protein content in µmol/mg and data are presented as mean value with standard deviation of three independent experiments.

The experiments showed, that UVA irradiation changed the metabolism of all metabolites investigated (alanine, L-isoeudine, threonine, lactica acid, valine, acetone, formic acid, methanol, tyrosine, acetic acid, glutamic acid, glycine, succinic acid, fumaricacid, 2-oxoglutaric acid, D-glucose-α, D-glucose-β, myo-inositol, arginine, 2-oxoiso caproicacid, asparagines, choline, cis-4-hydroxy-D-proline, phenylalanine, leucine, taurine and adenine compound) in the melanoma cell pellets from IM and MM. But these differences were heterogeneous among the different melanoma cell lines (WM 115, WM 793 and WM 266-4).

Treatment with UVA irradiation changed the production of the metabolite choline significantly (students t-test; $p<0.05$) in initial melanoma (WM 793) cells and production of the metabolites alanine, lactic acid, formic acid, cis-4-hydroxy-D-proline, leucine and adenine compound was changed significantly (students t-test; $p<0.05$) in metastasizing melanoma (WM 266-4) cells (figure 21).

1.10 Investigation of UVA induced cell signaling pathways

UVA irradiation induced metabolic changes (figure 19, 20 and 21) and UVA induced Warburg effect persists beyond the last UVA irradiation (figure 18) and metabolic changes, induced by UVA irradiation could have functional relevance for tumor progression. In order to investigate the complex signal transduction mechanisms, which are responsible for UVA induced metabolic changes we analyzed early UVA induced signaling events, which are known in other dermal cells. Epidermal growth factor receptor (EGFR) and insulin-like growth factor receptor (IGFR) are early targets of UVA signaling.

Akt is a protein kinase that involved in PI3K/AKT/mTOR signaling (Bunney and Katan, 2010; Majewski *et al.,* 2004). Interestingly, Akt phosphorylation at serine 473 is present in the majority of immunohistologically investigated melanomas (Dhawan *et al.*, 2002) and it has been shown that increased glycolysis and overexpression of TKTL1 is correlated with the activation of Akt (Elstrom *et al.*, 2004; Langbein *et al.*, 2006) and activation of Akt is dramatically increased with melanoma progression (Dai DL *et al.,* 2005).

Furthermore, we analyzed hypoxia inducible factor 1 alpha (HIF1α), which mediates transcription of different target genes, associated with glycolysis and involved in various cellular processes in hypoxic microenvironment (Demaria *et al.,* 2010). The upregulation of HIF1 in many tumors such as head and neck cancer, cervical cancer

and renal cell carcinoma induced by hypoxia are associated with tumor progression (Kuphal *et al.,* 2010). It has been shown, that in malignant melanoma even in normoxic condition, HIF1 activity is increased, due to constitutive HIF1α activation that is regulated by ROS (Kuphal *et al.,* 2010). Poly ADP ribose polymerase 1 (PARP1) is an enzyme which has a role in DNA damage signaling and DNA strand break repairs, expressing its functionality by binding to damaged DNA (Polo and Jackson, 2011).

1.10.1 EGFR and IGFR internalization by UVA

Epidermal growth factor receptor (EGFR) and insulin-like growth factor receptor (IGFR) are early targets of UVA signaling and it is known that EGFR and IGFR signaling cascades are important during UV radiation mediated stress signaling (El-Abaseri *et al.*, 2006; Lopez-Camarillo *et al.*, 2012) (Baban *et al.,* in press). After activation both receptors are internalized from the surface of the membrane. To investigate the role of UVA irradiation on EGFR and IGFR signaling of melanoma cells, internalization of the EGFR and IGFR population was measured indirectly by detection of EGFR and IGFR on cellular surface with fluorescence labeled antibodies by FACS analysis (figure 22).

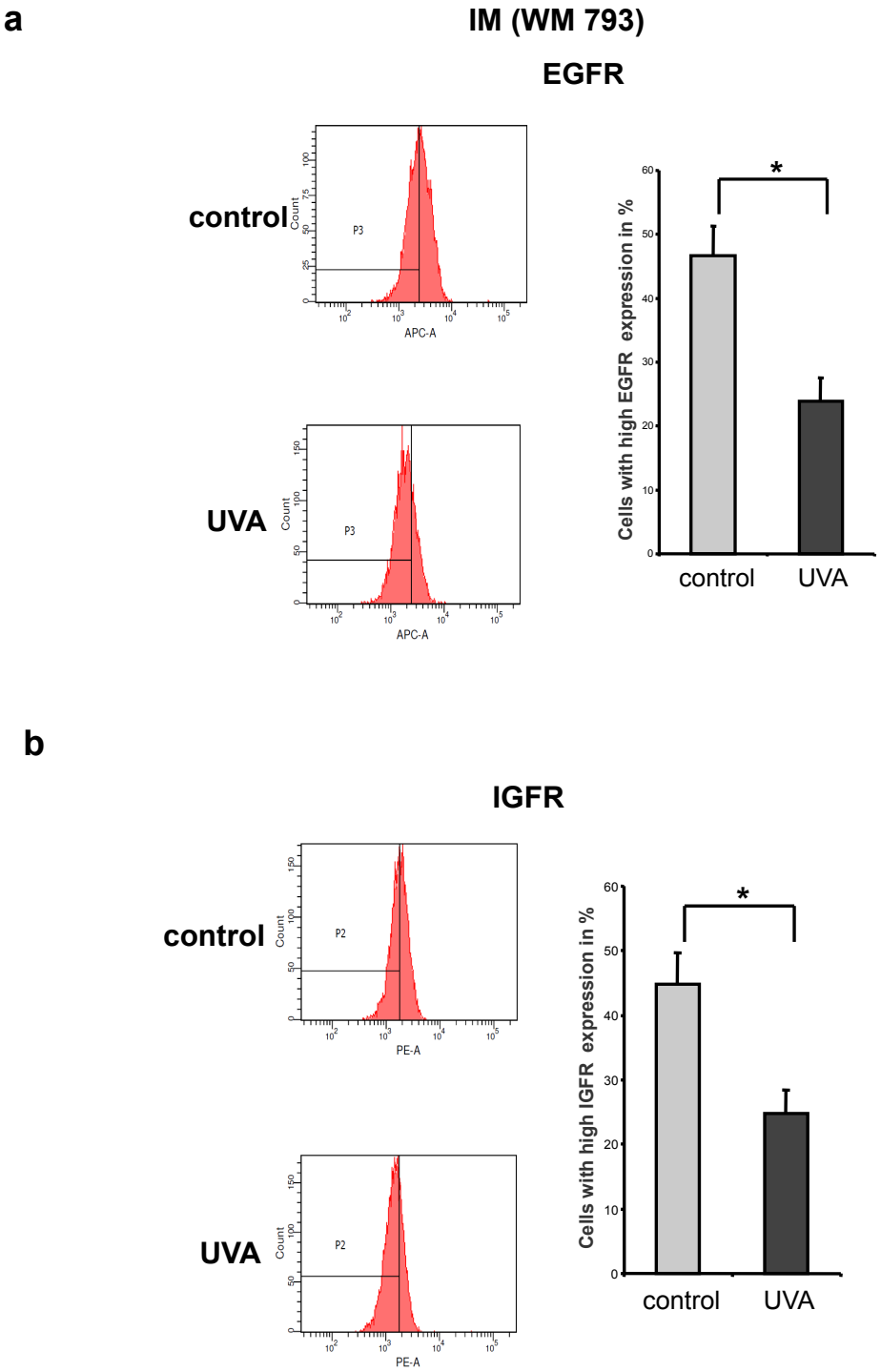

Figure 22. UVA induced internalization of EGFR and IGFR.

a-b. The fluorescence activity of EGFR and IGFR stained with fluorescent antibodies on the cellular surface of melanoma cells from initial melanoma (WM 793) treated with and without 6 J/cm^2 UVA irradiation was measured with FACS. The mean fluorescence intensity of UVA treated melanoma cells decreases significantly (students t-test; $p<0.05$) compared to control, showing enhanced internalization of EGFR and IGFR. Data are presented as mean value of three independent experiments with standard deviation.

We found a significant decrease in the EGFR of and IGFR population on cellular surface upon UVA treatment (figure 22). These results point to a higher UVA induced turnover of EGFR and IGFR and to a UVA induced activation of EGFR and IGFR.

1.10.2 EGFR activation

To investigate UVA induced EGFR activation, the level of phosphorylated (Tyr 1068) EGFR was determined with Western blot. The expression of phosphorylated EGFR (pEGFR) within the melanoma cells from IM was analyzed with and without UVA and normalized to the expression of beta actin (ß actin) as a house keeping protein. We could see a slight increase of phosphorylated EGFR (pEGFR) upon UVA irradiation. UVA irradiation significantly (students t-test; $p<0.05$) increased the level of phosphorylated EGFR (pEGFR) in initial melanoma (793WM) cell line (figure 23).

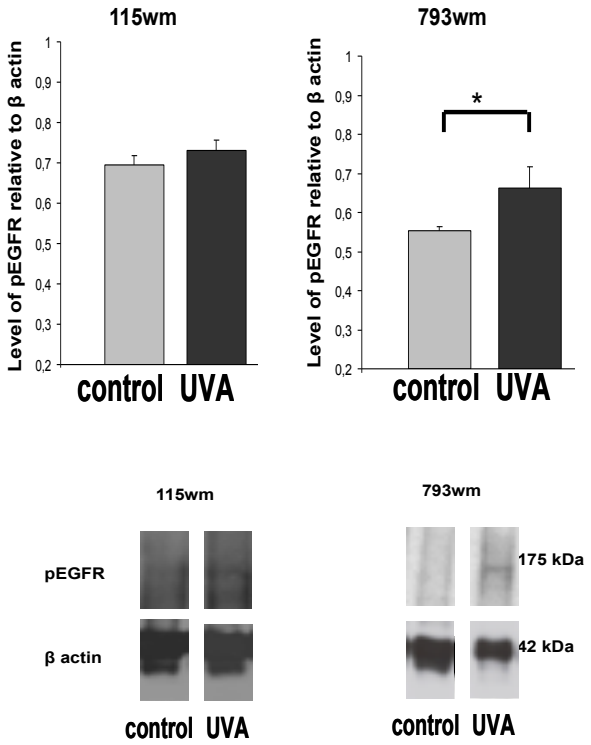

Figure 23. UVA irradiation enhanced activation of EGFR.

Melanoma cells from initial melanoma (IM) were irradiated with and without 6 J/cm^2 UVA three times daily for 4 consecutive days with subsequent detection of phosphorylated (Tyr 1068) EGFR and ß actin by Western blot and the level of pEGFR relative to ß actin was quantified densitometrically. Data represent the mean of three independent experiments with standard deviation.

1.10.3 Akt activation

Hyperactivation of the protein kinase Akt by phosphorylation at the serine residue 473 is associated with (Volker *et al.*, 2008) and UVA stimulation of the EGFR may activate protein kinase Akt as proliferative factor. In order to analyze the level of activated Akt upon UVA irradiation, melanoma cell lines from IM and MM were exposed to 6 J/cm^2 UVA three times daily for 4 consecutive days and after treatment the levels of phosphorylated (Ser 473) Akt was determined by Western blot. Repetitive UVA irradiation significantly (students t-test; $p<0.05$) enhanced the level of phosphorylated Akt (pAkt) in IM cells and it was also increased in MM cells (figure 24) (section from Baban *et al.,* in press).

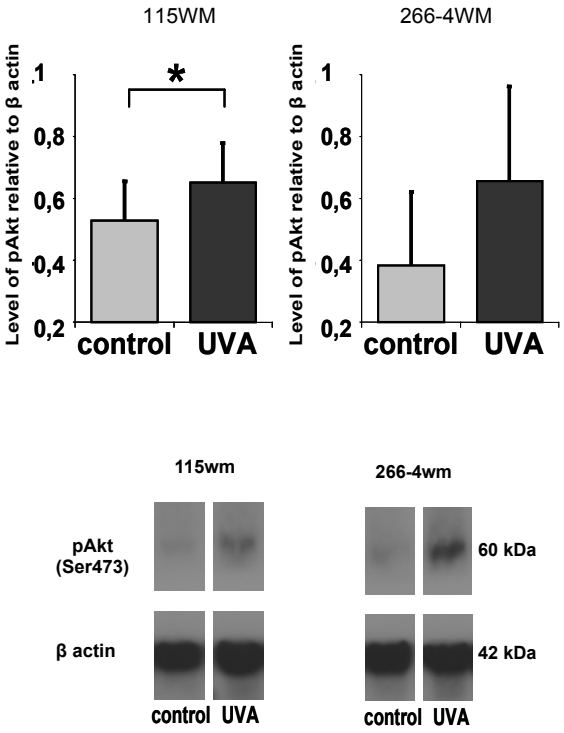

(section from Baban *et al.,* in press)

Figure 24. UVA irradiation enhanced activation of Akt.

Melanoma cell lines from initial melanoma (IM) and metastasizing melanoma (MM) were treated with and without 6 J/cm^2 UVA three times daily for 4 days with subsequent detection of phosphorylated (Ser 473) Akt and ß actin by Western blot and the level of pAkt relative to ß actin was quantified densitometrically. Data represent the mean of three independent experiments with standard deviation (section from Baban *et al.,* in press).

1.10.4 Transcription of HIF1α and PARP1 by real time PCR

Hypoxia inducible factors 1 (HIF1) is a transcription factor, which is associated with tumor growth and it could be affected by UVA induced ROS. Poly ADP ribose polymerase 1 (PARP1) or poly ADP ribose synthase 1 (PARP1) is involved in differentiation, proliferation and tumor transformation (Rojo *et al.,* 2012; Wang *et al.,* 2015), also PARP1 has role in single stranded DNA (ssDNA) breaks repair, which can occur after UVA irradiation and with its enzymatic activity NADH is needed, which can influence the metabolism. To determine the influences of UVA irradiation on expression of HIF1alpha (HIF1α) and PARP1, real time PCR was performed. UVA irradiation treatment for 4 days induced slight up regulation of HIF1α and PARP1 gene expression compared to untreated cells but the influences were not significant (students t-test; $p<0.05$) (figure 25).

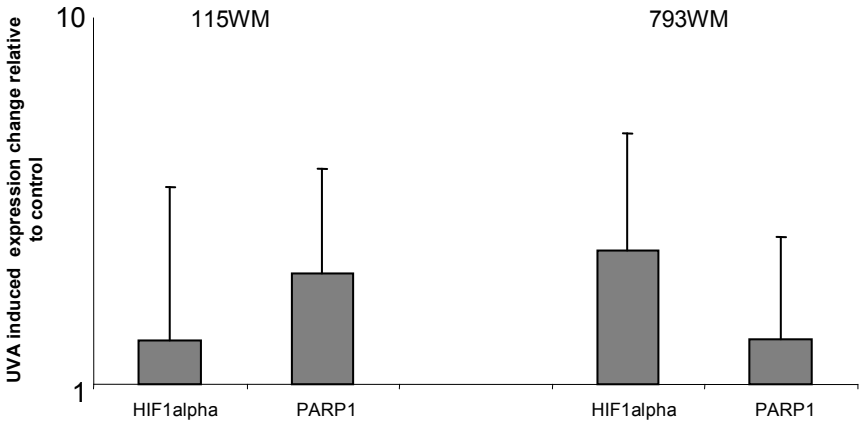

Figure 25. UVA irradiation influenced HIF1alpha and PARP1 gene expression.
The transcription level of HIF1alpha (HIF1α) and PARP1 relative to house keeping gene ß actin was compared with and without UVA irradiation. The transcription level of HIF1α and PARP1 was slightly increased after exposure to UVA irradiation but the changes were not significant. Data are presented, as mean value with standard deviation of three independent experiments and it is shown in $2^{-\Delta\Delta Ct}$ in logarithmic scale, which means the difference in the target gene between treated and control samples.

1.10.5 Analysis of HIF1α protein expression by Western blot

To investigate further UVA induction of HIF1α, melanoma cells from IM were exposed to UVA and after treatment the levels of HIF1α protein were determined by Western blot. The expression of total HIF1α protein within the cell was normalized to the expression of ß actin as a house keeping protein. We could see a slight

upregulation of HIF1α upon UVA irradiation compared to untreated melanoma cells but the increase was not significant (students t-test; p<0.05) (figure 26).

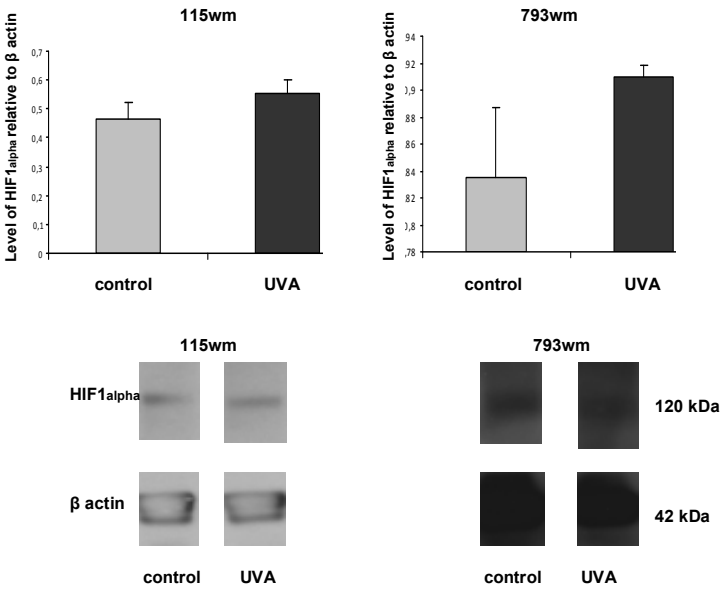

Figure 26. UVA irradiation influenced HIF1α expression.

Melanoma cell lines from initial melanoma (IM) were treated with and without 6 J/cm^2 UVA three times daily for 4 days with subsequent detection of HIF1α and ß actin by Western blot. The level of HIF1α relative to ß actin was quantified densitometrically. Slight upregulation of HIF1α was observed but it was unsignificant change upon UVA irradiation. Data represent the mean of three independent experiments with standard deviation.

1.11 Effect of UVA radiation on gene transcription of different genes involved in DNA repair

UVA radiation causes DNA damage, could interfere with DNA damage related genes that are upregulated upon DNA damage.

To investigate the expression level of different XP genes that are involved in nucleotide excision repair and different pro-apoptotic pathways, real time PCR was performed. By real time PCR analysis the effect of UVA irradiation on expression of the following genes, like XPA, XPB, XPC, XPD, XPE, XPF, XPG, CHK2, HR23a, HR23b, ATM, ATR, BRAC1, BRAC2, BRAC3, ERCC1, BAX, Bcl2, P21, P53 and MDM2 was examined (figure 27).

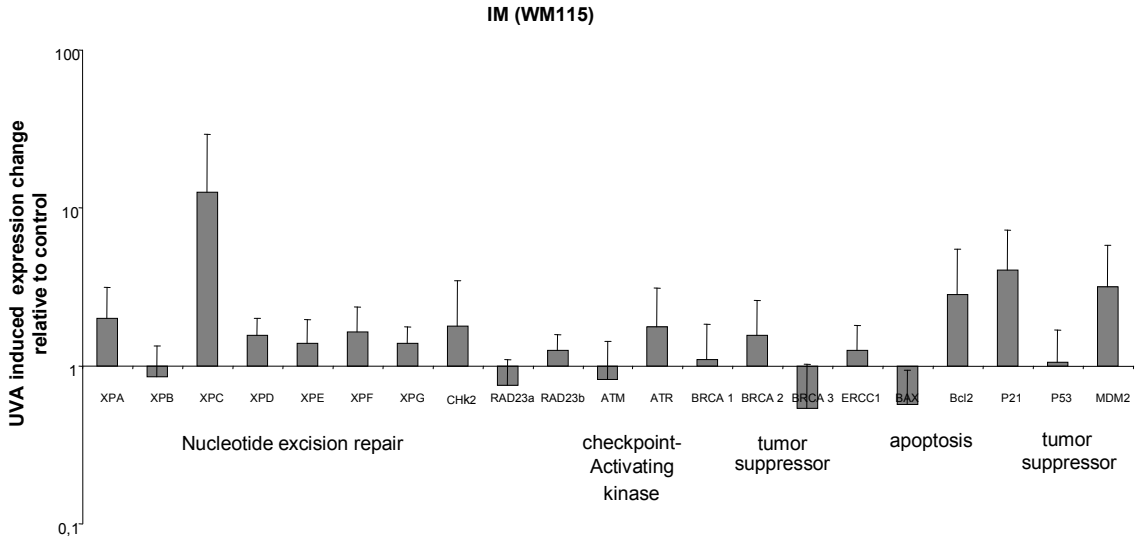

Figure 27. Effect of UVA irradiation on gene transcription of different genes involved in DNA repair.

Melanoma cell line (WM 115) was treated with and without 6 J/cm^2 UVA three times daily for 4 days, the transcriptional levels of XPA, XPB, XPC, XPD, XPE, XPF, XPG, CHK2, HR23a, HR23b, ATM, ATR, BRAC1, BRAC2, BRAC3, ERCC1, BAX, Bcl2, P21, P53 and MDM2 relative to house keeping gene ß actin were compared with and without UVA irradiation. The transcription level of XPC was increased after exposure to UVA irradiation but there were no significant changes in the transcription levels of the other genes investigated. Data are presented as mean value with standard deviation of three independent experiments and displayed in $2^{-\Delta\Delta Ct}$ logarithmic scale, which means the difference in the normalized target gene in the samples with and without UVA irradiation.

The transcription level of XPC is increased more then 10-fold after exposure to UVA irradiation but there were no significant changes in the transcription levels of the other investigated genes (figure 27).

Functional relevance of Warburg effect

1.12 MMPs and uPA expression in melanoma cells

An important step in melanoma progression is invasion of adjacent tissue, facilitated by proteases like matrix metalloproteinases (MMPs) and urokinase type plasminogen activator (uPA) and it was shown that MMP9 and uPA are activated during invasion of melanoma cells (Bianchini *et al.*, 2006; Tang *et al.*, 2013). We investigated the role of UVA irradiation in melanoma progression and invasion via lactic acid alone, which is a major derivate of the UVA induced Warburg effect. Treatment with 20mM lactic acid for 12hr is able to induce expression of MMPs and uPA in melanoma cell lines from IM and MM (figure 28) (section from Baban *et al.,* in press).

a

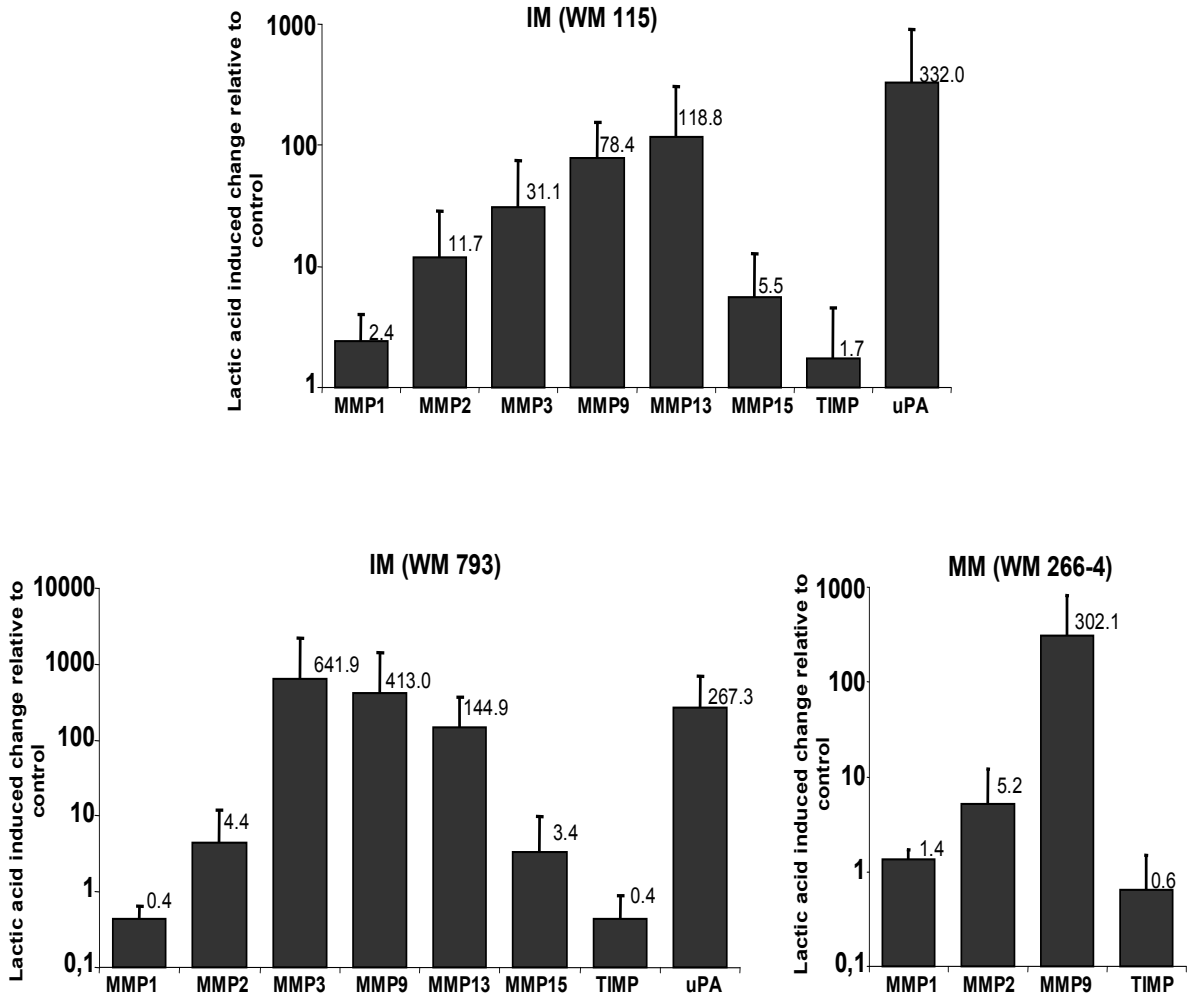

(section from Baban *et al.,* in press)

b

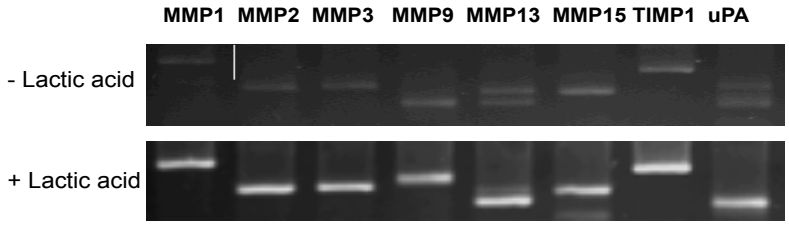

Figure 28. MMP and uPA expression are upregulated after exposure to lactate.

a. Melanoma cells from IM and MM were treated with and without 20mM lactic acid and transcriptional levels of MMP1, MMP2, MMP3, MMP9, MMP13, MMP15, TIMP1 and uPA relative to house keeping gene ß actin were compared with and without lactic acid. MMP and uPA transcription levels are increased after exposure to lactic acid, except MMP1 in initial melanoma cell (WM 793). Data are presented as mean value with standard deviation of at least four independent experiments and data are displayed in $2^{-\Delta\Delta Ct}$ logarithmic scale, which means the difference in the normalized target gene in the treated and untreated samples. (section from Baban *et al.,* in press)

b. Representative gel pictures of target and control amplicons of the real time PCR.

Lactic acid increased the transcription of MMP2, MMP3, MMP9, MMP13, MMP15 and uPA except MMP1 in initial melanoma cells (WM 793). In addition we found a slight induction of TIMP1 in melanoma cells but compared to the transcription levels of most MMPs and uPA these effects of lactate on TIMP1 transcription were negligible (Figure 28).

1.13 MMP2 and MMP9 activity

To show that either UVA irradiation or UVA irradiation associated lactic acid alone is capable to induce the secretion of active tumor relevant MMP2 and MMP9, melanoma cells from IM and MM were treated with and without UVA irradiation and ROS quencher or with lactic acid alone then secretion of active MMP2 and MMP9 was investigated by zymography (figure 29) (section from Baban *et al.,* in press).

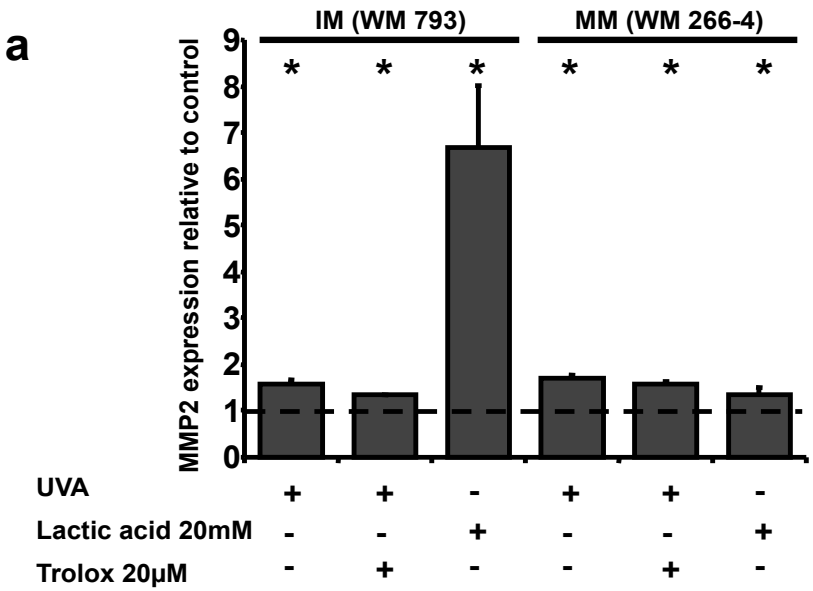

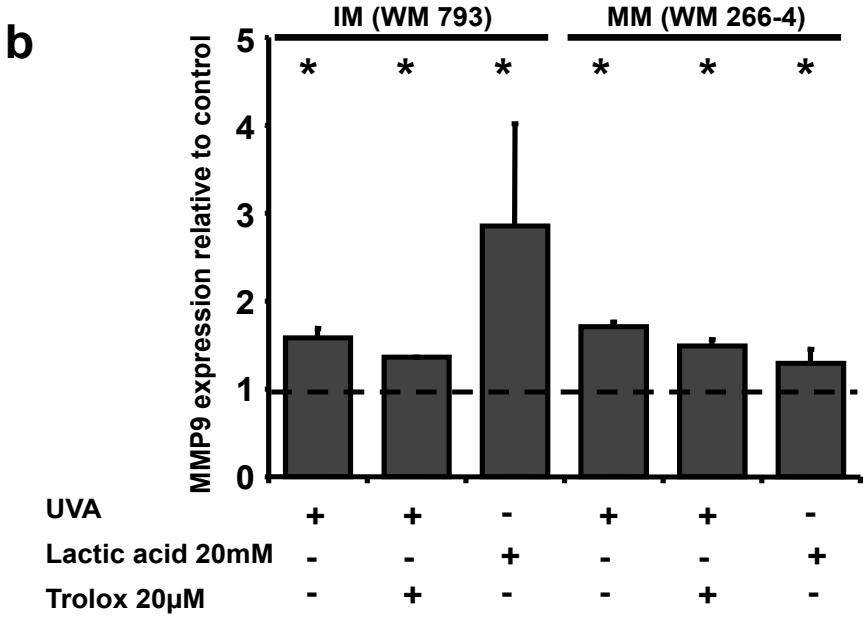

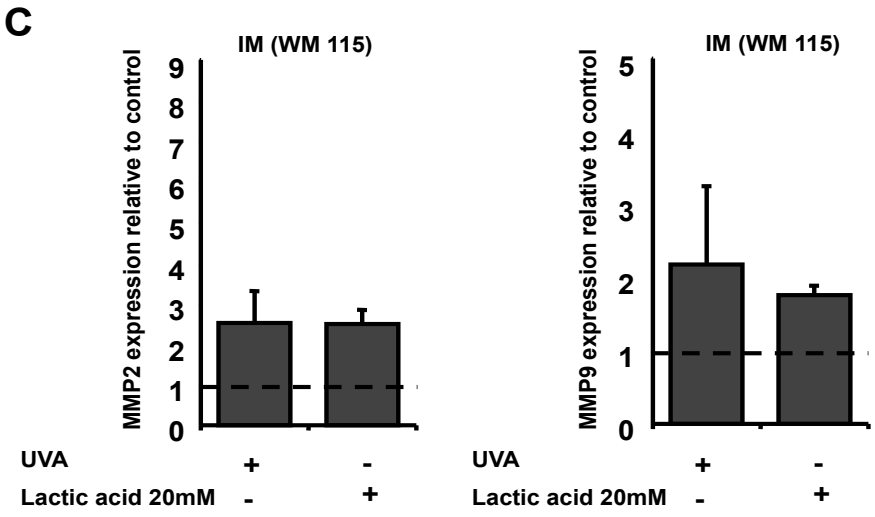

(section from Baban *et al.*, in press)

Figure 29. Zymography for MMP2 and MMP9 activity.

a-b. Different melanoma cells from IM and MM were treated with and without 6 J/cm^2 UVA or with and without 20mM lactic acid and the secretion of active MMP2 and MMP9 was measured with zymography. MMP2 and MMP9 expression are displayed relative to untreated expression samples. UVA irradiation and lactic acid alone significantly increased (students t-test; $p<0.05$) MMP2 and MMP9 secretion and ROS quencher Trolox slightly attenuated the effect. Data are presented as mean value of three independent experiments with standard deviation (section from Baban *et al.,* in press).

c. Melanoma cell line (WM115) was treated with and without UVA or with and without 20mM lactic acid then secretion of active MMP2 and MMP9 was measured with zymography. MMP2 and MMP9 expression is displayed relative to untreated expression samples. UVA irradiation and lactic acid alone increased MMP2 and MMP9 secretion. Data are presented as mean value of three independent experiments with standard deviation (section from Baban *et al.,* in press).

The result of either UVA irradiation, or UVA irradiation associated lactic acid was capable to induce secretion of active tumor relevant MMP2 and MMP9, which was performed with zymography indicate that UVA irradiation induced secretion of active MMP2 and MMP9 in IM and MM cell line, compared to control and UVA induced activity of MMP2 and MMP9 was slightly reduced in the presence of ROS quencher, indicating a partially ROS mediated mechanism of UVA induced MMP2 an MMP9 induction. Furthermore, treatment with lactic acid alone was capable to facilitate secretion of MMP2 and MMP9, when compared to control (figure 29) (section from Baban *et al.,* in press).

.

1.14 uPA activity

To investigate the effect of either UVA irradiation, or UVA irradiation associated lactic acid on the secretion and activation of tumor relevant protease uPA, the activity of uPA was measured in melanoma cell lines from IM and MM treated with and without 6 J/cm^2 UVA irradiation, 20µm ROS quencher Trolox and lactic acid alone (figure 30) (section from Baban *et al.,* in press).

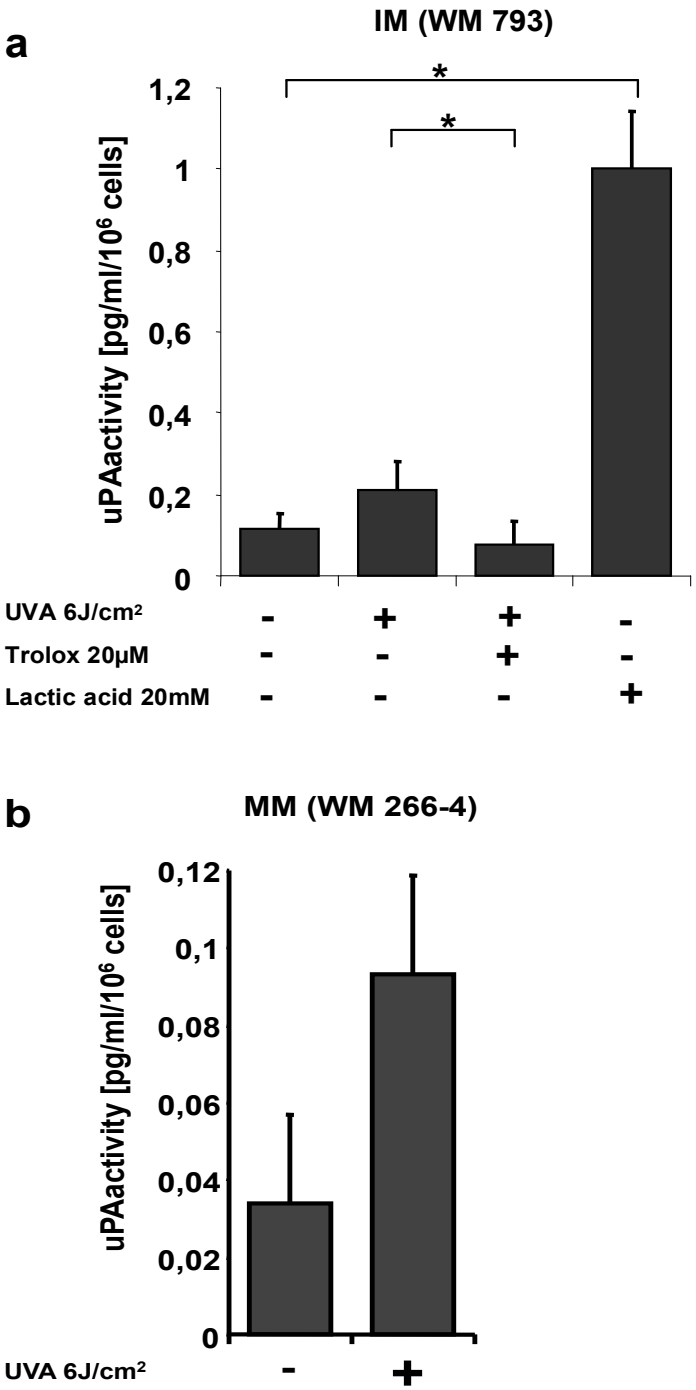

(section from Baban *et al.,* in press)

Figure 30. uPA activity induced by UVA irradiation.

a. Secretion and activation of uPA were measured in melanoma cells (WM 793), which were treated with and without 6 J/cm^2 UVA, 20µm ROS quencher Trolox, and 20mM lactic acid and normalized to number of cells. UVA induced uPA secretion and activation, ROS quencher decreased UVA induced uPA secretion and activation (students t-test; $p<0.05$). Treatment with lactic acid alone significantly (students t-test; $p<0.05$) induced uPA secretion and activation. Data are presented as mean value of three independent experiments with standard deviation (section from Baban *et al.,* in press).

b. Secretion and activation of uPA were measured in melanoma cells (WM 266-4) treated with and without UVA and normalized to number of cells. UVA induced uPA secretion and activation. Data are

presented as mean value of three independent experiments with standard deviation (section from Baban *et al.,* in press).

UVA irradiation induced secretion and activation of uPA in melanoma cells from IM and MM cell and UVA induced uPA secretion and activation was slightly reduced in the presence of ROS quencher, which indicates a partially ROS mediated mechanism of UVA induced uPA induction. Furthermore treatment with lactic acid alone was also capable to facilitate secretion and activation of uPA, compared to control in (WM 793) melanoma cells (Figure 30).

1.15 UVA enhanced Warburg effect increased invasion via lactate production

To test whether production of lactic acid, which can be induced by UVA mediated ROS, is functionally capable to enhance invasion of melanoma cells from IM and MM, we performed *in vitro* invasion assays. In these assays UVA irradiated melanoma cells and control (non irradiated) cells were grown on an artificial collagen matrix, where they invade this matrix according to their invasive potential. Melanoma cells were treated with and without 6 J/cm^2 UVA irradiation, 20µM ROS quencher Trolox, 5.5mM glycolytic inhibitor 2-DG and 20mM lactic acid (Figure 31) (section from Baban *et al.,* in press).

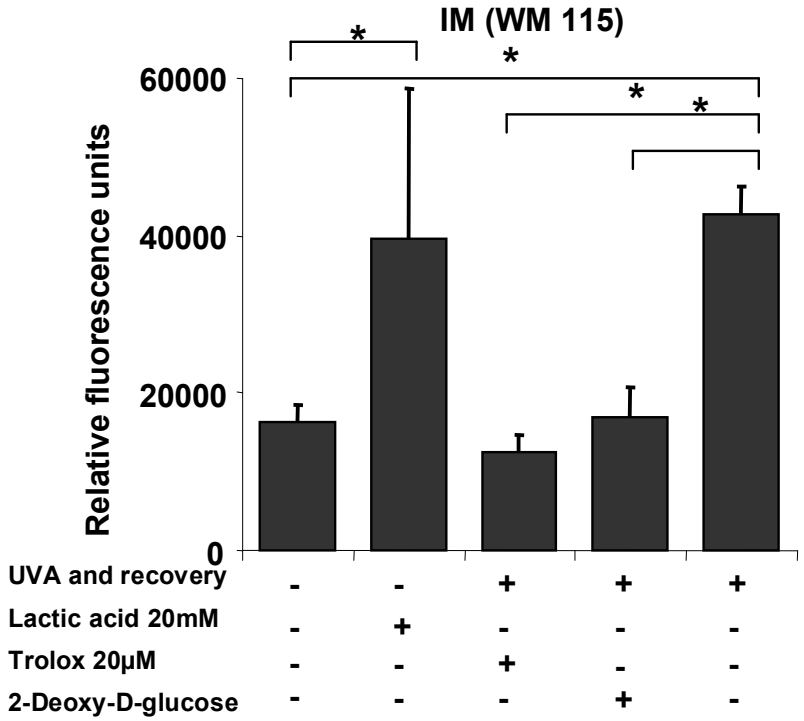

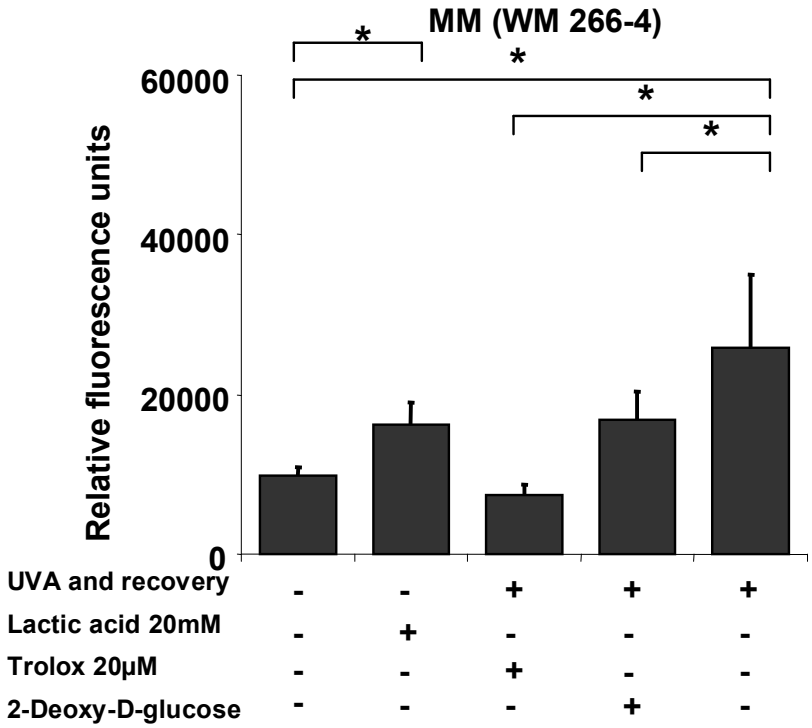

(section from Baban *et al.,* in press)

Figure 31. Lactic acid and UVA enhanced Warburg effect increased *in vitro* invasion in a ROS dependent way.

Invasive potential of melanoma cells from IM and MM after treatment with and without 6 J/cm^2 UVA, 20mM lactic acid, 20µm ROS quencher Trolox and inhibitor of glycolysis 2-DG were measured with *in vitro* invasion assay after recovery. UVA radiation as well as addition of lactic acid increased invasive potential of melanoma cells while addition of ROS quencher Trolox and inhibitor of glycolysis 2-DG decreased invasive potential. Data are presented as mean value with standard deviation of three independent experiments. UVA radiation as well as lactic acid alone enhanced *in vitro* invasion via ROS dependent way (figure 31) (section from Baban *et al.,* in press).

In the invasion assay, UVA irradiation significantly (students t-test; $p<0.01$) increased invasion of melanoma cells from IM and MM and this effect was partially ROS mediated as the ROS quencher Trolox significantly (students t-test; $p<0.01$) attenuated UVA induced invasion. Similarly, the inhibitor of glycolysis 2-DG significantly (students t-test; $p<0.01$) attenuated UVA induced invasion in IM and MM cells. Treatment of melanoma cells with lactic acid alone significantly (students t-test; $p<0.01$) increased invasion to an extent comparable to UVA irradiation. These data show that addition of lactic acid can mimic the UVA induced increase of the invasive potential *in vitro* (figure 31). This lactate production subsequently can lead to

increased expression of MMPs and uPA, which is resulting in increased invasiveness of UVA treated melanoma cells.

1.16 UVA induced invasion is facilitated by MMP and uPA

To investigate to which extent the UVA or lactic acid induced invasion is facilitated either by MMP proteases or by uPA protease, we tested invasive potential of UVA treated cells with and without inhibitors of MMP and uPA (figure 32) (section from Baban *et al.,* in press).

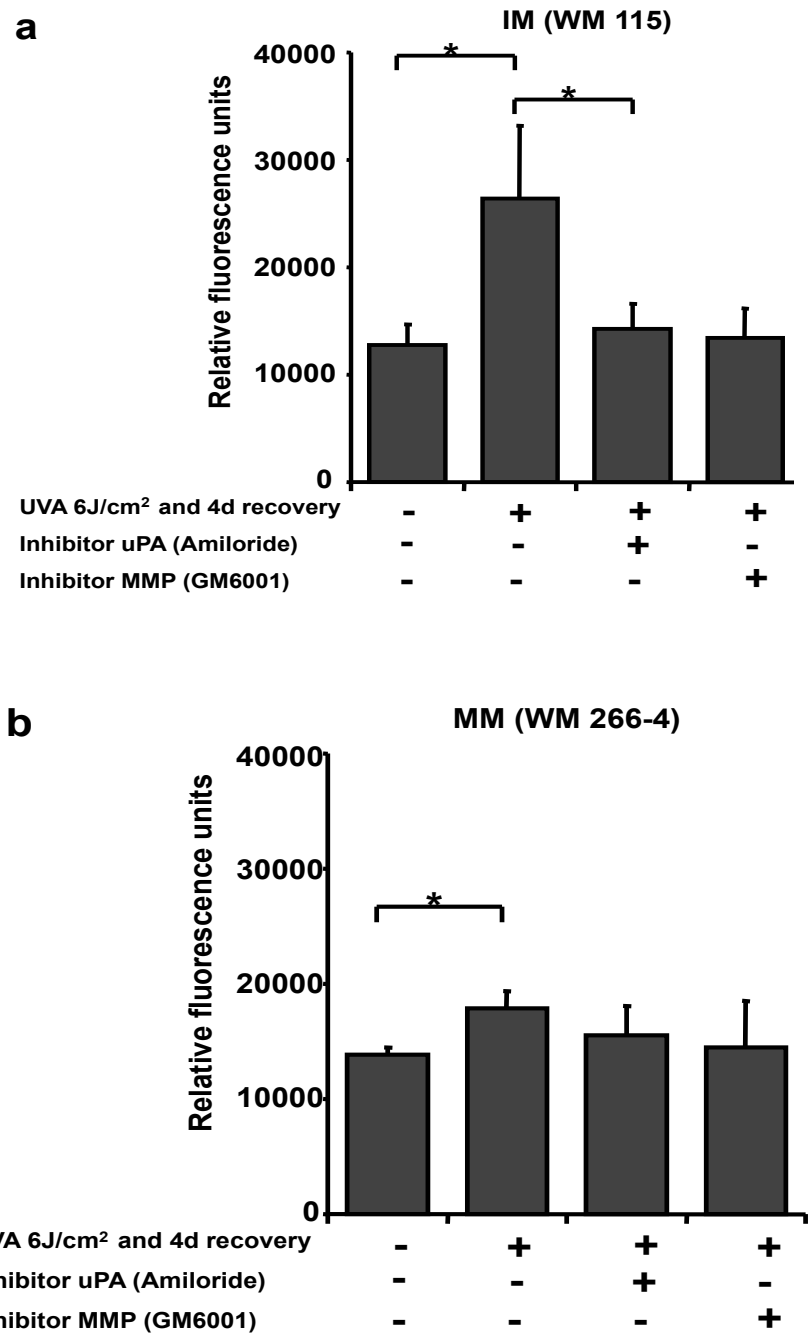

(section from Baban *et al.,* in press)

Figure 32. UVA enhanced invasion attenuated by MMP inhibitor GM6001 or uPA inhibitor Amiloride.

Invasive potential of melanoma cells from initial melanoma (IM) and metastasizing melanoma (MM) treated with and without repetitive 6 J/cm^2 UVA irradiation and with and without 10nM MMP inhibitor (GM6001) or 7µM uPA inhibitor (Amiloride) was measured by an *in vitro* invasion assay. Inhibitors of MMP and uPA decreased UVA induced invasion and the effect of the inhibitor was significantly influenced in melanoma cells from IM. Data are presented as mean value of three independent experiments with standard deviation (section from Baban *et al.,* in press).

Presence of a MMP inhibitor as well as an uPA inhibitor partially abrogated UVA induced invasive potential (figure 32), which indicates MMP as well as uPA are functionally needed for UVA induced invasion *in vitro*.

2. Effect of UVA irradiation on melanoma cells in skin reconstructs

To recapitulate the situation in human skin *in vivo* more closely, effect of UVA irradiation on melanoma cells from IM and MM in the skin reconstruct model was investigated. Skin reconstructs are three dimensional (3D) models of human skin, composed of a dermal layer, consisting of collagen and fibroblasts and an epidermal layer, containing keratinocytes and melanoma cells of different progression level, in our experiment were used. Skin reconstructs were prepared in collaboration with Dr. Tobias Sinnberg (working group of Prof. Birigit Schittek, University of Tuebingen).

2.1 Warburg effect within the human skin reconstruct tissue

The skin reconstructs with melanoma cells were irradiated with 6 J/cm^2 of UVA three times daily for 4 consecutive days and glucose uptake and lactate production was measured within the skin reconstruct tissue (figure 33) (section from Baban *et al.,* in press).

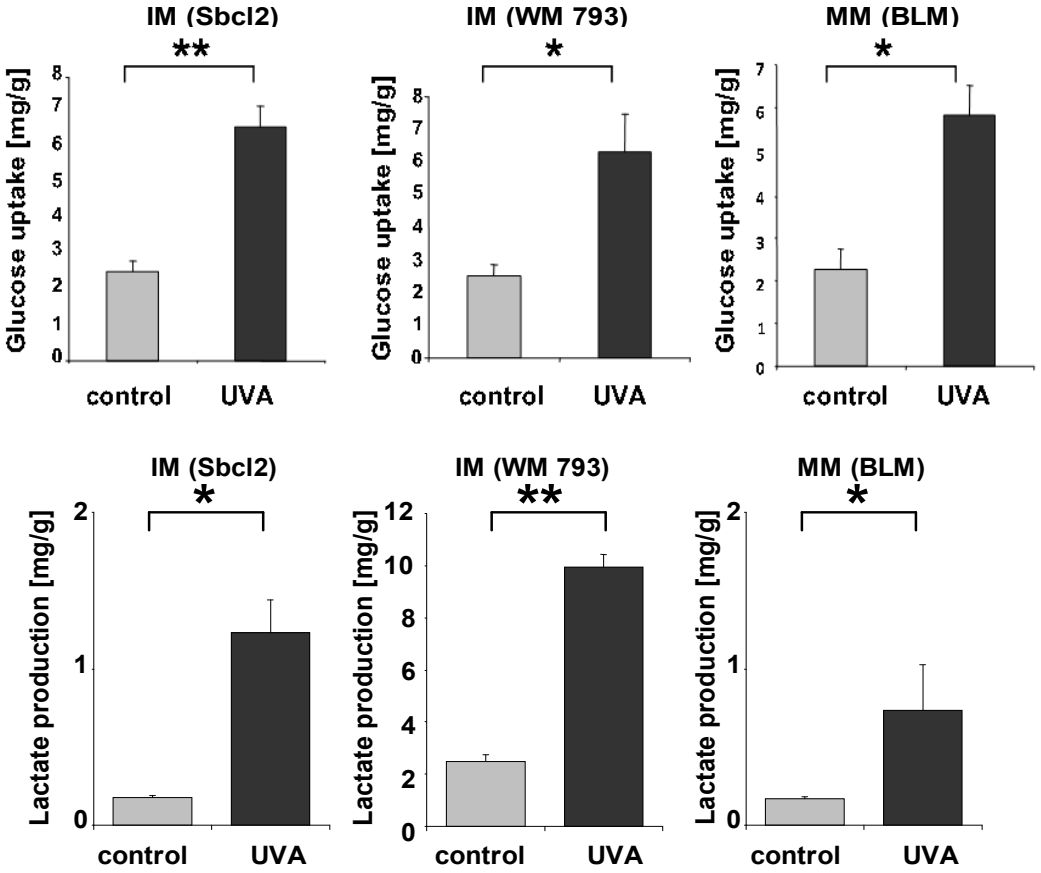

(section from Baban *et al.,* in press).

Figure 33. Effects of UVA irradiation on Warburg effect in the skin reconstruct tissues.

The skin reconstructs with melanoma cell lines from initial melanoma (IM) and metastasizing melanoma (MM) were treated repetitively with 6 J/cm^2 UVA three times daily for 4 consecutive days.

UVA irradiation significantly (students t-test; $p<0.05$) increased glucose uptake and lactate production within skin reconstruct tissues with IM and MM melanoma cells. Glucose uptake and lactate production value were normalized to total weight of respective skin reconstruct samples. Data are presented as mean value with standard deviation of three independent experiments (section from Baban *et al.,* in press).

Glucose uptake and lactate production were significantly (students t-test; $p<0.05$) increased upon UVA irradiation within skin reconstruct tissues with melanoma cell lines from IM and MM (figure 33).

2.2 Effect of ROS quencher Trolox on UVA induced Warburg effect in the human skin reconstructs

Since exposure to UVA irradiation generates ROS, we tested whether UVA induced Warburg effect in skin reconstructs with melanoma cell lines is ROS mediated within skin reconstruct tissues (figure 34 a) and supernatant of skin reconstructs (figure 34 b) by coincubation with 20µm ROS quencher Trolox.

a

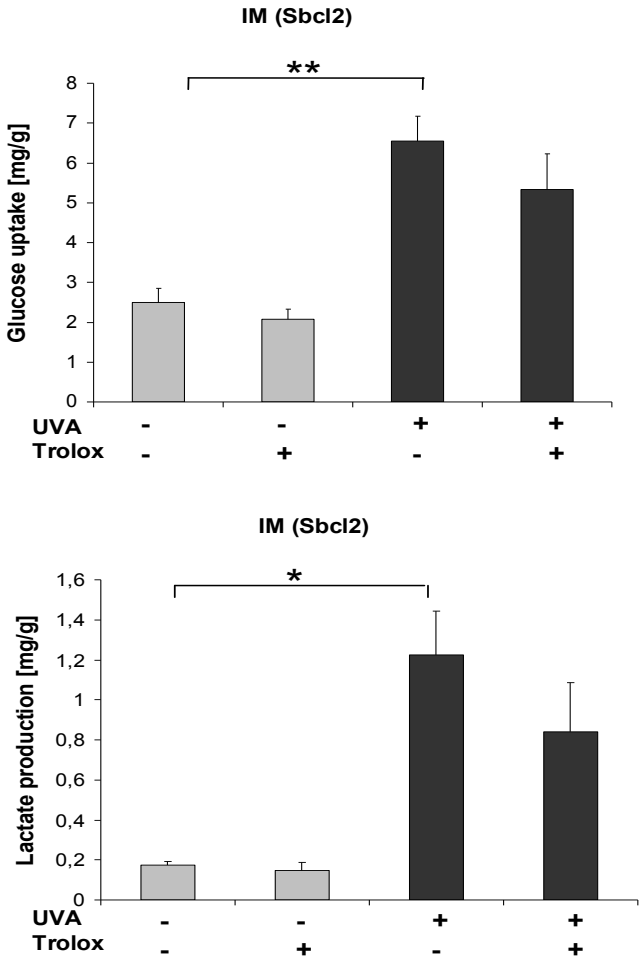

b

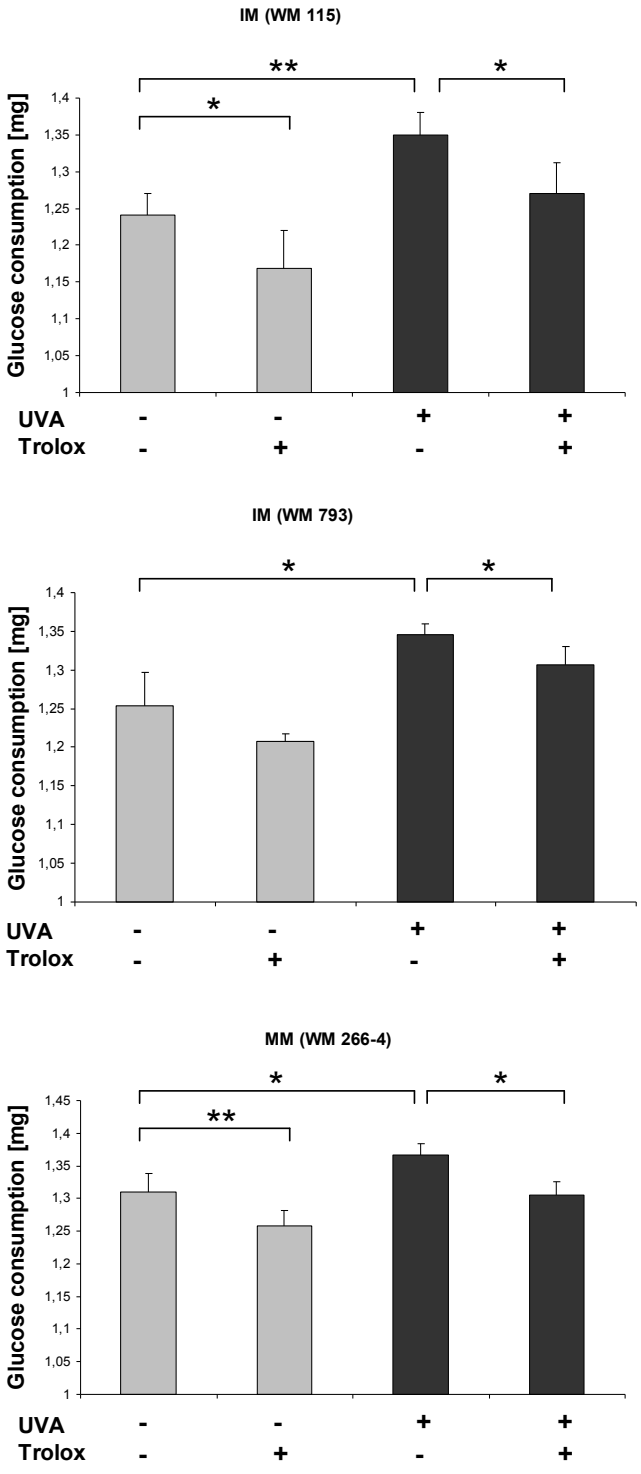
IM (WM 115)
Glucose consumption [mg]
1,4
1,35
1,3
1,25
1,2
1,15
1,1
1,05
1
**
*
*
UVA - - + +
Trolox - + - +
IM (WM 793)
Glucose consumption [mg]
1,4
1,35
1,3
1,25
1,2
1,15
1,1
1,05
1
*
*
UVA - - + +
Trolox - + - +
MM (WM 266-4)
Glucose consumption [mg]
1,45
1,4
1,35
1,3
1,25
1,2
1,15
1,1
1,05
1
*
**
*
UVA - - + +
Trolox - + - +

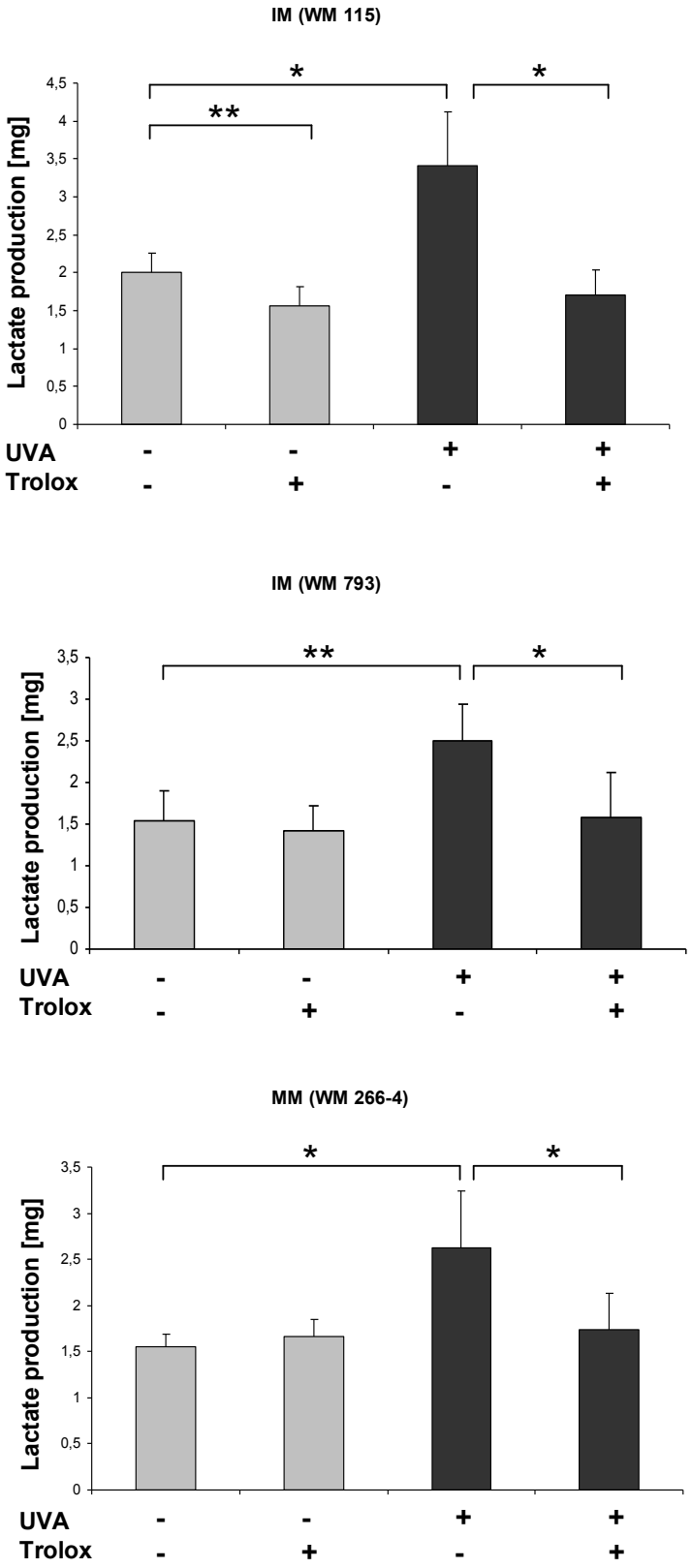

Figure 34. UVA induced Warburg effect is partially attenuated by ROS quencher Trolox.

UVA induced Warburg effect within the skin reconstruct tissues and in the supernatant of different melanoma cell lines from initial melanoma (IM) and metastasizing melanoma (MM) with and without ROS quencher Trolox was measured.

a. UVA induced Warburg effect is partially attenuated by decreasing glucose uptake and lactate production within the skin reconstruct tissues when they were treated with 20µm ROS quencher Trolox.
b. UVA induced Warburg effect is significantly (students t-test; $p<0.05$) attenuated by decreasing glucose consumption and lactate production with UVA treated samples in the supernatant of skin reconstructs when they were treated with 20µm ROS quencher Trolox.

In the supernatant of the skin reconstructs glucose consumption and lactate production was increased upon UVA irradiation and coincubation with ROS quencher Trolox decreased this effect, indicating a partially ROS mediated mechanism of UVA induced glucose consumption and lactate production within the skin reconstruct tissues and skin reconstruct supernanats (figure 34 a and b).

2.3 Effect of sunscreen product on UVA induced Warburg effect in the human skin reconstructs

Sunscreen product has a protective effect against sunburn, induced by UV radiation in human skin (Autier P., 2000; Kaur *et al.,* 2014). To show that sunscreen is capable to decrease the UVA induced Warburg effect, we treated human skin reconstruct with a sunscreen product during irradiation courses before measuring glucose consumption and lactate production in the supernatant of human skin reconstructs with and without sunscreen product and additionally with ROS quencher Trolox (figure 35).

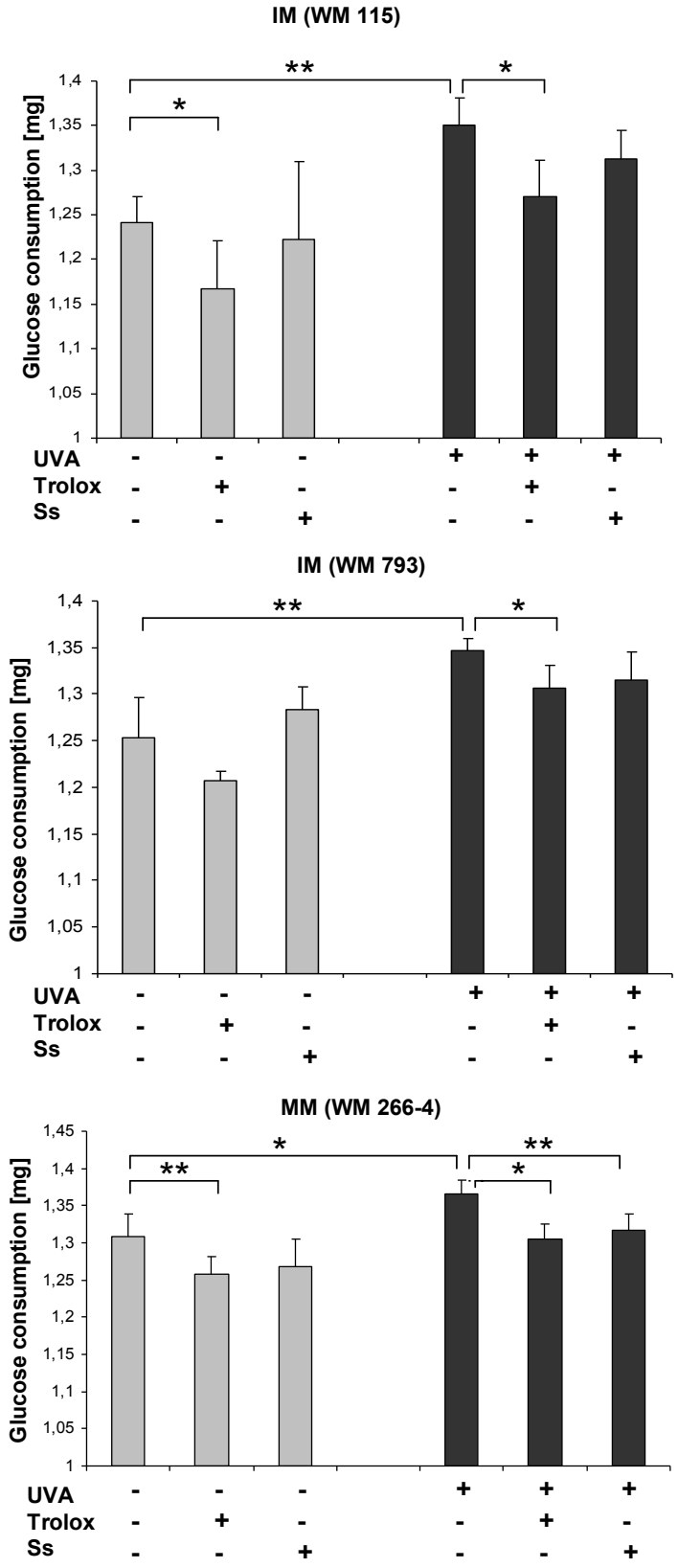
IM (WM 115)
Glucose consumption [mg]
1,4
1,35
1,3
1,25
1,2
1,15
1,1
1,05
1
**
*
*
UVA - - - + + +
Trolox - + - - + -
Ss - - + - - +
IM (WM 793)
Glucose consumption [mg]
1,4
1,35
1,3
1,25
1,2
1,15
1,1
1,05
1
**
*
UVA - - - + + +
Trolox - + - - + -
Ss - - + - - +
MM (WM 266-4)
Glucose consumption [mg]
1,45
1,4
1,35
1,3
1,25
1,2
1,15
1,1
1,05
1
*
**
**
*
UVA - - - + + +
Trolox - + - - + -
Ss - - + - - +

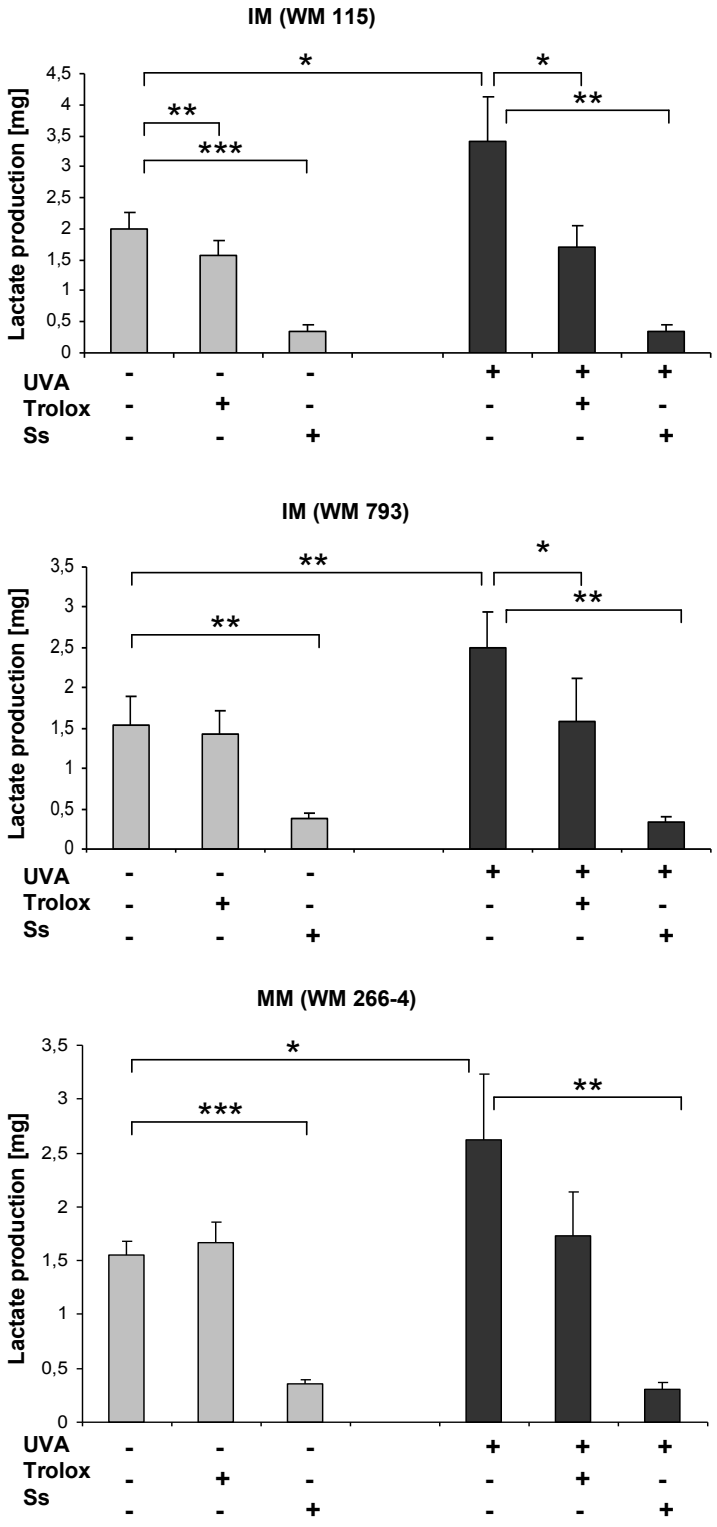

Figure 35. Influence of UVA induced Warburg effect in the supernatant of human skin reconstructs with sunscreen product.

Human skin reconstructs with melanoma cell lines from initial melanoma (IM) and metastasizing melanoma (MM) were treated repetitively with 6 J/cm^2 UVA three times daily for 4 consecutive days with and without sunscreen (Ss) product and 20µm ROS quencher Trolox. The glucose consumption and the lactate production were significantly increased upon UVA irradiation and UVA induced

increased glucose consumption and lactate production was significantly (students t-test; $p<0.05$) attenuated with 20µm ROS quencher Trolox and this effect with sunscreen (Ss) product was attenuated also in the supernatant of skin reconstructs. Data are presented as mean value with standard deviation of three independent experiments.

The UVA induced increased Warburg effect in the human skin reconstruct is significantly (students t-test; $p<0.05$) attenuated by application of a sunscreen product in MM cells (figure 35).

2.4 Transketolase activity in human skin reconstruct model

To recapitulate the human skin *in vivo* more closely, skin reconstructs with different melanoma cells from IM and MM were used to detect the influences of UVA irradiation on transketolase activity. For measurement of transketolase activity in skin reconstructs, the skin reconstruct was weighted and subsequently transketolase activity was measured calorimetrically as described above (figure 36).

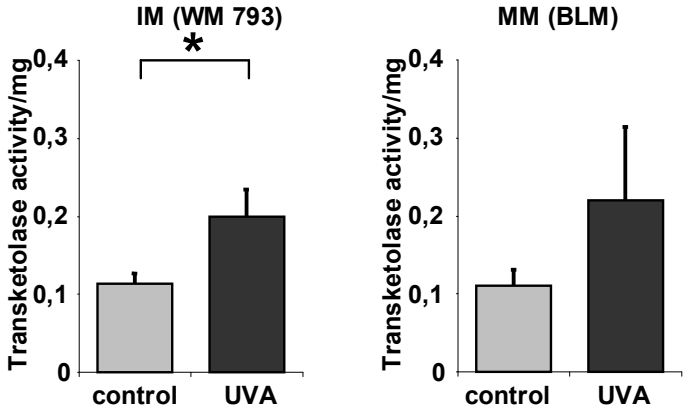

(section from Baban *et al.,* in press)

Figure 36. UVA irradiation enhanced transketolase activity in human skin reconstructs.
Human skin reconstructs with melanoma cell lines from initial melanoma (IM) and metastasizing melanoma (MM) were treated repetitively with 6 J/cm^2 UVA three times daily for 4 consecutive days and transketolase activity was determined by a colorimetric assay. Treatment with UVA irradiation increased transketolase activity in the skin reconstructs, the effect was significant (students t-test; $p<0.05$) in IM cells only. Data are presented as mean value of three independent experiments with standard deviation (section from Baban et al., in press).

Treatment with UVA irradiation increased transketolase activity in skin reconstructs with melanoma cells from IM and MM but increase in transketolase activity reached significance in skin reconstructs with IM cells (figure 36).

2.5 Effect of ROS quencher Trolox on UVA induced transketolase activity in the human skin reconstruct model

To investigate wether UVA induced transketolase activity in skin reconstructs with melanoma cell lines from IM and MM is ROS mediated, the skin reconstructs with different melanoma cell lines from IM and MM were irradiated with 6 J/cm^2 and treated with and without ROS quencher Trolox with a dose of 20µM during the irradiation course (figure 37).

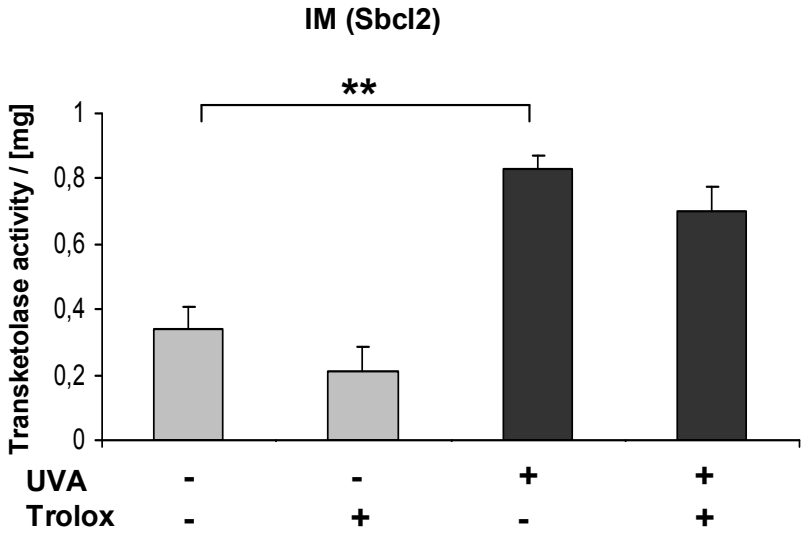

Figure 37. UVA induced transketolase activity attenuated by ROS quencher Trolox.
Human skin reconstructs with melanoma cell from initial melanoma (IM) were treated repetitively with UVA for three times daily for 4 consecutive days with and without Trolox. UVA treatment significantly (students t-test; $p<0.05$) increased transketolase activity in the skin reconstructs but the effect of ROS quencher Trolox was not significant (students t-test; $p<0.05$). Data are presented as mean value of three independent experiments with standard deviation.

ROS quencher Trolox attenuated UVA induced transketolase activity in skin reconstructs (figure 37).

2.6 Induction of MMP9 and uPA in human skin reconstructs by UVA irradiation

We want to know, whether UVA irradiation is able directly to induce MMP9 and uPA expression. Therefor, effect of UVA irradiation on MMP9 and uPA expression and secretion in skin reconstructs with melanoma cells from IM and MM was investigated by immunohistochemistry (figure 38) (section from Baban *et al.,* in press).

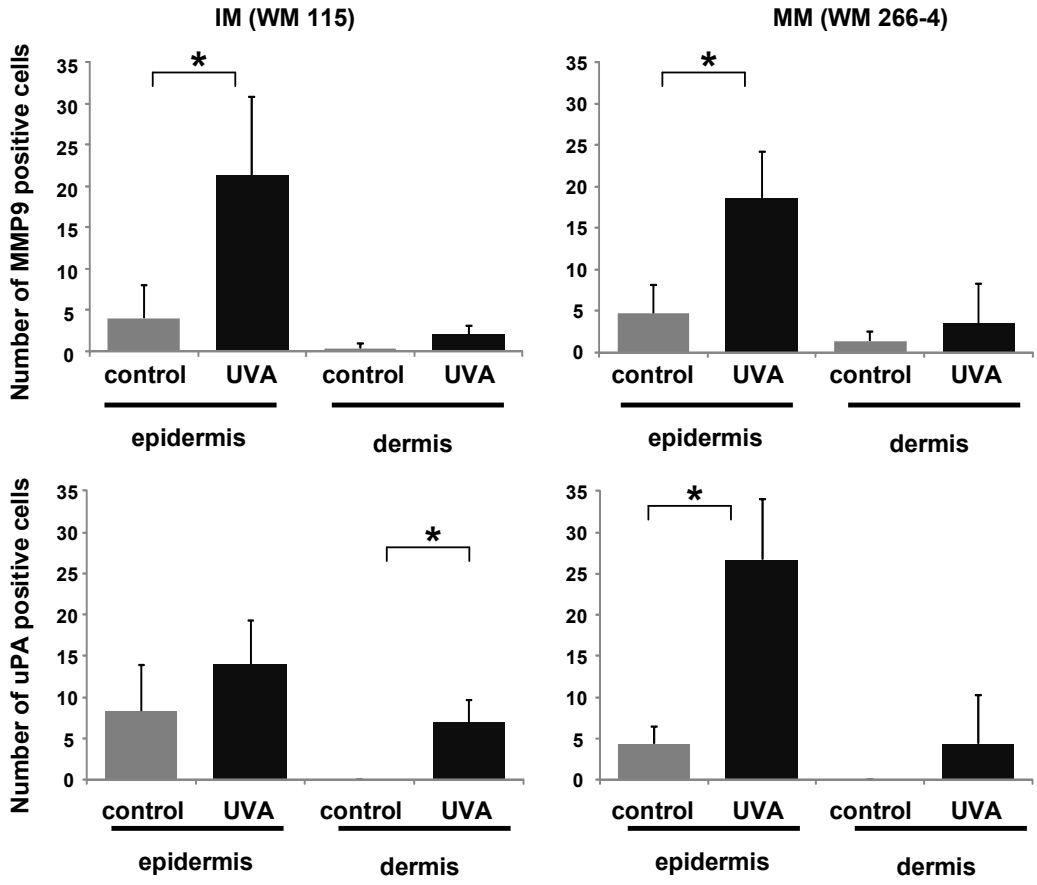

(section from Baban *et al.,* in press)

Figure 38. Expression of MMP9 and uPA in skin constructs upon UVA irradiation.

The skin reconstructs with melanoma cells from initial melanoma (IM) and metastasizing melanoma (MM) were irradiated with 6 J/cm^2 of UVA and the amount of MMP9 and uPA expression in epidermal and dermal layer was measured per visual field.

UVA irradiation was enhanced epidermal and dermal MMP9 expression in skin reconstructs. The effect was significantly (students t-test; $p<0.05$) induced in the epidermal layer of skin reconstructs with melanoma cells from IM and MM. UVA irradiation was enhanced epidermal and dermal uPA expression in skin reconstructs. Data are presented as mean values of at least three independent experiments with standard deviation (section from Baban *et al.,* in press).

UVA irradiation enhanced the expression of MMP9 and uPA tumor relevant proteases in skin reconstruct with melanoma cells. UVA irradiation significantly increased epidermal MMP9 expression of skin reconstructs with IM and MM cells. The result shows induction of tumor relevant MMP9 and uPA proteases upon UVA treatment (figure 38).

2.7 Invasion

Irradiation of skin reconstructs with epidermal melanoma cells from IM and MM enhanced MMP9 and uPA expression by 6 J/cm^2 of UVA (figure 38). We aimed to test the functional role of UVA irradiation toward invasion and metastasis of melanoma cells. Invasive potential of melanoma cells from IM and MM, using skin reconstructs model treated, with and without repetitive UVA irradiation was determined by S100 immunostaining (figure 39).

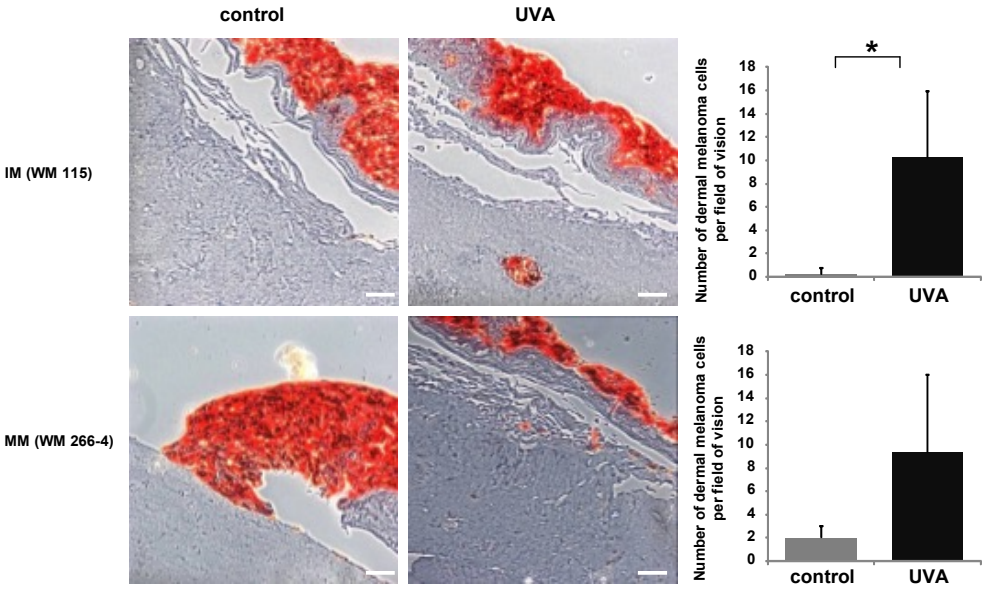

(section from Baban *et al.,* in press).

Figure 39. UVA irradiation induced invasion *in situ* in human skin reconstructs.

In repetitive UVA irradiated skin reconstructs with epidermal melanoma cells from initial melanoma (IM) and metastasizing melanoma (MM) more initial invasion of melanoma cells in the dermis is detected with melanoma specific S100 immunostaining compared to control. UVA irradiation enhanced invasion in skin reconstructs, the effect was singnificantly (students t-test; $p<0.05$) induced in IM cells. Dermal melanoma cells were counted per field of vision and are displayed as mean value with standard deviation of at least three independent experiments. Scale bar represents 70µm (section from Baban *et al.,* in press).

We found that pretreatment of UVA with subsequent recovery was capable to increase invasion.

Taken together, we could show that UVA treatment within physiological doses directly induced tumor relevant proteases. In addition to this, UVA irradiation increased initial dermal invasion of melanoma cells from IM and MM in skin reconstructs, which was verified by a histopathologist (Figure 39).

3. The role of mitochondrial DNA mutations in progression and invasion of melanoma cells

Functionality of mitochondria can be important for proliferating tumor cells, due to their role in metabolic processes and their role in apoptosis. On the other hand mutagenic events, due to UVA irradiation, can promote skin cancer onset and mutations in mitochondrial DNA (mtDNA), due to UVA irradiation and other sources with negative impact on mitochondrial functionality. The mitochondrial 4.9 kb large deletion is known to be induced by UVA and ROS and is considered as a marker deletion for mtDNA mutations (Berneburg *et al.,* 1999; 2006). The possible role of mtDNA common deletion in carcinogenesis is still discussed and the frequency of this deletion in melanomas as well as in nevi is still unknown.

3.1 Level of mtDNA common deletion in melanoma

To investigate the level of mtDNA deletion during carcinogenesis, histological samples were collected from four different groups of patients with normal nevi (benign), dysplastic nevi, melanoma (<1mm) and melanoma (>4mm). To avoid contamination from adjacent tissue we isolated the target tissue with Laser capture microdissection in cooperation with Prof. Röcken, Prof. Bauer (Department of Dermatology, University of Tuebingen) and Prof. Seeger (Department of Gynecology, University of Tuebingen). Nurgül Düzenli our lab assistant is involved in part of this experiment.

After tissue isolation by Laser capture microdissection and DNA extraction, real time PCR was performed to detect the quantity of this deletion in the tissues. To exclude bias, due to different age and sun exposure of the patients, the level of common deletion of the sample of the target tissue was normalized to a sample of normal skin adjacent to the sample from the same patient (figure 40).

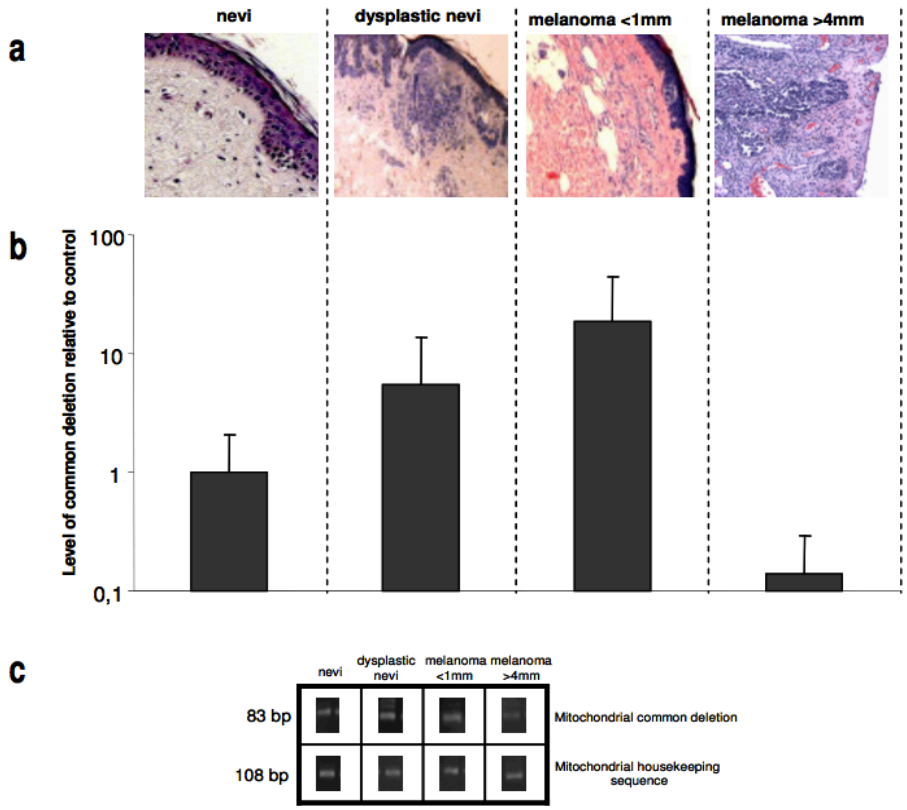

Figure 40.

The level of the mitochondrial common deletion decreased during melanoma progression.

a. In H&E stained histological samples (normal nevi, dysplastic nevi, melanoma <1mm and melanoma >4mm samples) the target tissue and control (non tumor epidermis tissues) were excised with Laser capture micro dissection.

b. The transcription level of common deletion was calculated as $2^{-\Delta\Delta Ct}$ values in normal nevi, dysplastic nevi, melanoma <1mm and melanoma >4mm samples. The transcription level of common deletion above 1 means the transcription level of target tissue was higher than the level in control tissue from the same patient. The level of common deletion in melanoma <1mm is higher than the level in control tissue and melanoma >4mm is lower than the level in control tissue from the same patient.

Data are presented as mean value of three independent samples from each group (normal nevi, dysplastic nevi and melanoma <1mm) and as mean value of two independent samples for melanoma >4mm with standard deviation.

c. Representative gel pictures of target and control amplicons of the real time PCR.

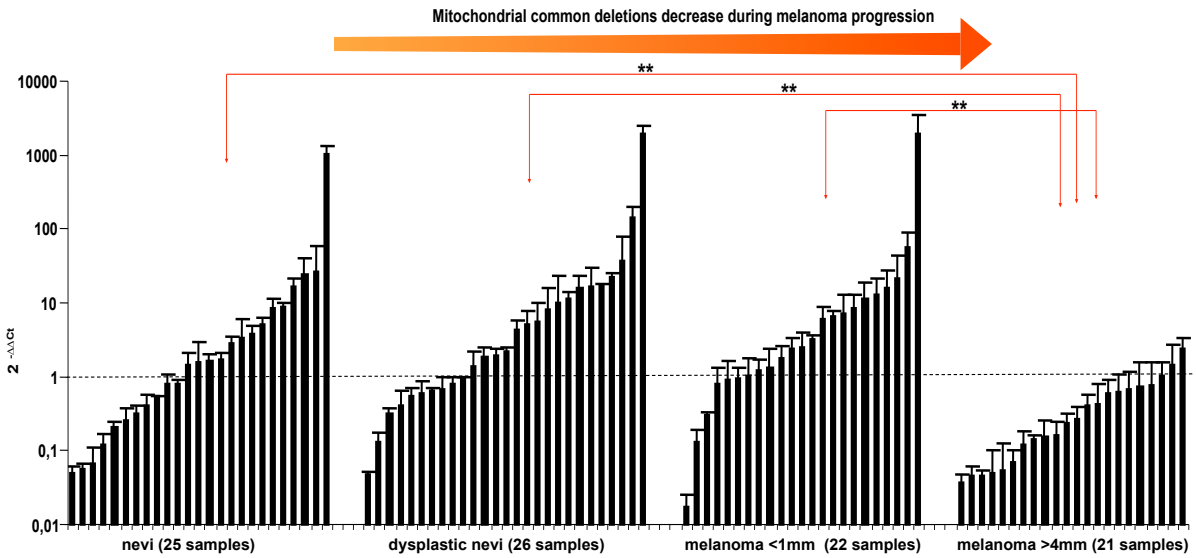

Figure 41. Measurement of the common deletion in 25 nevi samples, 26 dysplastic nevi samples, 22 melanoma of <1mm samples and 21 melanoma >4mm samples by real time PCR. The PCR result is displayed in $2^{-\Delta\Delta Ct}$ values, lower than 1 indicate lower amount of common deletion in target tissue compared to non tumor epidermal tissues, while values above 1 indicate higher amounts. Values $2^{-\Delta\Delta Ct}$ are displayed in logarithmic scale with standard deviation. In comparison to epidermal cells, melanoma >4mm together show significantly (student t-test $p<0.01$) lower levels of common deletion.

In histological human skin samples, we found that the average level of human common deletion in normal nevi and dysplastic nevi and melanoma >1mm samples is significantly higher than in control tissue from the same patient and in melanoma >4mm decreases significantly below the level of the control tissue from the same patient (figure 41). Interestingly, there is a tendency to high level of common deletion in initial melanoma. These findings point to a possible selection mechanism against the common deletion during melanoma progression.

E. Discussion

In many patients initial small melanomas are not discovered and patients continue solar exposure and it was shown that many patients even increase their sun exposure after diagnosis of initial melanoma (Idorn *et al.*, 2013) (Baban *et al.,* in press). The effect of a single neonatal high dose of UVB or UVA radiation for initiation of melanoma was shown previously in mice (Noonan *et al.*, 2003; Noonan *et al.*, 2012). In addition, recent work showed that UVB radiation promotes metastasis (Bald *et al.*, 2014). But despite its physiological relevance, it is still not clear how UVA irradiation influences progression of human initial melanoma cells (Baban *et al.,* in press).

In this study, we investigated the role of UVA irradiation on metabolism and progression of melanoma cell lines from initial melanoma (IM) and metastasizing melanoma (MM). We found that UVA irradiation alters metabolism, particularly UVA induced production of lactic acid. Furthermore, UVA irradiation as well as high concentrations of lactic acid increased expression and activity of MMPs and uPA and enhanced invasion *in vitro* (Baban *et al.,* in press).

Additionally, we investigated the level of mitochondrial DNA (mtDNA) common deletion, which can also be induced by UVA via ROS (Berneburg *et al.,* 1999), in normal nevi, dysplastic nevi, melanoma <1mm and melanoma >4mm samples.

1. Influence of UVA on Warburg effect

1.1 Influence of UVA on Warburg effect in melanoma cells

For most proliferating tumor cells the preference of aerobic glycolysis with increased glucose consumption and lactate production has been described as the Warburg effect (Warburg, 1956). The literature indicates that tumor cells benefit from the Warburg effect, since part of the glycolysis derived pyruvate can be used as precursor substances for further anabolic pathways like amino acid synthesis or fatty acid synthesis, as well as cholesterol synthesis (Vander Heiden *et al.*, 2009) (Baban *et al.,* in press). Our results demonstrate, that UVA induces the tumor associated Warburg effect in melanoma cell lines from initial melanoma (IM) and metastasizing melanoma (MM) partially in a dose dependent manner (figure 11). Upon UVA irradiation, these cells show an induction of glycolysis (figure 11, 12 and 15) with increased glucose consumption and lactate or lactic acid production (figure 11, 12 and 13). Although it has to be mentioned that UVA irradiation decreased survival of

the tumor cells in a dose dependent way (figure 10), the remaining viable cells have a higher rate of glucose consumption and lactate production per cell than unirradiated controls (figure 11 and 12) (Baban *et al.,* in press). Melanoma cells from IM have elevated rates of UVA induced Warburg effect, compared to melanoma cells from MM (figure 11). As a consequence of increased release of lactic acid into the medium, the pH in the medium decreased compared to unirradiated control (figure 13) (Baban *et al.,* in press). Exposure to UVA irradiation generates reactive oxygen species (ROS) (Meewes *et al.,* 2001). The metabolic changes we observe, seem to be partially mediated by ROS, since addition of ROS quenchers, enabled to prevent a UVA induced increase in the Warburg effect (figure 14). Interestingly, the UVA induced Warburg effect persisted for 5 days after cessation of the last UVA irradiation (figure 18), which could in part be attenuated by ROS quencher Trolox (figure 18) (Baban *et al.,* in press). This indicates a long lasting change in the metabolism of tumor cells, which goes beyond the time typically needed to repair UVA induced DNA damage. The long lasting increased glycolysis could be helpful for melanoma cell anabolic pathways, like amino acid synthesis or fatty acid synthesis and cholesterol synthesis through pyruvate, which is produced by UVA induced increase in aerobic glycolysis.

1.2 Influence of UVA on Warburg effect in skin reconstructs

Most *in vitro* experimental skin biology investigations were performed in monocultures but accumulating studies suggests, that skin cells behave differently when they are cultivated within a three dimensional (3D) culture model, were they can interact with other cells (Sun *et al.,* 2006; Mohapatra S *et al.,* 2007; Sun *et al.,* 2007; Kremer *et al.,* 2001). Therefore, skin reconstructs are more suitable to simulate the physiological situation in human skin.

In the 3D skin reconstruct model, melanoma cells can recapitulate the *in situ* phenotype and the biological characteristic of melanoma progression with the distinct growth phases (Meier *et al.,* 2000; Li *et al.,* 2011).

We used the skin reconstruct model also for our studies. Melanoma cells of different progression levels were seeded in the epidermal layer and the skin reconstructs were treated with and without UVA irradiation. Subsequently, glucose consumption and lactate production within the skin reconstruct tissues (figure 33) or in the supernatant of the skin reconstructs (figure 34 b) were measured. Similarly to the results of

monoculture experiments, we also found UVA induced increase in glucose consumption or uptake and increased lactate production compared to unirradiated control (Baban *et al.,* in press). UVA induced Warburg effect in skin reconstructs was again partially mediated via ROS, as the ROS quencher Trolox decreased UVA induced Warburg effect (figure 34). Before solar exposure, sunscreen products are often used, since they are able to absorb and protect skin against skinburn effect induced by UV (Autier P., 2000; Kaur *et al.,* 2014). We found that UVA induced Warburg effect was attenuated after application of a sunscreen product (figure 35). Decrease of UVA induced Warburg effect by a sunscreen product in the skin reconstruct model was similar to the effect of Trolox, indicating a protective effect of the sunscreen product against UVA induced progression of melanoma.

In the skin reconstructs high lactate concentrations could also be produced by surrounding cells like normal fibroblasts, during UVA irradiation (Morliere *et al.,* 1991; Coubomb *et al.,* 1996), as UVA irradiation is able to induce membrane damage through lipid peroxidation in fibroblasts and keratinocytes (Moysan *et al.,* 1996: Coubomb *et al.,* 1996). This effect is decreased by antioxidant vitamice E in fibroblast that where cultivated in 3D matrix models (Coubomb *et al.,* 1996). Indeed, keratinocytes and fibroblasts can produce lactate upon UVA irradiation via release of lactate dehydrogenase (Morliere *et al.,* 1991). But the additional production of lactate by fibroblasts and keratinocytes can enhance the functional consequences of lactate production, like MMP9 and uPA expressions in the IM cells and therefore enhance progression of IM cells.

2. Influence of UVA on transketolase activity

2.1 Influence of UVA on transketolase activity in melanoma cells

Another tumor relevant metabolic change is the activation of the pentose phosphate pathway, which provides tumor cells with components such as riboses, needed for nucleotide synthesis and nicotinamide adenine dinucleotide phosphate (NADPH), which is needed for other anabolic pathways (Boros *et al.,* 1997).

Transketolase isoform transketolase like 1 (TKTL1) is a main enzyme of the pentose phosphate pathway and part of the metabolic network supporting growth of tumor cells (Resendis-Antonio *et al.,* 2010) (Baban *et al.,* in press). It has been shown, that the expression of TKTL1 gene correlates with total transketolase activity and cell proliferation (Hu *et al.,* 2007; Zhang S *et al.*, 2008; Chen H *et al.,* 2009). Furthermore,

in many tumors, a strong correlation between the expression of TKTL1 and tumor progression was reported (Staiger e*t al.,* 2006; Volker *et al.,* 2008). In contrast to the work of Mayer A., no expression of TKTL1 in different malignant tumor cells was detected (Mayer A *et al.,* 2010). TKTL1 is also used as prognostic marker for highly proliferative cancers in cancer therapy (Langbein *et al.*, 2006).

We showed that UVA irradiation increased transketolase activity (figure 16) and despite different genetic background, every IM and MM investigated, tended to induce transketolase activity (figure 16 b). This effect was also observed for different doses of UVA irradiation, partially showing a dose dependent upregulation of transketolase activity (figure 16 a). This UVA enhanced transketolase activity in IM cells was dependent on UVA induced ROS, as addition of the ROS quencher Trolox reduced UVA induced transketolase activity (figure 17) (Baban *et al.,* in press). Interestingly, the UVA induced transketolase activity persisted for 5 days after cessation of the last UVA irradiation (figure 18), while its activity could in part be attenuated by ROS quencher Trolox (figure 18) (Baban *et al.,* in press), indicating a long lasting change in the metabolism of tumor cells, which goes beyond the time typically needed to repair UVA induced DNA damage. This long lasting activated pentosephosphate pathway could be of advantage for proliferating tumor cells, providing tumor cells with riboses, which are needed for nucleotide synthesis and nicotinamide adenine dinucleotide phosphate (NADPH), necessary for other anabolic pathways (Boros *et al.,* 1997).

2.2 Effect of UVA on transketolase activity in skin reconstructs

UVA increased transketolase activity in skin reconstructs (figure 36) (Baban *et al.,* in press) and this effect was slightly reduced in the presence of ROS quencher Trolox (figure 37), indicating a partially ROS mediated UVA induced transketolase activity in skin reconstructs. In the skin reconstructs, high transketolase activity could also be produced by surrounding cells like keratinocytes and normal dermal fibroblasts because during UV irradiation these cells for glucose catabolism turn to oxidative phase of pentose phosphate pathway, which is also mediated by ROS (Kuehne *et al.,* 2015). Indeed, keratinocytes and fibroblasts can increase transketolase activity upon irradiation.

Taken together, UVA induced, partially mediated by ROS, glycolysis with increased glucose consumption and lactic acid or lactate production and transketolase activity

(figure 42). This UVA induced long lasting change in the metabolism of tumor cells can support proliferation of the melanoma cells.

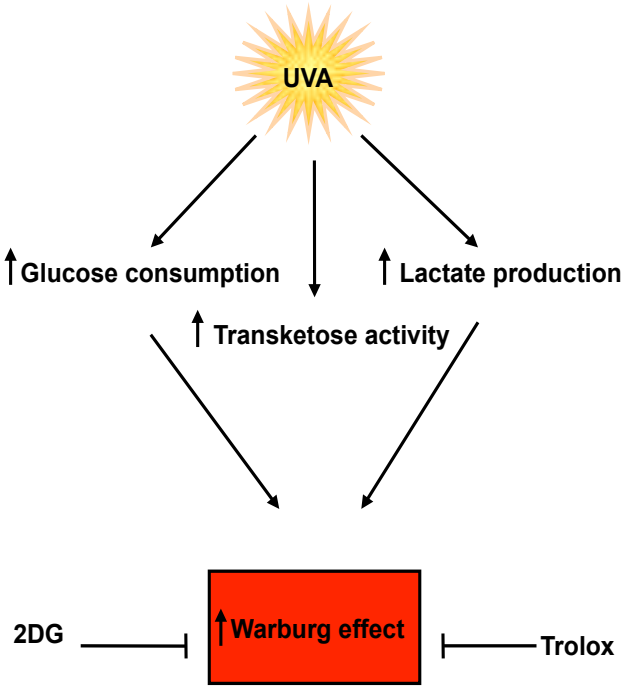

Figure 42. Summary of the effect of UVA irradiation in melanoma cells and skin reconstructs for Warburg effect and transketolase activity according to our data.
Increase of Warburg effect via UVA induced increase in glucose consumption and lactate production and UVA induced increase of Warburg effect was partially attenuated by ROS quencher Trolox and glycolysis inhibitor 2DG, and induction of transketolase activity by UVA irradiation.

3. Signal transduction mechanism of UVA induced Warburg effect

We demonstrated that UVA induced Warburg effect persists even 5 days beyond the last UVA irradiation (figure 18), indicating a long lasting change in the metabolism of tumor cells, which could be facilitated by modulations of signal transduction mechanisms. Therefore, we investigated stress associated signal transduction mechanisms, which are associated with UVA or UVB irradiation. Epidermal growth factor receptor (EGFR) signaling pathways and insulin like growth factor receptor (IGFR) signaling pathways are early targets of UVA signaling. EGFR and IGFR receptors are immediately activated upon UV irradiation and these pathways are involved in UVA induced metabolic changes in other dermal cells (El-Abaseri *et al.*, 2006; Lopez-Camarillo *et al.*, 2012).

Therefore, the EGFR and the IGFR population were analyzed in melanoma cell lines from IM and MM and a significant decrease in the EGFR and the IGFR population on the cellular surface upon UVA treatment was detected (figure 22). These results point to a higher UVA induced turnover of EGFR and IGFR and to a UVA induced internalization and activation of the EGFR and IGFR. Furthermore, the direct activation of EGFR upon UVA treatment was verified by Western blot (figure 23). EGFR activation leads to activation of pyruvate kinase M2 (PKM2), and then induces the expression of glycolytic enzymes, leading to an increased Warburg effect (Yang *et al.*, 2012) (Baban *et al.,* in press). Furthermore, EGFR and IGFR induced MAPK signaling could lead to transcriptional activation of glycolytic enzymes which are capable to facilitate long lasting induction of glycolysis. Further investigations concerning MAPK signaling and expression of glycolytic enzymes would be necessary to clarify this connection. The protein kinase Akt, involved in PI3K/AKT/mTOR signaling (Bunney *et al.,* 2010; Majeweki *et al.,* 2004), is necessary for cellular proliferation, progression and invasion. Akt is activated upon UVA treatment (figure 24). It has already been shown in melanoma, that Akt activation is highly associated with melanoma progression (Dai *et al.,* 2005). Considering this, our results support the idea that UVA irradiation enhances progression of initial melanoma cells.

Interestingly, an overexpression of Akt induces elevated glycolytic metabolism, furthermore, Akt increased glycolytic metabolism correlates with transketolase overexpression (Elstrom *et al.,* 2004; Langbein *et al.,* 2006).

Generation of ROS, which is one of the intermediate effects of UVA on cells, via induction of HIF1, could also lead to metabolic reprogramming towards Warburg effect (Haigis *et al.*, 2012). It was shown in melanoma cells that treating with an antioxidant (ROS quencher) attenuated HIF1α protein expression and HIF1 activity (Kuphal *et al.,* 2010) and inactivation of HIF1α changed the metabolism towards oxidative phosphorylation instead of aerobic glycolysis and therefore glycolysis rate decreased (Kluza *et al.,* 2012). Upon UVA irradiation a slight induction of HIF1 was visible, compared to control (figure 25 and 26) and this induction may be due to constitutive HIF1α activation, which could be regulated by ROS in malignant melanomas, even in normoxic condition (Kuphal *et al.,* 2010).

Taken together, our data indicate that UVA irradiation activates EGFR and IGFR as well as Akt and HIF1, this activation could influence long lasting induction of

glycolysis. Further investigation of the effects of inhibition of EGFR and IGFR signaling as well as the inhibition of Akt and HIF1 signaling on UVA induced expression of glycolytic enzymes would be necessary to clarify this question.

4. Functional relevance of UVA induced Warburg effect

Lactate levels of ~16mM were measured upon UVA irradiation of melanoma cells *in vitro* (Baban *et al.,* in press). Lactate concentrations of 11mM are shown in tumors *in vivo* (Serganova *et al.,* 2011). As lactic acid is detrimental for cellular viability, it is known that high levels of lactic acid are angiogenic (Dhup *et al.,* 2012) and immunosuppressive in monocytes via inhibition of TNF secretion (Dietl *et al.,* 2010). In addition, macrophages treated with lactic acid inhibited activation of CD8+ T cells (Ohashi *et al.,* 2013) (Baban *et al.,* in press).

Here we show that high levels of lactic acid have functional relevance as they induce transcription and secretion of MMPs and uPA and that UVA irradiation enhances invasion of melanoma cells.

4.1 Expression of MMPs and uPA

It has been shown, that induction of MMP2, MMP3, MMP9, MMP13, MMP15 are features of tumor progression (Orimoto *et al.,* 2008) and especially MMP 2, MMP3, MMP9, MMP13 and uPA are important proteases during melanoma progression (Bianchini *et al.,* 2006; Corte *et al.,* 2005; Girouard *et al.,* 2012; Ji *et al.,* 2013; Orimoto *et al.,* 2008; Rotte *et al.,* 2012; Tang *et al.,* 2013; Tas *et al.,* 2008; Tas *et al.,* 2005; Zigrino *et al.,* 2009). Also it has not been reported that MMP15 transcription is induced in melanoma. Here we show that UVA irradiation or lactic acid alone, a major derivate of the UVA induced Warburg effect, both are able to induce expression of all investigated proteases (MMPs and uPA) (figure 28), which are relevant for tumor progression in melanoma cells (Baban *et al.,* in press).

Furthermore, it was previously shown in other tumors that lactic acid is capable of increasing tumor cell migration by activation of MMP2 (Baumann *et al.,* 2009). In our experiments, IM cells show a transcriptional upregulation of MMP2, MMP3, MMP9, MMP13, MMP15 as well as uPA, compared to untreated control, upon treatment with lactic acid (figure 28) in physiological concentrations. In contrast to this, no significant upregulation of the inhibitors of MMPs, tissue inhibitor of matrixmetalloproteinases (TIMP1), can be found (figure 28) (Baban *et al.,* in press). Downregulation of TIMP

with upregulation of MMP3 is found in serum of patients with malignant melanoma (Tas *et al.,* 2005). The upregulation of MMPs and uPA is quite rapid, as it happens 12 hr after addition of lactic acid. So far it has not been reported, that MMP15 transcription is induced in melanoma. In hypoxic conditions lactic acid can also be produced (Pasteur effect), which is observed in melanoma (Scott *et al.,* 2011) and many other tumors. Using zymography we are able to show, that either UVA irradiation, or UVA irradiation associated lactic acid is capable of inducing secretion of active MMP2 and MMP9 (figure 29). UVA irradiation induced secretion of active MMP2 and MMP9 was slightly reduced in the presence of ROS quencher (figure 29 a and b), indicating a partially ROS mediated mechanism of UVA induced MMP2 and MMP9 induction. However, it is important to note that in our system, ROS quenchers cannot completely abrogate UVA mediated effects, indicating that either cumulative ROS production during UVA treatment exceeds the ROS detoxification capacity of Trolox, or other mechanisms, such as activation of MAPK, NFkB, ß-selectin or chemokine signaling may also be relevant (Baban *et al.,* in press).

Furthermore, treatment of cells with lactic acid alone was sufficient to facilitate secretion of MMP2 and MMP9 (figure 29). Additionally, UVA irradiation or addition of lactic acid alone enhanced secretion of uPA (figure 30) and UVA irradiation enhanced secretion of uPA was also partially ROS mediated (figure 30 a). Interestingly, lactic acid induced expression of MMPs and invasion in distant areas could be one efficient strategy of melanoma cells to run away from unfavorable areas with hypoxia, high lactic acid conditions and senescence inducing conditions (Mo *et al.,* 2013) (Baban *et al.,* in press).

4.2 Effect of UVA on MMP9 and uPA in skin reconstructs

UVA irradiation was also able to induce MMP9 and uPA expression in skin reconstructs with melanoma cells from IM and MM (figure 38) (Baban *et al.,* in press). Although it has to be mentioned, that MMP2 and MMP9 expression in skin reconstructs could be derived from keratinocytes and dermal fibroblasts (Eves *et al*., 2003). The contribution of keratinocytes and dermal fibroblasts to the MMP9 and uPA expression in skin reconstructs could be further investigated with additional immunohistochemistry methods.

4.3 UVA enhanced Warburg effect increases invasion of melanoma cells via production of lactic acid

The first step in melanoma progression is invasion of adjacent tissue, which is facilitated by proteases like matrix metalloproteinase (MMP) and urokinase type plasminogen activator (uPA) (described in paragraph 4.1 and 4.2). So far, it was reported that MMP9 and uPA are activated during invasion of melanoma cells (Tang *et al.,* 2013; Bianchini *et al.,* 2006).

The role of UVA induced Warburg effect for melanoma progression and invasion becomes clear, as we showed that lactate production subsequently led to increased expression of MMPs and uPA (figure 28, 29 and 30), resulting in increased invasiveness of the UVA treated melanoma cells (figure 31). We are the first to provide a functional link between UVA induced Warburg effect with enhanced lactic acid production and enhanced expression of MMP and uPA, which finally promotes enhanced invasion (Baban *et al.,* in press).

Our result of the *in vitro* invasion assay on melanoma invasion showed that UVA irradiation significantly increased invasion of melanoma cells and this effect was partially ROS mediated, as the ROS quencher Trolox significantly attenuated UVA induced invasion (figure 31). Similarly, the inhibitor of glycolysis (2DG) significantly attenuated UVA induced invasion (figure 31). Treatment of melanoma cells with lactic acid significantly increased invasion to an extent comparable to UVA irradiation. These data show, that addition of lactic acid can mimic the UVA induced increase of the invasive potential *in vitro* (Baban *et al.,* in press).

The presence of MMP inhibitor (GM6001) partially decreased the UVA induced invasive potential, as well as the presence of uPA inhibitor (amiloride) partially abrogated UVA induced invasive potential (figure 32), indicating that UVA or lactic acid induced invasion is partially facilitated either by MMP proteases or by uPA protease (Baban *et al.,* in press). These results further strengthen the direct role of these proteases in the process of invasion. Taken together, we could show that UVA as well as lactic acid alone directly induce tumor relevant proteases, MMPs as well as uPA and these proteases are functionally needed for UVA induced invasion *in vitro* (Baban *et al.,* in press).

We were able to demonstrate, that UVA irradiation enhances the Warburg effect in a partially ROS dependent fashion with increased lactate production, which induces MMP and uPA transcription, finally leading to increased invasion of tumor cells. This

demonstrates, that UVA irradiation is not only important in initiation of melanoma, but also during progression. These results support therapeutic strategies of using MMP inhibitors together with antioxidants and inhibitors of glycolysis. Furthermore, our findings support the therapeutic recommendation of continuous sun protection (Baban *et al.,* in press).

4.4 Invasion in skin reconstructs

It has been reported, that melanoma cells as well as other skin cells are able to express MMP9 and MMP2, which are involved in and facilitated melanoma cells invasion or progression in the skin reconstruct model (Eves *et al*., 2003), also was shown that invasive potential of melanoma cells in the skin reconstructs is determined by the melanoma cells themselves (van Kilsdonk JW *et al.,* 2010).

Staining of skin reconstruct slices with S100 staining showed that UVA irradiation significantly induced initial dermal invasion for IM cells but the effect was not significant for MM cells (figure 39). These data obtained with skin reconstructs demonstrate that UVA induced invasion of tumor cells, is a process, which is essential for melanoma metastasis (Baban *et al.,* in press).

Taken together, we showed that UVA irradiation induced tumor relevant proteases (figure 29 and 38) and MMPs and uPA proteases are involved in UVA induced invasion. Since this effect was partially abrogated by MMPs inhibitors, we were able to demonstrate, that activity of MMPs is also needed for UVA induced invasion of melanoma cells. Furthermore, we could show that upon addition of uPA inhibitor, UVA induced invasion was decreased, again indicating that activity of uPA is needed for UVA induced invasion of melanoma cells (figure 32) (figure 43) (Baban *et al.,* in press).

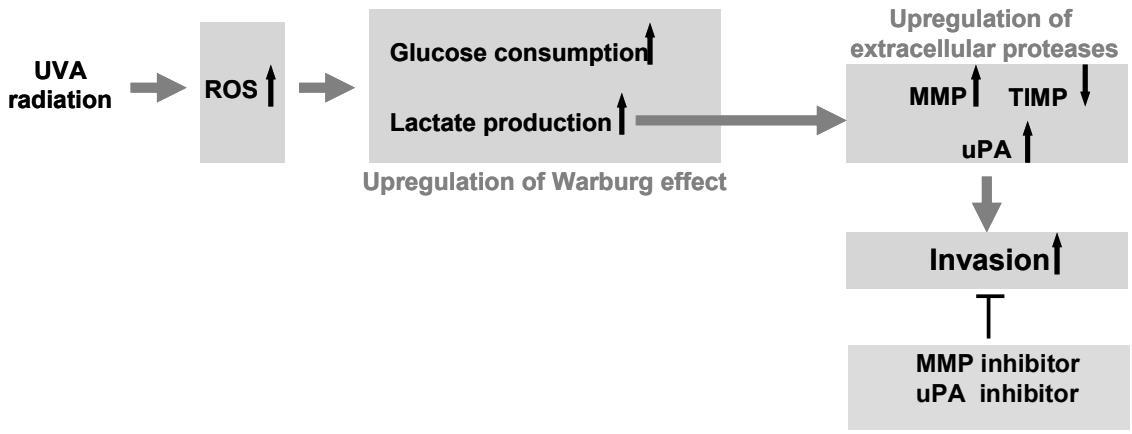

(modified from Baban *et al.,* in press)

Figure 43. Proposed model for functional relevance of UVA enhanced Warburg effect and invasion.
UVA enhanced glucose consumption and lactate production via production of ROS. Lactate production induced expression of MMPs and uPA and led to enhance invasive potential of melanoma cells. Furthermore, MMPs and uPA inhibitors attenuated the invasive potential of melanoma cells (Baban *et al.,* in press).

5. Influence of UVA on different metabolomics

Reprogramming of metabolic pathways is crucial in cancer cells, in order to adapt their bioenergetics and biosynthesis demands for tumorigenesis, progression, to escape from immune cells and resistance against chemotherapy (Furuta *et al.,* 2010; Dettmer *et al.,* 2013).

Changes in glycolysis, lipogenesis and tricarboxylic acid cycle in different stages of tumor progression were reported, which were associated with amino acid and nucleotide biosynthesis (Furuta *et al.,* 2010).

In collaboration with the University of Regensburg (Prof Gronwald) a large set of metabolites that are involved in several major metabolic pathways were analyzed by NMR spectroscopy (figure 19, 20 and 21). It has been shown in melanoma cells that all exhibited Warburg effect, characterized by increased glucose uptake and lactate production, when compared to melanocytes (Scott *et al.,* 2011).

We determined UVA induced increased Warburg effect through enhanced glucose consumption and lactate production in melanoma cells from IM and MM, compared to unirradiated control by NMR spectroscopy (figure 19) to support our previous data (discussed in paragraph 1.1 and 1.2).

Metabolism of amino acids (uptake and production) is also changed upon UVA treatment in the different melanoma cell lines (WM 115, WM 793 and WM 266-4) (figure 20). We detected that UVA irradiation induces L-isoleucine, threonine, valine, tyrosine, glutamine, arginine, phenylalanine, leucine and L-pyro glutamic acid in the supernatant of IM cells. While in the MM cells only tyrosine, phenyl alanine and L-pyro glutamic acid were significantly induced, other metabolomics, like formic acid and pyruvic acid were also significantly induced by UVA irradiation in different melanoma cell lines (figure 20).

The influence of UVA induced change in metabolites in melanoma cell pellets was less (figure 21), when compared to UVA induced metabolites change in the melanoma cell supernatant (figure 20). In IM cells no significant change in the

concentration of metabolomics was detected, yet the influence on different metabolomics in the MM cell pellet was only significant in alanine, lactic acid, formic acid, cis-hydroxy D-proline, leucine and adenine (figure 21).

It was shown, that melanoma cells are producing more alanine from glucose and consume more glutamine than melanocytes, and for fatty acid synthesis melanoma cells depend on glutamine substrate in hypoxic condition while during normoxic condition fatty acids are mostly produced from glucose (Scott, 2011).

In more detail, the major metabolic pathways such as amino acid synthesis, nucleic acid synthesis, glycolysis, glucose and lactate transport, pentose phosphate pathway, citrate cycle including 2-hydroxyglutarate, polyamine and methionine cycle, urea cycle, tryptophan metabolism, ROS quenchers like glutathione, fatty acid metabolism and cholesterol synthesis would be of interest for melanoma metabolism. Additionally, production and secretion of components for the extracellular matrix, like hyaluronic acid, which is involved in proliferation and migration of tumor cells should be monitored by the NMR technique and modifications of this technique.

Our conclusion, that analysis of metabolic differences in different stages of melanoma cells and primary cells may provide novel treatment options for a therapeutic benefit in melanoma cancer patients.

6. Common deletion

The importance of mitochondrial DNA (mtDNA) damage during carcinogenesis has recently been critically discussed with reports of varying mtDNA deletion frequencies in different tumors. High frequencies of the mtDNA 4977bp deletion, that is called common deletion, are associated with aging, especially photoaging (Berneburg *et al,* 2004; Hubbard K *et al.,* 2008).

In non melanoma skin cancer (squamous cell carcinoma and basal cell carcinoma) different types of mtDNA damages were investigated including mtDNA 4977bp deletion (Durham *et al.,* 2003) and the amount of mtDNA 4977bp deletion in squamous cell carcinoma and basal cell carcinoma, showed that most of these tumors had a decreased or undetectable amount of mtDNA 4977bp deletion, compared to prelesion non tumor tissue (Eshaghian *et al.,* 2006; Kamenisch *et al.,* 2006).

It has been shown in normal skin (non melanoma tissue) of melanomas patient, that the prevalence rate of mtDNA common deletion in darker skin was less than in those of lighter skin (high risk group of melanomas) (Hubbard K *et al.,* 2008).

The frequency of the mtDNA 4977bp deletion in melanoma tissue is still unknown and a possible role of this deletion in melanoma and other tumors is still discussed controversially.

It has been shown in some tumors, for example in oral cancer and colorectal cancer that the frequency of deleted mtDNA is decreasing proportionally during disease progression (Shieh *et al*., 2004; Chen *et al.,* 2011). Recently, it has been demonstrated that melanoma cells in an advanced stage have elevated rates of oxidative phosphorylation, compared to melanocytes (Barbi de Moura *et al*., 2012). Furthermore, it is known that mitochondrial function plays a prominent role in producing the energy, ATP through respiration, as well as in cellular metabolism. However, mitochondria has many other functions in addition to the production of ATP.

Our findings indicate that the increased level of mtDNA 4977bp deletion may be a transient phenomenon during early stage of melanomagenesis to advanced stage of melanoma, which predominately disappears later on.

The potential role of common deletion in the initial phase of melanoma as initial melanoma promoting factor and functional relevance of common deletion in initial phase of melanoma is still unclear and needs further investigation.

The frequency of the mtDNA common deletion in melanomas as wells as nevi is still unknown. Especially dysplastic nevi are an important risk factor for the development of melanoma. The aim of this study was to investigate the frequency of the mtDNA 4977bp deletion in melanomas of initial and advanced stages and in normal and dysplastic nevi. To accomplish this, samples were collected from four different groups of patients with normal nevi, dysplastic nevi, initial melanomas with tumor thickness smaller than 1mm and advanced melanomas with tumor thickness larger than 4mm.

Each group consisted of at least 20 patients and tissue adjacent to the lesion of each individual patient of each group, was used as control.

Tumor and non-tumor samples were confirmed by an independent pathologist, stained with hematoxylin and eosin (H&E) stain and then laser capture microdissected with a Laser capture microdissection (LCM2105) device to avoid

contamination with adjacent tissues of each sample. The frequency of common deletion in each sample was normalized to the respective control tissue of each individual patient. In most of the normal nevi, the dysplastic nevi and initial melanomas the frequency of the common deletion was higher when compared the adjacent control tissue (figure 40 and 41). The average frequency of common deletion in nevi samples was approximately 51 times higher than in adjacent control tissue (figure 40).

This tendency was also visible in the group with dysplastic nevi with an average increased frequency of approximately 93 times and in the group with initial melanomas with an average increased frequency of approximately 100 times (figure 40). Interestingly, the frequency of common deletion decreased dramatically in advanced stages to an average decreased frequency of approximately 0.5 times compared to adjacent control tissue (figure 40). This decrease in the frequency of the common deletion was highly significant, when compared to the frequencies of nevi and initial melanoma and high amount of mtDNA 4977bp deletion could be a transient phenomenon during early stages of melanomagenesis since we found a the tendency to higher amounts of common deletion, compared to epidermal tissue in nevi and dysplastic nevi.

High metabolism rates of advanced melanoma may also be a possible explanation, why these cells in metastasizing melanoma can afford lower levels of the common deletion, compared to initial melanoma cells. This appears reasonable, as proliferating cells, such as tumor cells, need an abundant supply of energy during proliferation and metastasis.

This finding indicates a possible selection mechanism during melanoma progression against high levels of common deletion and its depletion in advanced melanomas could serve as a tumor marker.

F. Abbreviation

Abbreviations	Description
%	Percentage
°C	Degree celsius
^{18}F	Fludeoxyglucose
2-DG	2-Deoxy-D-glucose
3D	Three dimensional
6-4PPs	(6-4) photoproducts
8oxoG	8-oxo-7,8-dihydro-2'-deoxyguanosine
AKT/mTOR	AKT/mammalian target of rapamycin
ATP	Adenosine triphosphate
BCC	Basal cell carcinoma
BER	Base excision repair
bp	Base pair
C-T or CC-TT transitions	Cytosine-thymine or Cytosinecytosine-Thyminethymine transitions
CC dimers	Cytosinecytosine dimers
cCdk4	Cyclin dependent kinase 4 genes
CD	Common deletion
cDNA	cComplementary DNA (cDNA)
CO_2	Carbon dioxide
CPDs	Cyclobutyl pyrimidine dimers
dl	Deciliter
DMBA	7,12-dimethyl benz anthracene
DMEM	Dulbecco's Modified Eagle Medium
DMSO	Dimethylsulfoxide
DNA	Deoxyribonucleic acid
DSBs	Double strand breaks
EGFR	Epidermal growth factor receptor
ELISA	Enzyme linked immunosorbent assay
ERK	Extracellular signal regulated kinases
FACS	Fluorescence activated cell sorting
FBS	Fetal bovine serum
g	Gram
GAPDH	Glyceraldehyde3-phosphate dehydrogenase
GLUT1	Glucose transporter 1
H&E stain	Hematoxylin and eosin stain
H^+	Hydron
H_2O	Water
HGF/SF	Hepatocyte growth factor/scatter factor
HIF1α	Hypoxia inducible factor 1 alpha
HR	Homologous recombination
hr	Hour

HRP	Horseradish peroxidase
IFNgamma/TNFalpha	Interferon gamma/tumor necrosis factor alpha
IGFR	Insulin-like growth factor receptor
IM	Initial melanoma
IR	Ionizing radiation
IS	Internal standard
J/cm^2	Joule/ square centimetre
l	Litre
LDH	Lactate dehydrogenase enzyme
MAPK	Mitogen activated protein kinases
MET gene	Metallothionein gene
min	Minute
ml	Millilitre
mm	Melimeter
MM	Metastasizing melanoma
mm^2	Square millimetre
mmole	Millimole
MMP1	Matrix metalloproteinase 1
MMP10	Matrix metalloproteinase 10
MMP15	Matrix metalloproteinase 15
MMP13	Matrix metalloproteinase 13
MMP2	Matrix metalloproteinase 2
MMP3	Matrix metalloproteinase 3
MMP9	Matrix metalloproteinase 9
mRNA	Messenger RNA
mtDNA	Mitochondrial DNA
MTT	(3-(4,5-dimethylthiazol-2-yl)-2,5-diphenyltetrazolium bromide)
NAD^+	Oxidized nicotinamide adenine dinucleotide
NADH	Reduced nicotinamide adenine dinucleotide
$NADP^+$	Oxidized Nicotinamide adenine dinucleotide phosphate
NADPH	Nicotinamide adenine dinucleotide phosphate
nDNA	Nuclear DNA
NER	Nucleotide excision repair
NHEJ	Non homologous end joining
nm	Nanometer
NMR spectroscopy	Nuclear magnetic resonance spectroscopy
NOS	Nitric oxide syntheses
NOX	Nicotinamide adenine dinucleotide phosphate oxidase
O.D	Optical density
O_2	Oxygen
p53 gene	Tumor protein gene
PARP1	Poly ADP ribose polymerase 1
PBS X1	Dulbecco's phosphate buffered saline 1x
PCR	Polymerase chain reaction
PDK3	Pyruvate dehydrogenase kinase 3

PET	Positron emission tomography
pg	Picogram
PI3K	Phosphor inositide 3 kinase
PTEN	Phosphatase and tensin homolog
PVDF	Hydrophobic polyvinylidene difluoride
RAS	Rat sarcoma
RGF	Radial growth phase
RNA	Ribonucleic acid
ROS	Reactive oxygen species
rpm	Round per minute
rRNA	Ribosomal RNA
RT	Room temperature
RT-PCR	Reverse transcription polymerase chain reaction
RTK	Receptor tyrosine kinase
RTK	rRceptor tyrosine kinases
SCC	Squamous cell carcinoma
sec	Second
siRNA	Small interfering RNA
SOD	Super oxide dismutase
SPECT	Single-photon emission computed tomography
SSBs	Single strand breaks
T-G transversions	Tyrosine-Guanosine transversions
TC/CT dimers	Thyminecytosine/cytosinethymine dimers
TIMP	Tissue inhibitor of metalloproteinasses
TKT 1	Transketolase like 1
tRNA	Transfer RNA
TT dimers	Thyminethymine dimers
uPA	Urokinase plasminogen activator
US	United States
UV	Ultraviolet
UVA	Ultraviolet A
UVB	Ultraviolet B
UVC	Ultraviolet C
VGF	Vertical growth phase
WHO	World health organization
XP	Xeroderma pigmentosum
β actin	Beta actin
µg	Microgram
µl	Microliter

Table 20. Abbreviation and their definition.

G. Literature

Airola K, Karonen T, Vaalamo M, Lehti K, Lohi J, Kariniemi AL, Keski-Oja J,Saarialho-Kere UK. Expression of collagenases-1 and -3 and their inhibitorsTIMP-1 and -3 correlates with the level of invasion in malignant melanomas. Br J Cancer. 1999 May;80(5-6):733-43.

Alfarouk KO, Verduzco D, Rauch C, Muddathir AK, Bashir AH, Elhassan GO, Ibrahim ME, Orozco JD, Cardone RA, Reshkin SJ, Harguindey S. Erratum: Glycolysis, tumor metabolism, cancer growth and dissemination. A new pH-based etiopathogenic perspective and therapeutic approach to an old cancer question. Oncoscience. 2014 Dec 18;2(4):317. eCollection 2015

American Cancer Society. Cancer Facts & Figures 2015. Atlanta: American Cancer Society; 2015.

Armstrong BK, Kricker A. The epidemiology of UV induced skin cancer. J. Photochem Photobiol B. 2001 Oct;63(1-3):8-18.

Armstrong BK, Kricker A. How much melanoma is caused by sun exposure? Melanoma. Res. 1993 Dec;3(6):395-401.

Autier P. Do high factor sunscreens offer protection from melanoma? West J Med. 2000 Jul;173(1):58. Review.

Baban TS, Kamenisch Y, Schuller W, von Thaler AK, Sinnberg T, Metzler G, Bauer J, Schittek B, Garbe C, Rocken M, Berneburg M. UVA-irradiation induces melanoma invasion via enhanced Warburg effect. J Invest Dermatology, in press.

Baczynska KA, Pearson AJ, O'Hagan JB, Heydenreich J. Effect of altitude on solar UVR and spectral and spatial variations of UV irradiances measured inWagrain, Austria in winter. Radiat Prot Dosimetry. 2013 May;154(4):497-504.

Bald T, Quast T, Landsberg J, Rogava M, Glodde N, Lopez-Ramos D, Kohlmeyer J, Riesenberg S, van den Boorn-Konijnenberg D, Hömig-Hölzel C, Reuten R, Schadow B, Weighardt H, Wenzel D, Helfrich I, Schadendorf D, Bloch W, Bianchi ME, Lugassy C,Barnhill RL, Koch M, Fleischmann BK, Förster I, Kastenmüller W, Kolanus W, HölzelM, Gaffal E, Tüting T. Ultraviolet-radiation-induced inflammation promotes angiotropism and metastasis in melanoma. Nature. 2014 Mar 6;507(7490):109-13.

Balk SJ; Council on Environmental Health; Section on Dermatology. Ultraviolet radiation: a hazard to children and adolescents. Pediatrics. 2011Mar;127(3):e791-817. Review. Coulomb B, Lebreton C, Mathieu N, Morlière P. UVA-induced oxidative damage in fibroblasts cultured in a 3-dimensional collagen matrix. Exp Dermatol. 1996 Jun;5(3):161-7.

Ballard JW, Whitlock MC. The incomplete natural history of mitochondria. Mol. Ecol. 2004 Apr;13(4):729-44.

Barbi de Moura M, Vincent G, Fayewicz SL, Bateman NW, Hood BL, Sun M, Suhan J, Duensing S, Yin Y, Sander C, Kirkwood JM, Becker D, Conrads TP, Van Houten B, Moschos SJ. Mitochondrial respiration--an important therapeutic target in melanoma. PLoS One. 2012;7(8):e40690.

Bardeesy N, Wong KK, DePinho RA, Chin L. Animal models of melanoma: recent advances and future prospects. Adv Cancer Res. 2000;79:123-56.

Battie C, Verschoore M. Cutaneous solar ultraviolet exposure and clinical aspects of photodamage. Indian J Dermatol Venereol Leprol. 2012 Jun;78 Suppl. 1:S9-S14.

Baumann F, Leukel P, Doerfelt A, Beier CP, Dettmer K, Oefner PJ, Kastenberger M, Kreutz M, Nickl-Jockschat T, Bogdahn U, Bosserhoff AK, Hau P. Lactate promotes glioma migration by TGF-beta2-dependent regulation of matrix metalloproteinase-2. Neuro Oncol. 2009 Aug;11(4):368-80.

Beissert S, Loser K. Molecular and cellular mechanisms of photocarcinogenesis. Photochem Photobiol. 2008 Jan-Feb;84(1):29-34.

Berneburg M, Gattermann N, Stege H, Grewe M, Vogelsang K, Ruzicka T, Krutmann J. Chronically ultraviolet-exposed human skin shows a higher mutation frequency of mitochondrial DNA as compared to unexposed skin and the hematopoietic system. Photochem Photobiol. 1997 Aug;66(2):271-5.

Berneburg M, Grether-Beck S, Kürten V, Ruzicka T, Briviba K, Sies H, Krutmann. Singlet oxygen mediates the UVA-induced generation of the photoaging-associated mitochondrial common deletion. J Biol Chem. 1999 May28;274(22):15345-9.

Berneburg M, Plettenberg H, Krutmann J. Photoaging of human skin. Photodermatol Photoimmunol Photomed. 2000 Dec;16(6):239-44.

Berneburg M, Plettenberg H, Medve-König K, Pfahlberg A, Gers-Barlag H, Gefeller O, Krutmann J. Induction of the photoaging-associated mitochondrial common deletion in vivo in normal human skin. J Invest Dermatol. 2004May;122(5):1277-83.

Berneburg M, Gremmel T, Kurten V, et al. (2005) Creatine supplementation normalizes mutagenesis of mitochondrial DNA as well as functional consequences. J Invest Dermatol 125:213-20.

Berthon HA, Kuchel PW, Nixon PF. High control coefficient of transketolase in the nonoxidative pentose phosphate pathway of human erythrocytes: NMR, antibody, and computer simulation studies. Biochemistry. 1992 Dec 29;31(51):12792-8.

Besaratinia A, Synold TW, Xi B, Pfeifer GP. G-to-T transversions and small tandem base deletions are the hallmark of mutations induced by ultraviolet a radiation in mammalian cells. Biochemistry. 2004 Jun 29;43(25):8169-77.

Bianchini F, D'Alessio S, Fibbi G, Del Rosso M, Calorini L. Cytokine-dependent invasiveness in B16 murine melanoma cells: role of uPA system and MMP-9. Oncol. Rep. 2006 Mar;15(3):709-14.

Birch-Machin MA, Tindall M, Turner R, Haldane F, Rees JL. Mitochondrial DNA deletions in human skin reflect photo- rather than chronologic aging. J Invest Dermatol. 1998 Feb;110(2):149-52.

Bogliolo M, Izzotti A, De Flora S, Carli C, Abbondandolo A, Degan P. Detection of the '4977 bp' mitochondrial DNA deletion in human atherosclerotic lesions. Mutagenesis. 1999 Jan;14(1):77-82.

Boros LG, Puigjaner J, Cascante M, Lee WN, Brandes JL, Bassilian S, Yusuf FI, Williams RD, Muscarella P, Melvin WS, Schirmer WJ. Oxythiamine and dehydroepiandrosterone inhibit the nonoxidative synthesis of ribose and tumor cell proliferation. Cancer Res. 1997 Oct 1;57(19):4242-8.

Bradl M, Klein-Szanto A, Porter S, Mintz B. Malignant melanoma in transgenic mice. Proc Natl Acad Sci U S A. 1991 Jan 1;88(1):164-8.

Brenner M, Hearing VJ. The protective role of melanin against UV damage in human skin. Photochem Photobiol. 2008 May-Jun;84(3):539-49.

Bunney TD, Katan M. Phosphoinositide signalling in cancer: beyond PI3K and PTEN. Nat Rev Cancer. 2010 May;10(5):342-52.

Chen H, Yue JX, Yang SH, Ding H, Zhao RW, Zhang S. Overexpression of transketolase-like gene 1 is associated with cell proliferation in uterine cervix cancer. J Exp Clin Cancer Res. 2009 Mar 30;28:43.

Chen T, He J, Shen L, Fang H, Nie H, Jin T, Wei X, Xin Y, Jiang Y, Li H, Chen G, Lu J, Bai Y. The mitochondrial DNA 4,977-bp deletion and its implication in copy number alteration in colorectal cancer. BMC Med Genet. 2011 Jan 13;12:8.

Cohen C, Zavala-Pompa A, Sequeira JH, Shoji M, Sexton DG, Cotsonis G, Cerimele F, Govindarajan B, Macaron N, Arbiser JL. Mitogen-actived protein kinase activation is an early event in melanoma progression. Clin Cancer Res. 2002 Dec;8(12):3728-33.

Comito G, Calvani M, Giannoni E, Bianchini F, Calorini L, Torre E, Migliore C, Giordano S, Chiarugi P. HIF-1α stabilization by mitochondrial ROS promotes Met-dependent invasive growth and vasculogenic mimicry in melanoma cells. Free Radic Biol Med. 2011 Aug 15;51(4):893-904.

Comoglio PM, Boccaccio C. Scatter factors and invasive growth. Semin Cancer Biol. 2001 Apr;11(2):153-65.

Correia M, Thiagarajan V, Coutinho I, Gajula GP, Petersen SB, Neves-Petersen MT. Modulating the structure of EGFR with UV light: new possibilities in cancer therapy. PLoS One. 2014 Nov 11;9(11):e111617.

Corte MD, Gonzalez LO, Corte MG, Quintela I, Pidal I, Bongera M, Vizoso F. Collagenase-3 (MMP-13) expression in cutaneous malignant melanoma. Int J Biol Markers. 2005 Oct-Dec;20(4):242-8.

Cortopassi GA, Arnheim N. Detection of a specific mitochondrial DNA deletion in tissues of older humans. Nucleic Acids Res. 1990 Dec 11;18(23):6927-33.

Coulomb B, Lebreton C, Mathieu N, Morlière P. UVA-induced oxidative damage in fibroblasts cultured in a 3-dimensional collagen matrix. Exp Dermatol. 1996 Jun;5(3):161-7.

Csete B, Lengyel Z, Kádár Z, Battyáni Z. Poly(adenosine diphosphate-ribose) polymerase-1 expression in cutaneous malignant melanomas as a new molecular marker of aggressive tumor. Pathol Oncol Res. 2009 Mar;15(1):47-53

Dai DL, Martinka M, Li G. Prognostic significance of activated Akt expression in melanoma: a clinicopathologic study of 292 cases. J Clin Oncol. 2005 Mar 1;23(7):1473-82.

Dani MA, Dani SU, Lima SP, Martinez A, Rossi BM, Soares F, Zago MA, Simpson AJ. Less DeltamtDNA4977 than normal in various types of tumors suggests that cancer cells are essentially free of this mutation. Genet Mol Res. 2004 Sep 30;3(3):395-409.

Davies H, Bignell GR, Cox C, Stephens P, Edkins S, Clegg S, Teague J, Woffendin H, Garnett MJ, Bottomley W, Davis N, Dicks E, Ewing R, Floyd Y, Gray K, Hall S, Hawes R, Hughes J, Kosmidou V, Menzies A, Mould C, Parker A, Stevens C, Watt S, Hooper S, Wilson R, Jayatilake H, Gusterson BA, Cooper C, Shipley J, Hargrave D, Pritchard-Jones K, Maitland N, Chenevix-Trench G, Riggins GJ, Bigner DD, Palmieri G, Cossu A, Flanagan A, Nicholson A, Ho JW, Leung SY, Yuen ST, Weber BL, Seigler HF, Darrow TL, Paterson H, Marais R, Marshall CJ, Wooster R, Stratton MR, Futreal PA. Mutations of the BRAF gene in human cancer. Nature. 2002 Jun 27;417(6892):949-54. Epub 2002 Jun 9.

De Fabo EC, Merlino G. Sunscreen prevention of melanoma in man and mouse. Pigment Cell Melanoma Res. 2010 Dec;23(6):835-7

De Fabo EC, Noonan FP, Fears T, Merlino G. Ultraviolet B but not ultraviolet A radiation initiates melanoma. Cancer Res. 2004 Sep 15;64(18):6372-6.

Demaria M, Giorgi C, Lebiedzinska M, Esposito G, D'Angeli L, Bartoli A, Gough DJ, Turkson J, Levy DE, Watson CJ, Wieckowski MR, Provero P, Pinton P, Poli V. A STAT3-mediated metabolic switch is involved in tumour transformation and STAT3 addiction. Aging (Albany NY). 2010 Nov;2(11):823-42.

Dennis LK, Vanbeek MJ, Beane Freeman LE, Smith BJ, Dawson DV, Coughlin JA. Sunburns and risk of cutaneous melanoma: does age matter? A comprehensive meta-analysis. Ann Epidemiol. 2008 Aug;18(8):614-27.

Dettmer K, Vogl FC, Ritter AP, Zhu W, Nürnberger N, Kreutz M, Oefner PJ, Gronwald W, Gottfried E. Distinct metabolic differences between various human cancer and primary cells. Electrophoresis. 2013 Oct;34(19):2836-47.

Dhawan P, Singh AB, Ellis DL, Richmond A. Constitutive activation of Akt/protein kinase B in melanoma leads to up-regulation of nuclear factor-kappaB and tumor progression. Cancer Res. 2002 Dec 15;62(24):7335-42.

Dhup S, Dadhich RK, Porporato PE, Sonveaux P. Multiple biological activities of lactic acid in cancer: influences on tumor growth, angiogenesis and metastasis. Curr Pharm Des. 2012;18(10):1319-30.

Diaz-Moralli S, Tarrado-Castellarnau M, Alenda C, Castells A, Cascante M. Transketolase-like 1 expression is modulated during colorectal cancer progression and metastasis formation. PLoS One. 2011;6(9):e25323.

Dietl K, Renner K, Dettmer K, Timischl B, Eberhart K, Dorn C, Hellerbrand C, Kastenberger M, Kunz-Schughart LA, Oefner PJ, Andreesen R, Gottfried E, Kreutz MP. Lactic acid and acidification inhibit TNF secretion and glycolysis of human monocytes. J Immunol. 2010 Feb 1;184(3):1200-9.

Douki T, Reynaud-Angelin A, Cadet J, Sage E. Bipyrimidine photoproducts rather than oxidative lesions are the main type of DNA damage involved in the genotoxic effect of solar UVA radiation. Biochemistry. 2003 Aug 5;42(30):9221-6.

Du MX, Sim J, Fang L, Yin Z, Koh S, Stratton J, Pons J, Wang JJ, Carte B. Identification of novel small-molecule inhibitors for human transketolase by high-throughput screening with fluorescent intensity (FLINT) assay. J Biomol Screen. 2004 Aug;9(5):427-33.

Durham SE, Krishnan KJ, Betts J, Birch-Machin MA. Mitochondrial DNA damage in non-melanoma skin cancer. Br J Cancer. 2003 Jan 13;88(1):90-5.

Egeblad M, Werb Z. New functions for the matrix metalloproteinases in cancer progression. Nat Rev Cancer. 2002 Mar;2(3):161-74.

El-Abaseri TB, Putta S, Hansen LA. Ultraviolet irradiation induces keratinocyte proliferation and epidermal hyperplasia through the activation of the epidermal growth factor receptor. Carcinogenesis. 2006 Feb;27(2):225-31. Epub 2005 Aug 25.

Elstrom RL, Bauer DE, Buzzai M, Karnauskas R, Harris MH, Plas DR, Zhuang H, Cinalli RM, Alavi A, Rudin CM, Thompson CB. Akt stimulates aerobic glycolysis in cancer cells. Cancer Res. 2004 Jun 1;64(11):3892-9.

Eshaghian A, Vleugels RA, Canter JA, McDonald MA, Stasko T, Sligh JE. Mitochondrial DNA deletions serve as biomarkers of aging in the skin, but are typically absent in nonmelanoma skin cancers. J Invest Dermatol. 2006 Feb;126(2):336-44.

Eves P, Katerinaki E, Simpson C, Layton C, Dawson R, Evans G, Mac Neil S. Melanoma invasion in reconstructed human skin is influenced by skin cells--investigation of the role of proteolytic enzymes. Clin Exp Metastasis. 2003;20(8):685-700

Fears TR, Bird CC, Guerry D 4th, Sagebiel RW, Gail MH, Elder DE, Halpern A, Holly EA, Hartge P, Tucker MA. Average midrange ultraviolet radiation flux and time outdoors predict melanoma risk. Cancer Res. 2002 Jul 15;62(14):3992-6.

Fleury C, Bérard F, Leblond A, Faure C, Ganem N, Thomas L. The study of cutaneous melanomas in Camargue-type gray-skinned horses (2): epidemiological survey. Pigment Cell Res. 2000 Feb;13(1):47-51.

Folkard M, Prise KM, Turner CJ, Michael BD. The production of single strand and double strand breaks in DNA in aqueous solution by vacuum UV photons below 10eV. Radiat Prot Dosimetry. 2002;99(1-4):147-9.

Frezza C, Gottlieb E. Mitochondria in cancer: not just innocent bystanders. Semin Cancer Biol. 2009 Feb;19(1):4-11.

Fukushima S, Honda K, Awane M, Yamamoto E, Takeda R, Kaneko I, Tanaka A, Morimoto T, Tanaka K, Yamaoka Y. The frequency of 4977 base pair deletion of mitochondrial DNA in various types of liver disease and in normal liver. Hepatology. 1995 Jun;21(6):1547-51.

Furumoto S, Takashima K, Kubota K, Ido T, Iwata R, Fukuda H. Tumor detection using 18F-labeled matrix metalloproteinase-2 inhibitor. Nucl Med Biol. 2003 Feb;30(2):119-25.

Furuta E, Okuda H, Kobayashi A, Watabe K. Metabolic genes in cancer: their roles in tumor progression and clinical implications. Biochim Biophys Acta. 2010 Apr;1805(2):141-52.

Gambhir SS. Molecular imaging of cancer with positron emission tomography. Nat Rev Cancer. 2002 Sep;2(9):683-93.

Gendron SP, Mallet JD, Bastien N, Rochette PJ. Mitochondrial DNA common deletion in the human eye: a relation with corneal aging. Mech Ageing Dev. 2012 Feb-Mar;133(2-3):68-74.

Gerber B, Mathys P, Moser M, Bressoud D, Braun-Fahrländer C. Ultraviolet emission spectra of sunbeds. Photochem Photobiol. 2002 Dec;76(6):664-8.

Giancotti FG. Deregulation of cell signaling in cancer. FEBS Lett. 2014 Aug19;588(16):2558-70.

Gidanian S, Mentelle M, Meyskens FL Jr, Farmer PJ. Melanosomal damage in normal human melanocytes induced by UVB and metal uptake--a basis for the pro-oxidant state of melanoma. Photochem Photobiol. 2008 May-Jun;84(3):556-64.

Girouard SD, Laga AC, Mihm MC, Scolyer RA, Thompson JF, Zhan Q, Widlund HR, Lee CW, Murphy GF. SOX2 contributes to melanoma cell invasion. Lab Invest. 2012 Mar;92(3):362-70.

Godon C, Cordelières FP, Biard D, Giocanti N, Mégnin-Chanet F, Hall J,Favaudon V. PARP inhibition versus PARP-1 silencing: different outcomes in terms of single-strand break repair and radiation susceptibility. Nucleic Acids Res.2008 Aug;36(13):4454-64.

Goodall J, Wellbrock C, Dexter TJ, Roberts K, Marais R, Goding CR. The Brn-2transcription factor links activated BRAF to melanoma proliferation. Mol Cell Biol. 2004 Apr;24(7):2923-31.

Gomez-Raya L, Okomo-Adhiambo M, Beattie C, Osborne K, Rink A, Rauw WM. Modeling inheritance of malignant melanoma with DNA markers in Sinclair swine. Genetics. 2007 May;176(1):585-97.

Govindarajan B, Sligh JE, Vincent BJ, Li M, Canter JA, Nickoloff BJ, Rodenburg RJ, Smeitink JA, Oberley L, Zhang Y, Slingerland J, Arnold RS, Lambeth JD, Cohen C, Hilenski L, Griendling K, Martínez-Diez M, Cuezva JM, Arbiser JL. Overexpression of Akt converts radial growth melanoma to vertical growth melanoma. J Clin Invest. 2007 Mar;117(3):719-29. Epub 2007 Feb 22

Grimm M, Munz A, Teriete P, Nadtotschi T, Reinert S. GLUT-1(+)/TKTL1(+) coexpression predicts poor outcome in oral squamous cell carcinoma. Oral Surg Oral Med Oral Pathol Oral Radiol. 2014 Jun;117(6):743-53.

GROSS J, LAPIERE CM. Collagenolytic activity in amphibian tissues: a tissue culture assay. Proc Natl Acad Sci U S A. 1962 Jun 15;48:1014-22

Habano W, Nakamura S, Sugai T. Microsatellite instability in the mitochondrial DNA of colorectal carcinomas: evidence for mismatch repair systems in mitochondrial genome. Oncogene. 1998 Oct 15;17(15):1931-7.

Habano W, Sugai T, Yoshida T, Nakamura S. Mitochondrial gene mutation, but not large-scale deletion, is a feature of colorectal carcinomas with mitochondrial microsatellite instability. Int J Cancer. 1999 Nov 26;83(5):625-9

Haigis MC, Deng CX, Finley LW, Kim HS, Gius D. SIRT3 is a mitochondrial tumor suppressor: a scientific tale that connects aberrant cellular ROS, the Warburg effect, and carcinogenesis. Cancer Res. 2012 May 15;72(10):2468-72.

Heerdt BG, Augenlicht LH. Absence of detectable deletions in the mitochondrial genome of human colon tumors. Cancer Commun. 1990;2(3):109-11.

Hillig T, Thode J, Breinholt MF, Franzmann MB, Pedersen C, Lund F, Mygind H,Sölétormos G, Rudnicki M. Assessing HER2 amplification by IHC, FISH, and real-time polymerase chain reaction analysis (real-time PCR) following LCM in formalin-fixed paraffin embedded tissue from 40 women with ovarian cancer. APMIS.2012 Dec;120(12):1000-7.

Hoeijmakers JH. Genome maintenance mechanisms for preventing cancer. Nature. 2001 May 17;411(6835):366-74.

Hofmann UB, Westphal JR, Waas ET, Zendman AJ, Cornelissen IM, Ruiter DJ, van Muijen GN. Matrix metalloproteinases in human melanoma cell lines and xenografts: increased expression of activated matrix metalloproteinase-2 (MMP-2) correlates with melanoma progression. Br J Cancer. 1999 Nov;81(5):774-82.

Howe HL, Wingo PA, Thun MJ, Ries LA, Rosenberg HM, Feigal EG, Edwards BK. Annual report to the nation on the status of cancer (1973 through 1998), featuring cancers with recent increasing trends. J Natl Cancer Inst. 2001 Jun 6;93(11):824-42.

Hu LH, Yang JH, Zhang DT, Zhang S, Wang L, Cai PC, Zheng JF, Huang JS. The TKTL1 gene influences total transketolase activity and cell proliferation in human colon cancer LoVo cells. Anticancer Drugs. 2007 Apr;18(4):427-33.

Huang Q, Shen HM. To die or to live: the dual role of poly(ADP-ribose) polymerase-1 in autophagy and necrosis under oxidative stress and DNA damage.Autophagy. 2009 Feb;5(2):273-6.
Hubbard K, Steinberg ML, Hill H, Orlow I. Mitochondrial DNA deletions in skin from melanoma patients. Ethn Dis. 2008 Spring;18(2 Suppl 2):S2-38-43.

Idorn LW, Datta P, Heydenreich J, Philipsen PA, Wulf HC. A 3-year follow-upof sun behavior in patients with cutaneous malignant melanoma. JAMA Dermatol. 2014 Feb;150(2):163-8.

Inamdar GS, Madhunapantula SV, Robertson GP. Targeting the MAPK pathway in melanoma: why some approaches succeed and other fail. Biochem Pharmacol. 2010 Sep 1;80(5):624-37.

Jackson SP, Bartek J. The DNA-damage response in human biology and disease. Nature. 2009 Oct 22;461(7267):1071-8.

Jalal N, Haq S, Anwar N, Nazeer S, Saeed U. Radiation induced bystander effect and DNA damage. J Cancer Res Ther. 2014 Oct-Dec;10(4):819-33.

Jeffers M, Rong S, Anver M, Vande Woude GF. Autocrine hepatocyte growth factor/scatter factor-Met signaling induces transformation and the invasive/metastastic phenotype in C127 cells. Oncogene. 1996 Aug 15;13(4):853-6.

Jemal A, Siegel R, Xu J, Ward E. Cancer statistics, 2010. CA Cancer J Clin. 2010 Sep-Oct;60(5):277-300.

Jhappan C, Noonan FP, Merlino G. Ultraviolet radiation and cutaneous malignant melanoma. Oncogene. 2003 May 19;22(20):3099-112.

Ji MK, Shi Y, Xu JW, Lin X, Lin JY. Recombinant snake venom metalloproteinase inhibitor BJ46A inhibits invasion and metastasis of B16F10 and MHCC97H cells through reductions of matrix metalloproteinases 2 and 9 activities. Anticancer Drugs. 2013 Jun;24(5):461-72.

John A. D'Orazio1, Stuart Jarrett1, Amanda Marsch1, James Lagrew1 and Laura Cleary1 Melanoma — Epidemiology, Genetics and Risk Factors University of Kentucky College of Medicine, Markey Cancer Center, Department of Pediatrics, and Department of Molecular and Biomedical Pharmacology, Lexington, USA.

Kamenisch Y, Wenz J, Metzler G, Bauer J, Neubauer H, Garbe C, Röcken M, Berneburg M. The mitochondrial DNA common deletion is present in most basal and squamous cell carcinoma samples isolated by laser capture microdissection but generally at reduced rather than increased levels. J Invest Dermatol. 2007 Feb;127(2):486-90.

Kamenisch Y, Fousteri M, Knoch J, et al. (2010) Proteins of nucleotide and base excision repair pathways interact in mitochondria to protect from loss of subcutaneous fat, a hallmark of aging. J Exp Med 207:379-90.

Kaneko N, Vierkoetter A, Kraemer U, Sugiri D, Matsui M, Yamamoto A, Krutmann J, Morita A. Mitochondrial common deletion mutation and extrinsic skin ageing in German and Japanese women. Exp Dermatol. 2012 Jul;21 Suppl 1:26-30.

Kappes UP, Luo D, Potter M, Schulmeister K, Rünger TM. Short- and long-wave UV light (UVB and UVA) induce similar mutations in human skin cells. J Invest Dermatol. 2006 Mar;126(3):667-75.

Katiyar SK, Singh T, Prasad R, Sun Q, Vaid M. Epigenetic alterations in ultraviolet radiation-induced skin carcinogenesis: interaction of bioactive dietary components on epigenetic targets. Photochem Photobiol. 2012 Sep-Oct;88(5):1066-74

Kaur A, Thatai P, Sapra B. Need of UV protection and evaluation of efficacy of sunscreens. J Cosmet Sci. 2014 Sep-Oct;65(5):315-45.

Keleg S, Büchler P, Ludwig R, Büchler MW, Friess H. Invasion and metastasis in pancreatic cancer. Mol Cancer. 2003 Jan 22;2:14. Review.

Kelsall SR, Mintz B. Metastatic cutaneous melanoma promoted by ultraviolet radiation in mice with transgene-initiated low melanoma susceptibility. Cancer Res. 1998 Sep 15;58(18):4061-5.

Kessenbrock K, Plaks V, Werb Z. Matrix metalloproteinases: regulators of the tumor microenvironment. Cell. 2010 Apr 2;141(1):52-67.

Khalid Rahman Sudies on free radicals, antioxidants, and co-factors. Clin Interv Aging. 2007 June; 2(2): 219–236. Published online 2007 June.

Kluza J, Corazao-Rozas P, Touil Y, Jendoubi M, Maire C, Guerreschi P, Jonneaux A, Ballot C, Balayssac S, Valable S, Corroyer-Dulmont A, Bernaudin M, Malet-Martino M, de Lassalle EM, Maboudou P, Formstecher P, Polakowska R, Mortier L, Marchetti P. Inactivation of the HIF-1α/PDK3 signaling axis drives melanoma toward mitochondrial oxidative metabolism and potentiates the therapeutic activity of pro-oxidants. Cancer Res. 2012 Oct 1;72(19):5035-47.

Knebel A, Rahmsdorf HJ, Ullrich A, Herrlich P. Dephosphorylation of receptor tyrosine kinases as target of regulation by radiation, oxidants or alkylating agents. EMBO J. 1996 Oct 1;15(19):5314-25. .

Koch H, Wittern KP, Bergemann J (2001) In human keratinocytes the Common Deletion reflects donor variabilities rather than chronologic aging and can be induced by ultraviolet A irradiation. J Invest Dermatol 117:892-7.

Kotake K, Nonami T, Kurokawa T, Nakao A, Murakami T, Shimomura Y. Human livers with cirrhosis and hepatocellular carcinoma have less mitochondrial DNA deletion than normal human livers. Life Sci. 1999;64(19):1785-91.

Kremer M, Lang E, Berger A. Organotypical engineering of differentiated composite-skin equivalents of human keratinocytes in a collagen-GAG matrix (INTEGRA Artificial Skin) in a perfusion culture system. Langenbecks Arch Surg. 2001 Aug;386(5):357-63.

Kuehne A, Emmert H, Soehle J, Winnefeld M, Fischer F, Wenck H, Gallinat S, Terstegen L, Lucius R, Hildebrand J, Zamboni N. Acute Activation of Oxidative Pentose Phosphate Pathway as First-Line Response to Oxidative Stress in Human Skin Cells. Mol Cell. 2015 Aug 6;59(3):359-71.

Kuphal S, Winklmeier A, Warnecke C, Bosserhoff AK. Constitutive HIF-1 activity in malignant melanoma. Eur J Cancer. 2010 Apr;46(6):1159-69.

Langbein S, Zerilli M, Zur Hausen A, Staiger W, Rensch-Boschert K, Lukan N, Popa J, Ternullo MP, Steidler A, Weiss C, Grobholz R, Willeke F, Alken P, Stassi G, Schubert P, Coy JF. Expression of transketolase TKTL1 predicts colon and urothelial cancer patient survival: Warburg effect reinterpreted. Br J Cancer. 2006 Feb 27;94(4):578-85.

Lange CA, Tisch-Rottensteiner J, Böhringer D, Martin G, Schwartzkopff J, Auw-Haedrich C. Enhanced TKTL1 expression in malignant tumors of the ocular adnexa predicts clinical outcome. Ophthalmology. 2012 Sep;119(9):1924-9.

Lee CH, Wu SB, Hong CH, Yu HS, Wei YH. Molecular Mechanisms of UV-Induced Apoptosis and Its Effects on Skin Residential Cells: The Implication in UV-Based Phototherapy. Int J Mol Sci. 2013 Mar 20;14(3):6414-35.

Leiter U, Eigentler T, Garbe C. Epidemiology of skin cancer. Adv Exp Med Biol. 2014;810:120-40. Review.

Ley RD, Applegate LA, Padilla RS, Stuart TD. Ultraviolet radiation—induced malignant melanoma in Monodelphis domestica. Photochem Photobiol. 1989 Jul;50(1):1-5.

Ley RD. Dose response for ultraviolet radiation A-induced focal melanocytic hyperplasia and nonmelanoma skin tumors in Monodelphis domestica. Photochem Photobiol. 2001 Jan;73(1):20-3.

Li L, Fukunaga-Kalabis M, Herlyn M. The three-dimensional human skin reconstruct model: a tool to study normal skin and melanoma progression. J Vis Exp. 2011 Aug 3;(54). pii: 2937. doi: 10.3791/2937.

Liemburg-Apers DC, Willems PH, Koopman WJ, Grefte S. Interactions between mitochondrial reactive oxygen species and cellular glucose metabolism. Arch Toxicol. 2015 Aug;89(8):1209-26.

Linan Ha, Frances P Noonan†, Edward C De Fabo† and Glenn Merlino. Animal Models of Melanoma. J of Investigative Dermatology Symposium Proceedings (2005) 10, 86–88;

Lindahl T. Instability and decay of the primary structure of DNA. Nature. 1993 Apr 22;362(6422):709-15.

Liotta LA, Tryggvason K, Garbisa S, Hart I, Foltz CM, Shafie S. Metastatic potential correlates with enzymatic degradation of basement membrane collagen. Nature. 1980 Mar 6;284(5751):67-8.

Liu-Smith F, Dellinger R, Meyskens FL Jr. Updates of reactive oxygen species in melanoma etiology and progression. Arch Biochem Biophys. 2014 Dec 1;563:51-5

Livak, K. J. and T. D. Schmittgen, Analysis of relative gene expression data using real time quantitative PCR and the 2(-Delta Delta C(T)) Method. (2001). Methods 25(4): 402-408.

López-Camarillo C, Ocampo EA, Casamichana ML, Pérez-Plasencia C, Alvarez-Sánchez E, Marchat LA. Protein kinases and transcription factors activation in response to UV-radiation of skin: implications for carcinogenesis. Int J Mol Sci. 2012;13(1):142-72. .

Luanpitpong S, Talbott SJ, Rojanasakul Y, Nimmannit U, Pongrakhananon V, Wang L, Chanvorachote P. Regulation of lung cancer cell migration and invasion by reactive oxygen species and caveolin-1. J Biol Chem. 2010 Dec 10;285(50):38832-40.

.

Lunt SY, Vander Heiden MG. Aerobic glycolysis: meeting the metabolic requirements of cell proliferation. Annu Rev Cell Dev Biol. 2011;27:441-64.

Löffek S, Zigrino P, Angel P, Anwald B, Krieg T, Mauch C. High invasive melanoma cells induce matrix metalloproteinase-1 synthesis in fibroblasts by interleukin-1alpha and basic fibroblast growth factor-mediated mechanisms. J Invest Dermatol. 2005 Mar;124(3):638-43.

Majewski N, Nogueira V, Robey RB, Hay N. Akt inhibits apoptosis downstream of BID cleavage via a glucose-dependent mechanism involving mitochondrial hexokinases. Mol Cell Biol. 2004 Jan;24(2):730-40.

Marnett LJ. Oxyradicals and DNA damage. Carcinogenesis. 2000 Mar;21(3):361-70.

Mayer A, Von Wallbrunn A, Vaupel P. Glucose metabolism of malignant cells is not regulated by transketolase-like (TKTL)-1. Int J Oncol. 2010 Aug;37(2):265-71.

Mecherikunnel A, Duncan CH. Total and spectral solar irradiance measured at ground surface. Appl Opt. 1982 Feb 1;21(3):554-6.

Meewes C, Brenneisen P, Wenk J, Kuhr L, Ma W, Alikoski J, Poswig A, Krieg T, Scharffetter-Kochanek K. Adaptive antioxidant response protects dermal fibroblasts from UVA-induced phototoxicity. Free Radic Biol Med. 2001 Feb 1;30(3):238-47.

Meier F, Nesbit M, Hsu MY, Martin B, Van Belle P, Elder DE, Schaumburg-Lever G, Garbe C, Walz TM, Donatien P, Crombleholme TM, Herlyn M. Human melanoma progression in skin reconstructs : biological significance of bFGF. Am J Pathol. 2000 Jan;156(1):193-200.

Mitchell D, Paniker L, Sanchez G, Trono D, Nairn R. The etiology of sunlight-induced melanoma in Xiphophorus hybrid fish. Mol Carcinog. 2007 Aug;46(8):679-84.

Miyamura Y, Coelho SG, Schlenz K, Batzer J, Smuda C, Choi W, Brenner M, Passeron T, Zhang G, Kolbe L, Wolber R, Hearing VJ. The deceptive nature of UVA tanning versus the modest protective effects of UVB tanning on human skin. Pigment Cell Melanoma Res. 2011 Feb;24(1):136-47.

Mo J, Sun B, Zhao X, Gu Q, Dong X, Liu Z, Ma Y, Zhao N, Tang R, Liu Y, Chi J, Sun R. Hypoxia-induced senescence contributes to the regulation of microenvironment in melanomas. Pathol Res Pract. 2013 Oct;209(10):640-7

Mogensen M, Jemec GB. The potential carcinogenic risk of tanning beds: clinical guidelines and patient safety advice. Cancer Manag Res. 2010 Oct 28;2:277-82.

Mohapatra S, Coppola D, Riker AI, Pledger WJ. Roscovitine inhibits differentiation and invasion in a three-dimensional skin reconstruction model of metastatic melanoma. Mol Cancer Res. 2007 Feb;5(2):145-51

Morlière P, Moysan A, Santus R, Hüppe G, Mazière JC, Dubertret L. UVA-induced lipid peroxidation in cultured human fibroblasts. Biochim Biophys Acta. 1991 Jul 30;1084(3):261-8.

Moysan A, Clément-Lacroix P, Michel L, Dubertret L, Morlière P. Effects of ultraviolet A and antioxidant defense in cultured fibroblasts and keratinocytes. Photodermatol Photoimmunol Photomed. 1996 Oct-Dec;11(5-6):192-7.

Mouret S, Baudouin C, Charveron M, Favier A, Cadet J, Douki T. Cyclobutane pyrimidine dimers are predominant DNA lesions in whole human skin exposed to UVA radiation. Proc Natl Acad Sci U S A. 2006 Sep 12;103(37):13765-70.

Natali PG, Nicotra MR, Di Renzo MF, Prat M, Bigotti A, Cavaliere R, Comoglio PM. Expression of the c-Met/HGF receptor in human melanocytic neoplasms: demonstration of the relationship to malignant melanoma tumour progression. Br J Cancer. 1993 Oct;68(4):746-50.

Nicholson RI, Gee JM, Harper ME. EGFR and cancer prognosis. Eur J Cancer. 2001 Sep;37 Suppl 4:S9-15.

Nilsson M, Gullberg M, Dahl F, Szuhai K, Raap AK. Real-time monitoring of rolling-circle amplification using a modified molecular beacon design. Nucleic Acids Res. 2002 Jul 15;30(14):e66.

Nomura H, Sato H, Seiki M, Mai M, Okada Y. Expression of membrane-type matrix metalloproteinase in human gastric carcinomas. Cancer Res. 1995 Aug 1;55(15):3263-6

Noonan FP, Dudek J, Merlino G, De Fabo EC. Animal models of melanoma: an HGF/SF transgenic mouse model may facilitate experimental access to UV initiating events. Pigment Cell Res. 2003 Feb;16(1):16-25

Noonan FP, Recio JA, Takayama H, Duray P, Anver MR, Rush WL, De Fabo EC, Merlino G. Neonatal sunburn and melanoma in mice. Nature. 2001 Sep20;413(6853):271-2.

Noonan FP, Zaidi MR, Wolnicka-Glubisz A, Anver MR, Bahn J, Wielgus A, Cadet J, Douki T, Mouret S, Tucker MA, Popratiloff A, Merlino G, De Fabo EC. Melanoma induction by ultraviolet A but not ultraviolet B radiation requires melanin pigment. Nat Commun. 2012 Jun 6;3:884.

Noonberg SB, Benz CC. Tyrosine kinase inhibitors targeted to the epidermal growth factor receptor subfamily: role as anticancer agents. Drugs. 2000 Apr;59(4):753-67.

Ohashi T, Akazawa T, Aoki M, Kuze B, Mizuta K, Ito Y, Inoue N. Dichloroacetate improves immune dysfunction caused by tumor-secreted lactic acid and increases antitumor immunoreactivity. Int J Cancer. 2013 Sep1;133(5):1107-18.

Orimoto AM, Neto CF, Pimentel ER, Sanches JA, Sotto MN, Akaishi E, Ruiz IR. High numbers of human skin cancers express MMP2 and several integrin genes. J Cutan Pathol. 2008 Mar;35(3):285-91.

Page-McCaw A, Ewald AJ, Werb Z. Matrix metalloproteinases and the regulation of tissue remodelling. Nat Rev Mol Cell Biol. 2007 Mar;8(3):221-33.

Pang CY, Lee HC, Yang JH, Wei YH. Human skin mitochondrial DNA deletions associated with light exposure. Arch Biochem Biophys. 1994 Aug 1;312(2):534-8.

Parisi AV, Wong JC. An estimation of biological hazards due to solar radiation. J Photochem Photobiol B. 2000 Feb;54(2-3):126-30.

Patra KC, Hay N. The pentose phosphate pathway and cancer. Trends Biochem Sci. 2014 Aug;39(8):347-54. doi: 10.1016/j.tibs.2014.06.005. Epub 2014 Jul 15.

Peltomäki P, Gao X, Mecklin JP. Genotype and phenotype in hereditary nonpolyposis colon cancer: a study of families with different vs. shared predisposing mutations. Fam Cancer. 2001;1(1):9-15.

Pfeifer GP, You YH, Besaratinia A. Mutations induced by ultraviolet light. Mutat Res. 2005 Apr 1;571(1-2):19-31. Epub 2005 Jan 20.

Poillet-Perez L, Despouy G, Delage-Mourroux R, Boyer-Guittaut M. Interplay between ROS and autophagy in cancer cells, from tumor initiation to cancer therapy. Redox Biol. 2015;4:184-92.

Polo SE, Jackson SP. Dynamics of DNA damage response proteins at DNA breaks: a focus on protein modifications. Genes Dev. 2011 Mar 1;25(5):409-33.

Ramos J, Villa J, Ruiz A, Armstrong R, Matta J. UV dose determines key characteristics of nonmelanoma skin cancer. Cancer Epidemiol Biomarkers Prev.2004 Dec;13(12):2006-11.

Ramos MC, Steinbrenner H, Stuhlmann D, Sies H, Brenneisen P. Induction of MMP-10 and MMP-1 in a squamous cell carcinoma cell line by ultraviolet radiation. Biol Chem. 2004 Jan;385(1):75-86.

Rastogi RP, Richa, Kumar A, Tyagi MB, Sinha RP. Molecular mechanisms of ultraviolet radiation-induced DNA damage and repair. J Nucleic Acids. 2010 Dec 16;2010:592980.

Recio JA, Merlino G. Hepatocyte growth factor/scatter factor activates proliferation in melanoma cells through p38 MAPK, ATF-2 and cyclin D1. Oncogene. 2002 Feb 7;21(7):1000-8.

Redondo P, Lloret P, Idoate M, Inoges S. Expression and serum levels of MMP-2 and MMP-9 during human melanoma progression. Clin Exp Dermatol. 2005 Sep;30(5):541-5. PubMed PMID: 16045689.

Resendis-Antonio O, Checa A, Encarnación S. Modeling core metabolism in cancer cells: surveying the topology underlying the Warburg effect. PLoS One. 2010 Aug 25;5(8):e12383.

Rojo F, García-Parra J, Zazo S, Tusquets I, Ferrer-Lozano J, Menendez S,Eroles P, Chamizo C, Servitja S, Ramírez-Merino N, Lobo F, Bellosillo B,Corominas JM, Yelamos J, Serrano S, Lluch A, Rovira A, Albanell J. Nuclear PARP-1protein overexpression is associated with poor overall survival in early breastcancer. Ann Oncol. 2012 May;23(5):1156-64.

Rigel DS, Russak J, Friedman R. The evolution of melanoma diagnosis: 25 years beyond the ABCDs. CA Cancer J Clin. 2010 Sep-Oct;60(5):301-16

Rotte A, Martinka M, Li G. MMP2 expression is a prognostic marker for primary melanoma patients. Cell Oncol (Dordr). 2012 Jun;35(3):207-16.

Roux PP, Blenis J. ERK and p38 MAPK-activated protein kinases: a family of protein kinases with diverse biological functions. Microbiol Mol Biol Rev. 2004 Jun;68(2):320-44.

Sabourin CL, Freeman AG, Kusewitt DF, Ley RD. Identification of a transforming ras oncogene in an ultraviolet radiation-induced corneal tumor of Monodelphis domestica. Photochem Photobiol. 1992 Mar;55(3):417-24.

Sawaya RE, Yamamoto M, Gokaslan ZL, Wang SW, Mohanam S, Fuller GN, McCutcheon IE, Stetler-Stevenson WG, Nicolson GL, Rao JS. Expression and localization of 72 kDa type IV collagenase (MMP-2) in human malignant gliomas in vivo. Clin Exp Metastasis. 1996 Jan;14(1):35-42.

Serganova I, Rizwan A, Ni X, Thakur SB, Vider J, Russell J, Blasberg R, Koutcher JA. Metabolic imaging: a link between lactate dehydrogenase A, lactate, and tumor phenotype. Clin Cancer Res. 2011 Oct 1;17(19):6250-61.

Setlow RB, Grist E, Thompson K, Woodhead AD. Wavelengths effective in induction of malignant melanoma. Proc Natl Acad Sci U S A. 1993 Jul 15;90(14):6666-70.

Schenk G, Duggleby RG, Nixon PF. Heterologous expression of human transketolase. Int J Biochem Cell Biol. 1998 Mar;30(3):369-78.

Schenk G, Duggleby RG, Nixon PF. Properties and functions of the thiamine diphosphate dependent enzyme transketolase. Int J Biochem Cell Biol. 1998 Dec;30(12):1297-318.

Schäfers M, Riemann B, Kopka K, Breyholz HJ, Wagner S, Schäfers KP, Law MP, Schober O, Levkau B. Scintigraphic imaging of matrix metalloproteinase activity in the arterial wall in vivo. Circulation. 2004 Jun 1;109(21):2554-9. Epub 2004 May 3.

Schulman JM, Fisher DE. Indoor ultraviolet tanning and skin cancer: health risks and opportunities. Curr Opin Oncol. 2009 Mar;21(2):144-9

Scott DA, Richardson AD, Filipp FV, Knutzen CA, Chiang GG, Ronai ZA, Osterman AL, Smith JW. Comparative metabolic flux profiling of melanoma cell lines: beyond the Warburg effect. J Biol Chem. 2011 Dec 9;286(49):42626-34.

Sherburn TE, Gale JM, Ley RD. Cloning and characterization of the CDKN2A and p19ARF genes from Monodelphis domestica. DNA Cell Biol. 1998 Nov;17(11):975-81.

Shieh DB, Chou WP, Wei YH, Wong TY, Jin YT. Mitochondrial DNA 4,977-bp deletion in paired oral cancer and precancerous lesions revealed by laser microdissection and real-time quantitative PCR. Ann N Y Acad Sci. 2004 Apr;1011:154-67.

Smith ME, Kaulmann U, Ward JM, Hailes HC. A colorimetric assay for screening transketolase activity. Bioorg Med Chem. 2006 Oct 15;14(20):7062-5. Epub 2006 Jun 19.

Staibano S, Pepe S, Lo Muzio L, Somma P, Mascolo M, Argenziano G, Scalvenzi M, Salvatore G, Fabbrocini G, Molea G, Bianco AR, Carlomagno C, De Rosa G. Poly(adenosine diphosphate-ribose) polymerase 1 expression in malignant melanomas from photoexposed areas of the head and neck region. Hum Pathol. 2005 Jul;36(7):724-31.

Staiger WI, Coy JF, Grobholz R, Hofheinz RD, Lukan N, Post S, Schwarzbach MH, Willeke F. Expression of the mutated transketolase TKTL1, a molecular marker in gastric cancer. Oncol Rep. 2006 Oct;16(4):657-61.

Sternlicht MD, Werb Z. How matrix metalloproteinases regulate cell behavior. Annu Rev Cell Dev Biol. 2001;17:463-516.

Sun T, Jackson S, Haycock JW, MacNeil S. Culture of skin cells in 3D rather than 2D improves their ability to survive exposure to cytotoxic agents. J Biotechnol. 2006 Apr 10;122(3):372-81. Epub 2006 Jan 30.

Sun T, Norton D, McKean RJ, Haycock JW, Ryan AJ, MacNeil S. Development of a 3D cell culture system for investigating cell interactions with electrospun fibers. Biotechnol Bioeng. 2007 Aug 1;97(5):1318-28.

Swalwell H, Latimer J, Haywood RM, Birch-Machin MA. Investigating the role of melanin in UVA/UVB- and hydrogen peroxide-induced cellular and mitochondrial ROS production and mitochondrial DNA damage in human melanoma cells. Free Radic Biol Med. 2012 Feb 1;52(3):626-34.

Taanman JW. The mitochondrial genome: structure, transcription, translation and replication. Biochim Biophys Acta. 1999 Feb 9;1410(2):103-23.

Tang ZY, Liu Y, Liu LX, Ding XY, Zhang H, Fang LQ. RNAi-mediated MMP-9 silencing inhibits mouse melanoma cell invasion and migration in vitro and in vivo. Cell Biol Int. 2013 Aug;37(8):849-54.

Tas F, Duranyildiz D, Oguz H, Camlica H, Yasasever V, Topuz E. Circulating levels of vascular endothelial growth factor (VEGF), matrix metalloproteinase-3 (MMP-3), and BCL-2 in malignant melanoma. Med Oncol. 2008;25(4):431-6.

Tas F, Duranyildiz D, Oguz H, Disci R, Kurul S, Yasasever V, Topuz E. Serum matrix metalloproteinase-3 and tissue inhibitor of metalloproteinase-1 in patients with malignant melanoma. Med Oncol. 2005;22(1):39-44.

Tatarenkov A, Avise JC. Rapid concerted evolution in animal mitochondrial DNA. Proc Biol Sci. 2007 Jul 22;274(1619):1795-8.

Tokuraku M, Sato H, Watanabe Y, Seiki M. [Expression of membrane-type matrix metalloproteinase (MT-MMP) and activation of MMP-2 in lung cancer]. Nihon Rinsho. 1995 Jul;53(7):1822-6. Japanese.

Tucker MA, Goldstein AM. Melanoma etiology: where are we? Oncogene. 2003 May 19;22(20):3042-52.

Turnbull DJ, Parisi AV. Spectral UV in public shade settings. J Photochem Photobiol B. 2003 Jan;69(1):13-9.

Van Kilsdonk JW, Bergers M, Van Kempen LC, Schalkwijk J, Swart GW.Keratinocytes drive melanoma invasion in a reconstructed skin model. Melanoma Res. 2010 Oct;20(5):372-80.

Vander Heiden MG, Cantley LC, Thompson CB. Understanding the Warburg effect: the metabolic requirements of cell proliferation. Science. 2009 May 22;324(5930):1029-33.

Vincensi MR, d'Ischia M, Napolitano A, Procaccini EM, Riccio G, Monfrecola G, Santoianni P, Prota G. Phaeomelanin versus eumelanin as a chemical indicator of ultraviolet sensitivity in fair-skinned subjects at high risk for melanoma: a pilot study. Melanoma Res. 1998 Feb;8(1):53-8.

Völker HU, Hagemann C, Coy J, Wittig R, Sommer S, Stojic J, Haubitz I, Vince GH, Kämmerer U, Monoranu CM. Expression of transketolase-like 1 and activation of Akt in grade IV glioblastomas compared with grades II and III astrocytic gliomas. Am J Clin Pathol. 2008 Jul;130(1):50-7.

Wallace DC, Brown MD, Lott MT. Mitochondrial DNA variation in human evolution and disease. Gene. 1999 Sep 30;238(1):211-30.

Wallace DC. Mitochondria and cancer: Warburg addressed. Cold Spring Harb Symp Quant Biol. 2005;70:363-74.

Wallace DC. Mitochondrial DNA sequence variation in human evolution and disease. Proc Natl Acad Sci U S A. 1994 Sep 13;91(19):8739-46.

Walter RB, Kazianis S. Xiphophorus interspecies hybrids as genetic models of induced neoplasia. ILAR J. 2001;42(4):299-321.

Wang L, Cai W, Zhang W, Chen X, Dong W, Tang D, Zhang Y, Ji C, Zhang M. Inhibition of poly(ADP-ribose) polymerase 1 protects against acute myeloid leukemia by suppressing the myeloproliferative leukemia virus oncogene. Oncotarget. 2015 Sep 29;6(29):27490-504

WARBURG O. On respiratory impairment in cancer cells. Science. 1956 Aug 10;124(3215):269-70.

Wehner J, Horneck G. Effects of vacuum UV and UVC radiation on dry E. coli plasmid pUC19. I. Inactivation, lacZ- mutation induction and strand breaks. J Photochem Photobiol B. 1995 Apr;28(1):77-

Wittgen HG, van Kempen LC. Reactive oxygen species in melanoma and its therapeutic implications. Melanoma Res. 2007 Dec;17(6):400-9.

Yajima I, Kumasaka MY, Thang ND, Goto Y, Takeda K, Yamanoshita O, Iida M, Ohgami N, Tamura H, Kawamoto Y, Kato M. RAS/RAF/MEK/ERK and PI3K/PTEN/AKT Signaling in Malignant Melanoma Progression and Therapy. Dermatol Res Pract. 2012;2012:354191..

Yamaguchi R, Janssen E, Perkins G, et al. (2011) Efficient elimination of cancer cells by deoxyglucose-ABT-263/737 combination therapy. PLoS One 6:e24102.

Yamamoto M, Mohanam S, Sawaya R, Fuller GN, Seiki M, Sato H, Gokaslan ZL, Liotta LA, Nicolson GL, Rao JS. Differential expression of membrane-type matrix metalloproteinase and its correlation with gelatinase A activation in human malignant brain tumors in vivo and in vitro. Cancer Res. 1996 Jan 15;56(2):384-92.

Yang W, Zheng Y, Xia Y, Ji H, Chen X, Guo F, Lyssiotis CA, Aldape K, Cantley LC, Lu Z. ERK1/2-dependent phosphorylation and nuclear translocation of PKM2 promotes the Warburg effect. Nat Cell Biol. 2012 Dec;14(12):1295-304.

Yuan W, Wu S, Guo J, Chen Z, Ge J, Yang P, Hu B, Chen Z. Silencing of TKTL1 by siRNA inhibits proliferation of human gastric cancer cells in vitro and in vivo. Cancer Biol Ther. 2010 May 1;9(9):710-6. Epub 2010 May 8.

Zhang S, Yue JX, Yang JH, Cai PC, Kong WJ. Overexpression of transketolase protein TKTL1 is associated with occurrence and progression in nasopharyngeal carcinoma: a potential therapeutic target in nasopharyngeal carcinoma. Cancer Biol Ther. 2008 Apr;7(4):517-22. Epub 2008 Jan 2. Retraction in: Cancer Biol Ther. 2010 Jul 1;10(1):110..

Zhang Y, Dong Z, Bode AM, Ma WY, Chen N, Dong Z. Induction of EGFR-dependent and EGFR-independent signaling pathways by ultraviolet A irradiation. DNA CellBiol. 2001 Dec;20(12):769-79. P

Zhang Y, Rohde LH, Wu H. Involvement of nucleotide excision and mismatch repair mechanisms in double strand break repair. Curr Genomics. 2009 Jun;10(4):250-8.

Zigrino P, Kuhn I, Bäuerle T, Zamek J, Fox JW, Neumann S, Licht A, Schorpp-Kistner M, Angel P, Mauch C. Stromal expression of MMP-13 is required for melanoma invasion and metastasis. J Invest Dermatol. 2009 Nov;129(11):2686-93.

Zu XL, Guppy M. Cancer metabolism: facts, fantasy, and fiction. Biochem Biophys Res Commun. 2004 Jan 16;313(3):459-65.

H. Acknowledgements

I would like to express my thankfulness and appreciation to my supervisor Professor Dr. med. Mark Berneburg and also to Dr. York Kamenisch, for their brilliant advices, discussion and for allowing me to grow as a scientist and to develop my research project.

Besides my supervisor, I want to thank my PhD committee members, Professor H. Peter Rodemann and Professor Michael Schwarz and also my PhD defense examiners, Professor Jürgen Bauer, Professor Kamran Ghoreschi and Professor Ana J. Garcia Saez, for their helpful comments and suggestions.

My sincere thanks also goes to Prof. Dr. Bernd Pichler and Dr. Inka Montero for their systematic guidance and great effort into training me in the scientific field from the Faculty of Medicine University of Tuebingen

Thanks to Professor Martin Röcken for giving me the opportunity to perform my work in the laboratory of the Department of Dermatology, University of Tuebingen.

I want to mention and thank all other collaboration groups, that were involved in our project progression, especially Professor Gronwald from University of Regensburg, Professor Seeger from University of Tuebingen and Dr. Tobias Sinnberg, working group of Professor Brigit Schittek from University of Tuebingen. Also I want to thanks, Nurgül Düzenli, Evelyn Maczey and Eva Müller-Hermelink for their technical assistance.

I want to thank all my friends who supported me to reach my goal, especially Dr. Sara Giovannini and Christina Braunsdorf for giving helpful opinion and advice on our lab related work, I do not forget other colleagues in Rontgenweg 13/1 for the welcoming and friendly working atmosphere.

My gratefulness to my family, especially to my husband Dr.med Deedar Mustafa and my father Dr. Sherko Baban, for their constant support and encouragement throughout my PhD experience.

Finally, I want to appreciate financial support of my research project. This work was mainly funded by Kurdistan regional government ministry of higher education and scientific research.

In addition, part of the work was funded by Deutsche Krebshilfe 106223, Deutsche Krebshilfe 110210 and the melanoma research network.

Thanks…

Tarza S.A. Baban

I. Declaration of contribution

The concept of the project and the study design was mainly done by York Kamenisch and Mark Berneburg (with assistance Tarza Sherko Abdulkareem Baban). Experiments were performed by Tarza Sherko Abdulkareem Baban (with assistance of York Kamenisch), except the experiments listed in the section of collaboration groups were performed in collaboration.

Tarza Sherko Abdulkareem Baban and York Kamenisch analysed the data. Tarza Sherko Abdulkareem Baban, Mark Bernebrug and York Kamenisch interpreted and discussed the data. Figures and tables were created by York Kamenisch and Tarza Sherko Abdulkareem Baban. The manuscript was written by Tarza Sherko Abdulkareem Baban and revision and rewriting of the manuscript was done by York Kamenisch and Mark Berneburg.

Collaboration groups

1. Skin reconstructs preparation and histology were performed in collaboration with Dr.Tobias Sinnberg, Nurgül Düzenli, Evelyn Maczey and Eva Müller-Hermelink, Dr. med. Gisela Metzler, Prof. Jürgen Bauer, Prof. Birgit Schittek, Prof. Claus Garbe and Prof. Martin Röcken (University of Tuebingen).

2. Declaration of the figures (40 and 41):

Figure 40. The level of the mitochondrial common deletion decreased during melanoma progression

Figure 41. Measurement of the common deletion in 25 nevi samples, 26 dysplastic nevi samples, 22 melanoma of <1mm samples and 21 melanoma >4mm samples by real time PCR

This work was done in collaboration with Prof. Röcken, Claudia Braniek, Julia Wenz (Department of Dermatology) and Prof. Seeger (Department of Gynecology) University of Tuebingen.

Part of figure 41 experiment was performed by Nurgül Düzenli, and the rest of experiment was performed by Tarza Sherko Abdulkareem Baban.

3. Declaration of the figures (19, 20 and 21):

Figure 19. UVA induced Warburg effect analyzed by NMR spectroscopy

Figure 20. Change of metabolites upon UVA irradiation in the supernatant of melanoma cells

Figure 21. Change of metabolites upon UVA irradiation in the melanoma cell pellets

Analysis of samples by NMR spectroscopy was done in collaboration with Prof. Dr. Wolfram Gronwald, Philipp Schwarzfischer, Prof. Dr. Oefner and Prof. Dr. Marina Kreutz (University of Regensburg).